ADDIS ABABA UNIVERSITY

CENTER FOR ENVIRONMENTAL SCIENCE

Ecosystem service valuation and spatial modeling of carbon stock, tree species diversity, and soil erosion in Bale Mountains Ecoregion, Ethiopia

By

Girma Ayele Bedane

Supervisor: Gudina Legese Feyisa (PhD, Associate Professor)

Co supervisor: Feyera Senbeta (PhD, Professor)

A dissertation submitted to the Center for Environmental Science

Presented in Partial Fulfillment of the Requirements for the Degree of Doctor of Philosophy in Environmental Science Addis Ababa University

ADDIS ABABA, ETHIOPIA

January 2025

Ecosystem service valuation and spatial modeling of carbon stock, tree species diversity, and soil erosion in Bale Mountains Ecoregion, Ethiopia

By

Girma Ayele Bedane

Supervisor: Gudina Legese Feyisa (PhD, Associate Professor)

Co supervisor: Feyera Senbeta (PhD, Professor)

A thesis submitted to the Center for Environmental Science

Presented in Partial Fulfillment of the Requirements for the Degree of Doctor of Philosophy in Environmental Science Addis Ababa University

Addis Ababa, Ethiopia

January 2025

ABSTRACT

Ecosystem service valuation and spatial modeling of carbon storage, tree species diversity, and soil erosion in Bale Mountains Ecoregion, Ethiopia
By Girma Ayele, January 2025, Addis Ababa University

The Bale Mountains Ecoregion (BMER) has been facing severe deforestation, and land degradation driven by land use and land cover (LULC) changes that alarmingly impact its ecosystem conditions. Despite the severity of these challenges, there has been inadequate scientific knowledge on how these drivers affect the spatial distribution of ecosystem attributes and ecosystem service values (ESVs). This PhD research has aimed to contribute to address the knowledge gap, employing extensive ground-based geospatial data collection, remotely sensed satellite imagery, and advanced spatial modeling to explore the condition of the BMER ecosystem using various indicators of ecosystem attributes. Landsat images of the years 2010, 2015, and 2022 were acquired, and standard image pre-processing and analysis techniques were applied to generate LULC data and examine ecosystem dynamics. The LULC was used to conduct ecosystem service valuation by applying adopted coefficients for each service to the corresponding ecosystem areas at the BMER. At the same scale, soil loss was estimated and mapped for 2010 and 2022 using the Revised Universal Soil Loss Equation (RUSLE) and the Geographic Information System (GIS). Additionally, 236 sample plots were randomly selected in the forest of BMER to map the spatial distribution of Aboveground Carbon Density (ACD) and species diversity using kriging techniques.The maps of species indices were classified into six categories and related with a deforesation area map occurred during 2010 and 2022 to quanitify impacts of an area of deforesation on different classes of forest attributes using Zonal stitistics in ArcGIS map. Zooming into detail, additional forest data were collected from 1,122 sample plots in the Harana Forest to model the impacts of biophysical factors on ACD and the abundance of dominant tree species, applying Random Forest (RF), Artificial Neural Network (ANN), and Generalized Linear Model (GLM) approaches. The findings showed a significant decline in the ESV of BMER, from US$ 103 billion in 2010 to US$ 92.5 billion in 2022. Forest ecosystems showed a marked decrease in value, from US$ 94.5 billion to US$ 82.2 billion, while water ecosystem services declined from US$ 38.6 billion to US$ 35.4 billion. Climate regulation services experienced a reduction of US$ 76.4 million, whereas farmland ESV increased from US$ 4.81 billion to US$ 7.12 billion over the same period. Soil loss also worsened, with mean soil loss increasing from 0–306 t/ha/yr in 2010 to 0–391 t/ha/yr in 2022. The total soil loss increased from 4.5 million tons to 7.5 million tons between 2010 and 2022. Farmland was the most affected, accounting for 56.06% of total soil loss in 2010 and 68.9% in 2022. The ACD between 63 to 118 t/ha accounted for 54% of the total forest area, while a maximum of ACD of 282 and 336 t/ha accounted for only 0.3%. Species richness was unevenly distributed, with the highest class (24.00–28.29) covering 877 ha (0.1%) of the total area, while the lowest class (2.55–6.84) occupied 32%. The deforestation of 10,356 ha resulted in losses of species richness in a class of (6.84 to 11.13). The deforestation of 7,746 ha caused a loss of the Shannon-Weiner diversity indices (1.36 to 1.67). Biotic factors primarily influenced the spatial distribution of ACD in the Harana forest. The abundance of dominant tree species was influenced by elevation, temperature, rainfall, clay content, and potassium levels. In conclusion, this research provides a spatially explicit, quantitative scientific understanding of the ecosystem conditions of BMER. These findings provide critical empirical evidence to inform conservation interventions and strategies for sustainable ecosystem management of the BMER.

ACKNOWLEDGMENTS

I extend my deepest gratitude to my supervisor, Dr. Gudina Legese Feyisa, for his invaluable guidance throughout the entire study of my PhD research. From the initial stages of research design to the completion of this thesis report, his expertise and support have been instrumental in shaping the direction and quality of my work. I am especially grateful for his provision of training in environmental modeling which proved essential in the execution of this research work. I am profoundly indebted to Dr. Gudina for his unwavering encouragement when I faced the challenge of getting sponsorship for my research study as a self-sponsored PhD candidate. His steadfast belief in my capabilities and his patience during setbacks were pivotal in enabling me to persist and ultimately complete my research. The understanding and support demonstrated by Dr. Gudina have left an enduring impact on me. Similarly,

I humbly extend my deepest gratitude to my Co-supervisor, Professor Feyera Senbeta, for his invaluable guidance and support throughout my research journey. Professor Feyera played a pivotal role in shaping my research direction by raising important questions that needed to be addressed. His insightful inputs and expertise were instrumental in refining the focus of my work and ensuring the required academic rigor. I would like to extend my special thanks to Professor Seyoum Leta for inspiring me to pursue my PhD study at the Center for Environmental Science at Addis Ababa University. I am grateful to Dr. Amare Haileslassie for his support in continuing my rigorous research work. I want to extend my sincere gratitude to Farm Africa for granting me access to the soil data of the study area and facilitating the forest data collection process both for the purposes of this study and forest management. I would like to extend my sincere thanks to my colleagues Tewodros Gezahgan, Sahlemariam Mezmure, and Seyoum Gebrekidan for their invaluable support during the forest data collection process.

I am also grateful to my friend Merga Diyesa for his support in downloading the Landsat imagery and for his continual encouragement throughout this journey. I extend my gratitude to Samuel Teshome and Nigat Dejene for their encouragement and support, which motivated me to persevere through the rigorous journey of pursuing my PhD work. Importantly, I am deeply grateful to the community members and government technical staff in Delo Mena and Haran Buluk woredas for their invaluable support during the data collection process in the Harana Forest. Last but certainly not least, I extend my heartfelt thanks and appreciation to my family members Meseret Kasa, Dawit Girma, and Dagim Girma for their unwavering support and encouragement throughout my academic journey.

TABLES OF CONTENT

LIST OF TABLES

LIST OF FIGURES

ABBREVIATIONS

ACD	Aboveground Forest Carbon Density per plot
ANNs	Artificial Neural networks
BMER	Bale Mountains Ecoregion
DBH	Diameter at Breast Height
DEM	Digital Elevation Model
ENVI	Environmental for Visualizing Images
ESV	Ecosystem service valuation
FAO	Food and Agricultural Organization
GIS	Geographical Information System
GIS	Geographical Information systems
GLMs	Generalized Linear Models
GPS	Geographical Positioning System
IPBES	Intergovernmental Platform on Biodiversity and Ecosystem Services
IPCC	Intergovernmental Panel on Climate Change
ISRIC	International Soil Reference and Information Centre
LULC	Land use and land cover
LULCC	Land use and land cover change
OLI	Operational Land Imager images
REDD+	Reducing emissions from deforestation and forest degradation plus
RF	Random Forest
SDMs	Species Distribution Models
SPSS	Statistical Package for the Social Sciences
TEEB	The Economics of Ecosystems and Biodiversity
UNDP	United Nations Development Programmee
UNFCCC	United Nations Framework Convention on Climate Change
USGS	The United States Geological Survey
UTM	Universal Transverse Mercator Coordinate

LIST OF PUBLICATIONS FROM THIS PhD THESIS

Four scientific papers have been produced in this PhD work, two of which are published in the journal **Ecological Processes**, which is published by **Springer.** The remaining three are in the full scientific manuscript stage and are currently under review.

i. Bedane, G.A., Feyisa, G.L. & Senbeta, F. (2022). Spatial Distribution of Above Ground Carbon Density in Harana Forest, Ethiopia. *Ecol Process* 11(4). Doi.Org/10.1186/S13717-021-00345-X. **Annex 8, published article**

ii. Bedane GA, Feyisa G.L., & Senbeta F (2022). Modeling effects of abiotic factors on the abundances of eight woody species in the Harana forest using artificial networks, random forest, and generalized linear models. *Ecol Process* 11(10). doi.org/10.1186/s13717-023-00424-1. **Annex 9, published article**

iii. Bedane GA, Feyisa GL, Senbeta F, & Haileslassie A (2025). Dynamics of Ecosystem Service Value in response to Land Use and Land Cover Changes in the Bale Mountains Ecoregion, Ethiopia, **Annex 10, Draft *manuscript***

iv. Bedane GA, Feyisa, GL & Senbeta F **(**2025). Soil Loss Estimation and differentiating Erosion Susceptible Areas using RUSEL and ArcGIS techniques in the case of Bale Mountains Ecoregion, Ethiopia, **Annex 11, Draft *manuscript***

v. Bedane GA, Feyisa GL & Senbeta F (2025)**.** Geostatistical application in the spatial mapping of forest attributes in the Bale Mountains Ecoregion, Ethiopia, **Annex 12, Draft *manuscript***

CHAPTERS 1: INTRODUCTION

1.1.Background

The Earth comprises various ecosystems that provide multiple benefits for societal well-being (MEA, 2005; Fenta *et al*., 2020). The concept of ecosystem refers to "the functional unit comprising all the organisms in a particular place interacting with one another and with their physical environment and interconnected by an ongoing flow of energy and a cycling of materials" (Kumar and Mina, 2021). Nevertheless, most global ecosystems have been affected by land use and land cover (LULC) change, deforestation, soil erosion, biodiversity loss, and environmental pollution (Nguyen *et al*., 2012; Rendon *et al*., 2019). The LULC change has reduced the value of global ecosystem services from US$145 trillion in 2007 to US$125 trillion in 2011 (Costanza *et al*., 2014). Particularly, deforestation has become the second global source of carbon emission next to fossil fuel by releasing 5.9 GtCO2 annually (Gorte and Sheikh, 2010; Neba, 2013). The annual carbon emissions from deforestation in tropical areas account for 20% to 25% of global greenhouse gases (Moutinho and Schwartzman, 2015). In the meantime, biodiversity has been threatened in tropical forest areas (Neves *et al*., 2010; Kumari *et al*., 2021; Teferi *et al*., 2021) where tropical forests are estimated to harbor 40,000 to 53,000 species (Labrière *et al*., 2016). Soil is another component of the ecosystem which is a foundation of the terrestrial ecosystem (Baer and Birgé, 2018; Pham *et al*., 2018); but the soil conditions in different ecosystems have been globally affected by LULC change (Das *et al*., 2021; Pham *et al*., 2018; Gong *et al*., 2022). Available literature has shown that more than one million ha of global land has been affected by water erosion (Thomas *et al*., 2018); which has resulted in the loss of 75 billion tons of fertile soil annually from agricultural fields (Gong *et al*., 2022). Besides, a worldwide loss of 25 to 40 billion tons of surface soil has resulted in a direct economic loss of about US $ 4,00 billion (Das *et al*., 2021).

These environmental challenges have negatively impacted the conditions of ecosystems to the degree of impairing the ability of ecosystems to sustain the flow of ecosystem services (Rendon *et al*., 2019; Wulder *et al*., 2024). These pressing challenges have necessitated research studies to understand the dynamics in the extent and conditions of ecosystems (Rendon *et al*., 2019; Lof *et al.*, 2022; Wulder *et al*., 2024). Because reliable spatial information on ecosystem conditions is important in informing conservation policy (Tanács *et al.*, 2022). Ecosystem assessment has become an essential tool to examine spatial and temporal dynamics of ecosystems using various indicators of ecosystem attributes (Hatziiordanou *et al*., 2019; Rendon *et al*., 2019; Zhang *et al*., 2023). In line with this, an ecosystem can be defined as a system consisting of biotic and abiotic factors with the flow of solar energy and the cycling of nutrients (Lindeman,1942; Riisgard, 2017; Kumar and Mina, 2021). The term extent refers to the area of the ecosystem (Lof *et al.,* 2022) while ecosystem condition describes the quality of structural and functional components of ecosystems in providing a sustainable flow of ecosystem services (Unnasch *et al*., 2008; Hatziiordanou *et al*., 2019; Rendon *et al*., 2019; Lof *et al.,* 2022).

The structural and functional components of ecosystems are important to characterize the integrity of ecosystems (Verdonschot *et al*., 2020). The ecosytem structure comprises biotic and abiotic elements (Cao *et al.,* 2014; Monga *et al*., 2017). The biotic elements consist of living organisms in a given ecosystem while abiotic factors include non-living components (Balasubramanian, 2008; Jeyanny *et al*., 2014; Prasad, 2022). The functional component includes ecological processes such as photosynthesis, sequestration of carbon dioxide, evapotranspiration, and cycling of nutrients that could be processed by the structural component of the ecosystem (Collinge, 2010; Götzl *et al*., 2013; Selivanov *et al*., 2021; Monga *et al*., 2017). The functional processes could provide ecosystem services to the benefit of people (Tan *et al*., 2020; Nchimbi, 2021; Zhang *et al*., 2023). Technically, ecosystem services are defined as "benefits people obtain from ecosystems" (MEA, 2005). This indicates that the functional roles of the ecosystem are more apparent in terms of ecosystem services (Sheate *et al*., 2012; Baiqiu *et al*., 2019). The ecosystem services are classified into four categories (1) provisioning services which include goods and services directly derived from ecosystems (Silvis and Heid., 2013; Deeksha *et al*., 2022; Tamire *et al*., 2023), (2) regulating services that comprise a regulation of climate change and preventing soil erosion (MEA, 2005; Selivanov and Hlaváčková, 2021), (3) Cultural services entail the non-material benefits that people obtain from nature in form of recreation, aesthetics, and spiritual values (Ding, 2006; Silvis and Heid, 2013); and (4) Supporting services comprise of roles of the ecosystem such as soil formation, photosynthesis, and water purification (Silvis and Heid., 2013; Deeksha *et al*., 2022).

Ecosystem assessment in this research study has aimed to examine the extent and conditions of ecosystems using ecosystem service valuation, spatial analysis, and ecological modeling (Hein, 2014; Maes *et al*., 2015; Balzan *et al*., 2018; Simeon and Wana 2024). The technique of ecosystem services valuation focuses on expressing the benefits of different ecosystems in terms of the monetary value at the scale of the BMER. Spatial analysis and modeling are used to examine the spatial distributions of ecosystem attributes at different spatial scales. The ecosystem attributes refer to the characteristics of ecosystems that can be measured using indicators (Mwakisunga *et al*., 2012; Vayreda *et al*., 2012; Yu *et al*., 2016; Czúcz *et al*., 2021). There are various indicators of attributes to assess ecosystem conditions (Rendon *et al*., 2019); while indicators are supposed to be simple to extract the required information and easily communicated to be understood by wider audiences (Reyers *et al*., 2010). The indicators of ecosystem attributes could be classified into physical, compositional, and functional indicators (Hadjibiros, 2014; Rendon *et al*., 2019; Czúcz *et al*., 2021).

The physical indicators are used to measure aggregated attributes of biotic and abiotic elements such as population density, biomass, abundance, and species richness for living organisms (Reyers *et al*., 2010; Czúcz *et al*., 2021; Lof *et al.* 2022). In this indicator category, indicators of living factors can be an accumulation of chemicals and the magnitude of soil loss (Hadjibiros, 2014; Czúcz *et al*., 2021). The compositional indicators of attributes consist of variables that are combined from different indicators to represent the aspects of ecosystem components using a single index such as the Shannon-Wiener Index diversity index (Reyers *et al*., 2010; Rendon *et al*., 2019; Czúcz *et al*., 2021). The functional indicators are used to quantify the ecosytem functional in terms of biogeochemical and physical indicators (Rendon *et al*., 2019; Czúcz *et al*., 2021). However, the measurement of functional roles is often conducted in terms of quantifying the value of ecosystem services using valuation techniques (Czúcz *et al*., 2021; Liu *et al*., 2021; Sharma *et al*., 2021; Wen *et al*.,2021).

Valuation is defined as the process of putting a monetary value on ecosystem services (Losonci, 2012; Schröter, 2015; Sharma *et al*., 2021). The valuation of ecosystem services has been widely growing in research to estimate the benefits of ecosystem services in economic values (Shuang *et al*., 2010; Selivanov and Hlaváčková, 2021). Particularly, Following the publication of MEA in 2005, a valuation of ecosystem services has been widely promoted by the TEEB, and IPBES (Silvis and Heid, 2013; Costanza *et al*., 2014; Tinch *et al*., 2019; Sharma *et al*., 2021). Recognizing that the valuation of ecosystem services could have various advantages. Primarily, it is useful to quantify and internalize the worth of the ecosystem in monetary value (Losonci, 2012; Schröter, 2015). Second, it supports policy-makers in making an informed decision (Barbier *et al*., 2009; Costanza *et al*., 2014; Hong and Izuru, 2019; Hadley *et al*., 2011). Third, it provides information on the extent of ESV loss and gain (Mulatu,1976; Kumar, 2005; Hegg, 2006; Fentaa *et al*., 2020). The fourth, benefit is that expressing ecosystem services in the monetary value is the most pragmatic language to communicate with policymakers, private sectors, and researchers to inform the consequences of losing ecosystem services (Gómez-Baggethun *et al*., 2009; Silvis and Heid., 2013; Selivanov and Hlaváčková, 2021).

Apart from valuation, spatial analysis and modeling techniques have been widely used to describe the conditions of ecosystem attributes in terms of the spatial information bearing that each attribute possesses a defined spatial location on the Earth (Liedtke, 2011; Szmyt and Stoyan, 2014). Spatial analysis such as spatial prediction or spatial interpolation is important to produce maps of ecosystem attributes by predicting the values of an object at un-sampled locations based on the known values collected from the sample locations (Rebelo and Jones, 2009; Wang, 2013; Liedtke, 2011; Wahab, 2017; Hein, 2014). Kriging in geostatistics is one of the prediction techniques that have been widely used to produce continuous surface maps of attributes by considering the influences of distance and degree between the known sample points (Samui, and Sitharam 2011; Lichtenstern, 2013). These maps are useful for visualizing the locations and patterns of ecosystem attributes at various spatial and temporal scales (Chatzinikolaou *et al.*,2012; Hein, 2014). Particularly, in the disciplines of ecology, agronomy, meteorology, geosciences, and forestry (Li, 2022). In forestry, spatial prediction is used to produce the spatial distribution maps of carbon stock and species diversity (Maes *et al*., 2012; Götzl *et al*., 2013; Ifo *et al*., 2016).

Moreover, models have become vital tools to examine complex ecological interactions; whereas a model is defined as a simplified representation of the real world (Jeffers, 1988; Hadjibiros, 2014; Wang, 2021). Alternatively, the model can be defined as a "formulation that mimics a real-world phenomenon by which prediction can be made" (Sanders, 2007). Seemingly, modeling can be conceptualized as a process of creating a simplified representation of reality (Fedra,1993; Kumar, 2021; Legesse *et al*., 2022). In ecology, models have been used to uncover the hidden relationships that could not be directly visible by looking at the organisms including concealed implications of interactions within biotic elements and between biotic and abiotic components (Jopp *et al*., 2011; Tenedório and Rocha, 2018). In this sense, most ecological models require two categories of inputs which are referred to as the dependent and independent variables (Meier, 2011; Wang, 2013). A dependent variable is a value of an attribute subjected to a modeling process while the independent variables are factors that influence the state of the dependent variable (Jiang, 2012).

The most commonly used models in the research of ecology include the Generalized linear models (GLMs), Random Forest Models (RF), and Artificial neural networks (ANNs) among many others (Guisan *et al*., 2002; Aksu *et al*., 2019; Zhang *et al*., 2019; Yudaputra *et al*., 2019). GLM model is suitable for ecological data as it does not require the assumption of normal distribution whereas most ecological data cannot fulfill the assumption of normal distribution (Guisan *et al*., 2002). The RF and ANN models are machine-learning algorithms where both algorithms do not require the stringent assumption of the normal distribution of dependent variables and are efficient in handling complex ecological interactions (Cutler *et al*., 2007; Vincenzia, 2011). Apart from the ecological models, there are calibrated erosion models such as the Revised Universal Soil Loss Equation (RUSLE) to estimate the magnitude of soil loss and mapping erosion-susceptible areas (Renard *et al*., 1997; Jemal, 2021; Kolli *et al*., 2021; Gong *et al*., 2022).

Regarding the hierarchical structure of this research study, the first three objectives are studied at a broader geographical scale of the Bale Mountains Ecoregion (BMER) while two objectives have been addressed at the Harana Forest Ecosystem. Harana forest ecosystem is the largest of all six forest priority areas and it serves as a buffer zone to the Bale Mountains National Park (BMNP) in the south and southwest parts of the BMER. The three research objectives that have been conducted at the scale of BMER include the valuation of ecosystem services, soil erosion modeling by integrating RUSEL with GIS, and producing spatial distribution maps of ACD and species diversity using kriging. Zooming into details, influences of biophysical factors on the spatial distribution of ACD have been modeled in the Harana Forest including modeling of impacts of abiotic factors on spatial distributions of the selected dominant tree species. The ACD in this study is operationally defined as the sum of the above-ground carbon stock of all trees within a plot of 15-meter radius. Similarly, species abundance refers to the count of individuals of each selected dominant tree species in a given plot of 15-meter radius.

1.2.Statement of the Problems

Anthropogenic factors have exerted continual pressures on global ecosystem conditions mainly in developing countries (Simeon and Wana 2024). Ethiopia is one of the developing countries losing its ecosystems in different parts of the country. These ecosytem destructions have resulted in the decline of the ecosystem services value of the country from US$ 483 billion to 397 billion losing 17.7% of ESV between 2000 and 2015 (Sutton *et al.*, 2016). BMER is one of the areas in the country that is affected by anthropogenic factors such as deforestation, habitat fragmentation, overgrazing, and soil erosion (Gashaw, 2015; Hagos et al., 2018). The BMER is one of 34 global biodiversity hotspot areas contributing to global biodiversity conservation (Nelson, 2012). Concerning the magnitude of the impacts of soil erosion on ecosystems, it has been reported that the size of cropland in the BMER has increased from 136.39 km^2 in 1973 to 572.19 km^2 in 1987 at the expense of forest resources (Kidane *et al.*, 2012). The other similar research study reported a loss of 123,751 ha of forest ecosystem between 1985 and 2015 where the area of cropland in the BMER increased by 292,294 ha (Hailemariam *et al.*, 2016).

Apart from these direct challenges, sustainable management of ecosystems has often been constrained by a lack of information and understanding of the condition of ecosystems (Reyers *et al.*, 2010). This challenge has been apparent in the BMER where there has been scanty information on the potential value of ecosystem services and the extent of losses in ecosytem services value in the BMER as previous research studies have focused only on investigating the impacts of LULC changes on ecosystems (Kidane *et al*, 2012; Hailemariam *et al*., 2016) without considering its implications on the ecosytem services of the BMER in terms of monetary value. This has highlighted a clear gap that this research study has been necessitated to address the identified gap through conducting the valuation of ecosystem services for different ecosystem types in the BMER at different periods of 2010, 2015, and 2022 based on the classification of Land Use and Land cover (LULC) types. LULC) tyes have been widely used as a proxy for the estimation of values of ecosystem services (Maes *et al*., 2015; Solomon *et al*., 2019).

Regarding the impact of soil erosion, it has been reported that soil erosion is one of the environmental challenges that affect ecosystems in BMER (Hagos *et al*., 2018). However, sufficient information has not been available on the extent of soil loss including spatial patterns of the soil losses. The study reported by Ketema *et al*., (2024) has shown the loss of 546,769.92 tons of soil with an average soil loss of 32 $^{-t}$ ha^{-1} yr^{-1} from the Welmel catchment in the Southern parts of BMER. However, the indicated study has been limited to a few locations and has not been sufficient to provide a full picture of soil loss in the entire BMER. This was the reason why this study initiated to address the identified gap by modeling soil erosion using the RUSLE and GIS techniques.

Tropical forests have been the subject of several research studies to understand the conditions of forest ecosystems in mitigating the impacts of climate change and biodiversity conservation (Ifo *et al*.,2016). Nevertheless, most of the research studies in the past have focused on estimating floristic characteristics without considering the spatial dimension of ecosystem attributes (Benítez *et al*., 2016). This infers that the spatial dimension of forest attributes has not been sufficiently studied to describe the spatial distributions of forest attributes by relating to geographical locations. The issue of missing spatial information in research studies has remained an obvious limitation in forest research studies in Ethiopia (Asefa *et al*., 2020; Teferi *et al*., 2021). For instance, stock of forest carbon stock has been estimated in the BMER by Asante *et al*., (2013), without mapping the spatial distribution patterns of the above-ground carbon stock. Additionally, different research studies have been conducted in the BMER to characterize the floristic composition of forest ecosystems using species diversity indices but these studies could not sufficiently demonstrate how the indices of tree species have been spatially configured in the Harana forest ecosystems (Lulekal *et al*., 2008; Yineger *et al*., 2008; Kewessa *et al*. 2019).

This study has aimed at addressing the identified gap by producing the spatial distribution maps of the ACD and species diversity at the broader scale of BMER using geostatistical techniques because the spatial information on ACD directly supports the understanding of how different parts of the forest area contribute to climate change mitigation efforts (Sales *et al*., 2007; Labrière *et al*., 2016). Correspondingly, the spatial information on tree species can have different implications. Primarily, it helps to easily understand the number of species richness or species diversity associated with a given area of forest ecosystem (Chisholm *et al*., 2018). Secondly, it helps to estimate the magnitude of tree species and species diversity losses in the case of deforestation (Whitmore and Sayer, 1992; Neves *et al*., 2010; Berhanu *et al*., 2023).

Additionally, the lack of sufficient understanding of the relationship between forest tree attributes and environmental factors has not been sufficiently studied and it has remained a hot topic in the study of ecology (Redowan 2015; Ifo *et al.*, 2016; Naidu and Kumary, 2016). The Harana forest ecosystem in the BMER has shared a common challenge as the previous studies have not provided an emphasis on the spatial dimensions of forest attributes, particularly on the ACD and species abundances (Yineger *et al*., 2008; Asante *et al*., 2013; Kewessa *et al*., 2019). Identifying these gaps, this study has employed different modeling techniques to determine the impacts of biophysical factors on the spatial distributions of the ACD including investigating the influences of abiotic factors on the abundance of dominant tree species in the Harana forest ecosystem. This information could be highly important and directly contributes to strengthing sustainable forest management based on empirical evidences.

1.3.General objective of the study

The overall objective of this study is to assess the extent and conditions of the spatial and temporal dynamics of ecosystem attributes at the broader geographical scale of the Bale Mountains Ecoregion (BMER) and examine the impacts of biophysical factors on spatial distributions of forest attributes at the local scale of Harana forest to produce the empirical evidence that could support decision-making process to strengthen the conservation efforts in the Bale Mountains Ecoregion.

1.4.Specific objectives of the study

The specific objectives of this study are structured to address the identified interdependent research problems across various geographical settings, ranging from the broader scale of the Bale Mountains Ecoregion (BMER) to the local scale of the Harana Forest that are outlined below:

i. Assessing ecosystem dynamics and estimating the monetary value of ecosystem services
ii. Quantifying the extent of soil loss and identifying erosion susceptibility areas within different ecosystems
iii. Predicting spatial distributions of above-ground forest carbon and tree species diversity in the forest ecosystem
iv. Modeling the influences of biophysical factors on the ACD and producing spatial distribution of ACD in the Harana forest ecosystem, and
v. Analyzing impacts of abiotic factors on the abundances of dominant tree species and predicting the spatial distributions of the abundances of each dominant tree species in the Harana Forest

CHAPTER 2: LITERATURE REVIEW

2.1. Ecosystem services valuation in monetary values

2.1.1 Ecosystem services value in perspectives of environmental and ecological economics

In the second half of the 20th century, environmentalists started to understand the limitations of conventional economics and extended the scope of economic analysis of traditional economics by incorporating the economic impacts of the environment in decision-making processes (Silvis and Heide *et al*., 2013; Biswa, 2023). This has paved the way for the development of environmental and ecological economics as new disciplines (Silvis and Heid; Biswa, 2023). Environmental economics has focused on utility, welfare, costs, and benefits whereas ecological economics tends to incorporate ecological sustainability criteria of productivity, stability, and resilience of ecosystems (Silvis and Heide *et al*., 2013). Ecological economics has advocated sustainable and equitable distribution of natural resources over time, and it encompasses diversified approaches to integrate relevant natural and social sciences (Silvis and Heide *et al*., 2013; Biswa, 2023). Ecological economics have shown more concern about the over-exploitation of natural resources and the production of wastes beyond the Earth's carrying capacity, but environmental economics focuses on market failure as the main cause of environmental problems (Silvis and Heide *et al*., 2013; Sharma *et al*., 2021). With all these understandings, economists have started measuring the value of ecosystem services using the concept of total economic value (Sharma *et al*., 2021). A total economic value (TEV) helps to assign value to ecosystem services which are classified as use and non-use values (Kumar, 2005; Biswa, 2023). The use-values comprise the actual and optional use-values (Watson, 2007). The actual use values include direct and indirect use values (Watson, 2007; Silvis and Heide *et al*., 2013). The direct use-value refers to the benefit obtained from actual use of environmental goods or services which could be consumptive and non-consumptive (Watson, 2007; Losonci, 2012). Consumptive use values include food, water, fish, timber, and hydropower, while the non-consumptive use values include recreational and educational services (Hegg, 2006; Silvis and Heide *et al*., 2013). The indirect use values are derived from the indirect uses of ecosystem services such as cycling of soil nutrients, watershed protection, and crop pollination (Hegg, 2006; Silvis and Heide *et al*., 2013). The optional value refers to the goods and services that are not used at present but it has the potential to be used in the future (Kumar, 2005; Watson, 2007; Silvis and Heide *et al*., 2013; Selivanov and Hlaváčková, 2021). For instance, if an unknown disease will occur in the future and existing plants may cure yet unknown disease such plants are considered to have an optional value (Barbier *et al*., 2009). The non-use values of ecosystem services include bequest and existence values (Brander *et al*., 2010; Losonci, 2012). A bequest value is the value that individuals put on the ecosystem services with the understanding that ecosystems could have potential uses in the future (Kumar, 2005; Watson, 2007;

Silvis and Heide *et al*., 2013). On the other hand, the existence value refers to satisfaction of knowing an ecosystem element continues to exist without being used now or in the future as nature has its right to exist (Losonci, 2012; Silvis and Heide *et al*., 2013; Hadley *et al*., 2011; Selivanov and Hlaváčková, 2021). These basics of environmental and ecological economics have laid the foundation for the Millennium ecosystem assessment that has brought ecosystem services into the domain of economics (Barbier *et al*., 2009; Sharma *et al*., 2021; Biswa, 2023). Following the publication of the Millennium ecosystem assessment in 2005, the valuation of ecosystem services has received worldwide attention from scientists, managers, and policy-makers (MEA, 2005; Spash, 2008; Schröter, 2015; Sharma *et al*., 2021). Importantly, the TEEB, and IPBES have played important roles in promoting the valuation of ecosystem services (Silvis and Heide *et al*., 2013; Costanza *et al*., 2014; Tinch *et al*., 2019; Sharma *et al*., 2021).

The process of ecosystem services valuation has been necessitated for the reason that the majority of ecosystem services lack a price tag as services are not valued in markets (Kumar, 2005; Silvis and Heide *et al*., 2013; Hadley *et al*., 2011). Ecosystem service valuation can be defined as a process by which people put monetary value on the flows of ecosystem goods and services to internalize the worth of the given ecosystem (Losonci, 2012; Schröter, 2014; Sharma *et al*., 2021). Nevertheless, ecosystem service valuation has been a contentious topic between the utilitarian and deontological philosophers (Hegg, 2006). The outlook of utilitarianism is anthropocentric with a view that nature has to serve people as an instrument to fulfill human welfare (Kumar, 2005; Hegg, 2006; Schröter, 2014). Deontologists argue that nature has biocentric or intrinsic value that cannot be quantified in monetary value and ecosystem services valuation is unnecessary and inappropriate where ecosystems contain infinite worth which cannot be quantified (Hegg, 2006; Liu *et al*., 2010; Tinch *et al*., 2019). In this aspect, advocates of deontology have a concern that valuation could provide misleading information to society as all services of an ecosystem cannot be exhaustively quantified in monetary value (Hegg, 2006; Silvis *et al*., 2013).

Differently, supporters of utilitarian philosophy insist that the ecosystem services valuation is useful to internalize the worth of ecosystems without denying the biocentric value of nature (Liu *et al*., 2010; Schroter *et al*., 2014; Schröter, 2014; Tinch *et al*., 2019). In this regard, assigning economic value to ecosystem services in monetary terms helps to establish a common unit to make a comparison of the benefits of various ecosystems (Kumar, 2005; Barbier *et al*., 2009; Hadley *et al*., 2011). Along this arguement, various methods and techniques have been developed to quantify the use and non-use values of ecosystem services (Silvis and Heide *et al*., 2013; Hadley *et al*., 2011; Sharma *et al*., 2021). The methods of ecosystem services valuation can be broadly classified into direct market-based and none market-based approaches (Mulatu,1976; Sharma *et al*., 2021). Additionally, a benefit transfer approach has been widely used in literature to quantify ecosystem services based on the adopted value though is not an independent method of valuation (Barbier *et al*., 2009; Sharma *et al*., 2019; Biswa, 2023). Having this, there has been increased interest in the adaptation of the benefits transfer approach because the primary data collection of ecosystems is much more expensive in terms of costs, and time resources (Barbier *et al*., 2009; Liu *et al*., 2010; Silvis and Heide *et al*., 2013; Biswa, 2023). The adavantagoe of the benefit transfer technique is that it is quicker and cheaper than undertaking primary valuation (Watson,2007; Hegg, 2006).

2.1.2. Methods and Techniques of Ecosystem Services Valuation

The direct market-based valuation method comprises three techniques such as market price-based, production function, and cost-based approaches (Watson, 2007; Brander *et al*., 2010; Selivanov and Hlaváčková, 2021). A market price-based method uses the prices of ecosystem services that are traded on the markets based on what people are willing to pay for received ecosystem services or goods (Liu *et al*., 2010; Selivanov and Hlaváčková, 2021). In the technique of production function, researchers estimate how much a given ecosystem service contributes to the delivery of another service that is traded on the existing market (Hegg, 2006; Liu *et al*., 2010; Selivanov and Hlaváčková, 2021). For example, the value of ecosystem services on water purification can be estimated using the increased revenues from selling quality water on the market (Hegg, 2006; Watson, 2007; Selivanov and Hlaváčková, 2021). However, this method is criticized for different reasons. First, it is tough to understand the relationships between inputs and output services to quantify how much of the input services are used to produce certain products (Brander *et al*., 2010). Second, the interconnectivity and interdependencies of ecosystem services may increase the likelihood of double-counting of values of ecosystem services (Brander *et al*., 2010). Third, all ecosystem regulation functions cannot be directly related to the service intended to be valued (Hegg, 2006).

On the other hand, a cost-based valuation method assumes that the values of ecosystem services can be defined at least as avoided cost because of the services of ecosystem (Selivanov and Hlaváčková, 2021). This method includes damage avoided cost, mitigation (restoration) cost, replacement cost, and substitute costs (Watson, 2007; Brander *et al*., 2010; Selivanov and Hlaváčková, 2021). A damage cost avoided method is known as a preventive expenditure method or averting cost method that defines the value of ecosystem services as the costs associated with the hypothetical damage avoided because of the existence of the ecosystem services (Selivanov and Hlaváčková, 2021). The avoided cost method estimates costs that would have been incurred in the absence of ecosystem services (Brander *et al*., 2010; Liu *et al*., 2010). The mitigation cost (restoration cost method) assumes the value of certain ecosystem services is equal to the expenditure incurred for the mitigation of the negative effects that can be caused due to the degradation of the ecosystem such as a purification cost of polluted drinking water (Selivanov and Hlaváčková, 2021). The main difference between the mitigation and damage cost-avoided is that the damage cost avoidance is hypothetical (Selivanov and Hlaváčková, 2021).

The replacement cost method estimates the value of an ecosystem service as the costs associated with replacing what has been missed (Brander *et al*., 2010; Selivanov and Hlaváčková, 2021). For example, if the forest stand is cleared, the value of the forest stand will be equal to at least the costs of planting a new forest stand (Liu *et al*., 2010; Selivanov and Hlaváčková, 2021). The replacement cost method is heavily criticized as it is not known if individuals can incur the actual replacement costs or not (Watson, 2007). Moreover, it is challenging to exactly define what attributes should be restored as it is technically impossible to restore an ecosystem to its original state (Hegg, 2006). Finally, the substitute cost approach is the method used to estimate the cost of ecosystem services such as the incurred costs of building a water storage tank as a substitute for a lost lake (Selivanov and Hlaváčková, 2021).

The indirect market valuation method includes the revealed preference and stated preference to measure non-use values of ecosystem services in terms of monetary units (Haab and McConnell, 2002; Hegg, 2006; Selivanov and Hlaváčková, 2021). The revealed preference method assumes ecosystem service values can be revealed through observable consumer behaviors in which a given environmental good is indirectly purchased (Hadley *et al*., 2011; Selivanov and Hlaváčková, 2021). In line with this, the revealed preference assesses the relationship between the demand for marketable goods versus a preference for related non-marketable goods or services (Tinch *et al*., 2019). The most widely used revealed preference methods consist of travel cost (TCM), hedonic pricing, and averting behavior methods (Liu *et al*., 2010; Hadley *et al*., 2011; Hegg, 2006; Losonci, 2012; Silvis and Heide *et al*., 2013). The travel cost method is commonly used for the assessment of recreational ecosystem services (Selivanov and Hlaváčková, 2021). By estimating costs incurred by an individual during traveling and expenditures made on site including the cost of time (Hegg, 2006; Watson, 2007; Tinch *et al*., 2019). In this method, it implies that the value of a particular ecosystem service can be measured as the time spent and costs incurred to access recreational service (Liu *et al*., 2010; Selivanov and Hlaváčková, 2021). The hedonic pricing method compares the price of a non-markable ecosystem service with that of a similar price of marketable goods (Hegg, 2006; Watson, 2007; Brander *et al.,* 2010). For instance, the value of a lake ecosystem can be expressed considering the difference between the price of real estate located near a lake as compared to a similar real estate located far apart from the lake (Brander *et al*., 2010; Selivanov and Hlaváčková, 2021). The hedonic method only works if changes in services of the non-market good have an observable impact on the demand for a market good (Tinch *et al*., 2019). However, the hedonic method has a limitation as researchers determine which variables should be included in the price function where the missing variable may exist and influence the value of an asset (Hegg, 2006). The averting behavior valuation method is another approach that helps to estimate the value of ecosystem services by capturing costs that people are willing to pay to avoid a negative impact happening in the future (Mulatu,1976; Hegg, 2006; Tinch *et al*., 2019).

The stated preference method provides a hypothetical questionnaire to respondents to let people assign a value to improve the quality of environmental services (Haab and McConnell, 2002; Brander *et al*., 2010; Losonci, 2012; Selivanov and Hlaváčková, 2021). The most commonly used stated preference valuation method consists of contingent valuation (CV), choice valuation (CM), and choice experiment (Haab and McConnell, 2002; Brander *et al*., 2010; Hanley *et al*., 2019; Losonci, 2012; Hadley, *et al*., 2011).

The contingent valuation method uses questionnaire to ask people how much they would be willing to pay (WTP) to preserve or restore ecosystem services (Hegg, 2006; Brander *et al*., 2010; Hanley *et al*., 2019; Selivanov and Hlaváčková, 2021) or their willingness to accept (WTA) compensation for some change in ecological service (Hegg, 2006; Liu *et al*., 2010; Losonci, 2012). However, the contingent valuation method has an inherent limitation in the sense that the estimated value does not come from actual payments rather it comes from the responses of individuals to a hypothetical scenario (Brander *et al*., 2010; Losonci, 2012).

The choice valuation model or choice modeling (CM) attempts to model the decision process of an individual in a given context where individuals are given two or more alternatives with the shared attributes of services to be valued (Brander *et al*., 2010; Selivanov and Hlaváčková, 2021). In this method, the value of ecosystem services is assessed based on the respondent's WTP through a process of ecosystem service rating or choosing from the list of alternatives (Selivanov and Hlaváčková, 2021). Finally, the choice experiment (conjoint analysis) method is used to estimate the value of ecosystem services using a questionnaire in which respondents have to choose one option from the list of alternatives (Selivanov and Hlaváčková, 2021).

The benefit transfer approach is a technique in which an estimated ESV from available databases or study location can be used to estimate ESVs of the same ecosystem service at another similar location (Barbier *et al*., 2009; Liu *et al*., 2010; Costanza *et al*., 2014; Sharma *et al*., 2019). The high cost and length of time to undertake monetary valuation studies have led to an increased interest in the adaptation of the benefits transfer approach (Barbier *et al*., 2009; Liu *et al*., 2010; Silvis and Heide *et al*., 2013; Biswa, 2023). In this regard, the benefit transfer technique has the advantage of being quicker and cheaper than undertaking primary valuation (Watson,2007; Hegg, 2006). The benefit transfer technique could provide reliable estimates of the ESV if it is used correctly (Hegg, 2006). Otherwise, it introduces uncertainty if the original data is not accurate and the site does not share similar environmental characteristics (Watson, 2007; Barbier *et al.*, 2009). The above section has provided a sufficient theoretical understanding of the concept of ecosystem services valuation while the next section emphasizes spatial analysis of ecosystem attributes to create spatial distribution maps for ecological attributes.

2.2. Spatial dimension of ecological attributes in

Ecological research studies for long years have been dominated by nonspatial dimensions focusing on the statistical computation without considering spatial dimension of the attributes of the ecosystem (Pelissar *et al*., 2018; Cooper *et al*., 2023). This implies that the classical statistics implicitly assume that every un-sampled location can be represented by a mean value of the sample plots (Kalivas *et al*., 2013; Szmyt, and Stoyan, 2014). Nevertheless, the likelihood of having an equal mean value in every location does not exist in nature (Ifo *et al*., 2016; Thorson, 2016). In the meantime, the sample point data from the field may not provide spatial information on the attributes of interest while the spatial information helps to understand how the attributes are distributed in geographical space (Rebelo and Jones, 2009; Wang, 2013).

Progressively, the innovation of the spatial analysis techniques has brought a paradigm shift in providing a unique set of techniques (Fischer, 2006; Skidmore *et al*., 2011), particularly innovation of geographical information position (GPS) for the data collection (Li, 2008; Zhu *et al*., 2018; Zhang *et al*., 2023), and Geographic Information Systems (GIS) for spatial analysis (Vogiatzakis, 2003; Fortin and Dale, 2006; Wang, 2021; Lof *et al*., 2022). Spatial analysis involves spatial interpolation whereas spatial interpolation can be defined as the process of estimating values of the given attributes for un-sampled locations based on the known values from the sample locations (Webster and Oliver, 2007; Sciarrettam and Trematerra, 2014). The term spatial interpolation is often interchangeably used with the term spatial prediction (Zhu *et al*., 2018). Spatial prediction can be also defined as the technique of estimating the values of the object of interest at un-sampled locations based on data collected from sample plots (Liedtke, 2011; Wahab, 2017; Zhu *et al*., 2018).

The techniques of spatial interpolation have been conceivable by the circumstance that every object on Earth has location-based information such as geometric data (coordinates and topology) including attributes (Fedra, 1993; Haining, 2004; Fortin and Dale, 2006; Jiang, 2012). Geometric data comprise coordinates, area, and shape of a given object (Fedra, 1993; Paramasivam and Venkatramanan, 2019). Topology refers to the spatial relationships between adjacent features (Fedra, 1993; Haining, 2004); whereas attributes refer to values that provide information about the object (Haining, 2004). Therefore, spatial interpolation techniques have been commonly employed in research of various disciplines such as ecology, agronomy, meteorology, geosciences, and environmental management to produce continuous surface maps (Fortin and Dale, 2006; Hein, 2014: Sciarrettam and Trematerra, 2014; Li, 2022; Lof *et al.,* 2022).

Techniques of spatial analysis could be broadly categorized into deterministic and geostatistical techniques (Rossi *et al.* 1992; Fortin and Dale, 2006; Vargas-Guzman *et al.*, 2004). Deterministic techniques are flexible and easy to use as users can easily manipulate the required parameters (Hengl, 2007). The deterministic techniques do not require stringent assumptions because all relationships are defined by mathematical functions (Holling *et al.*, 1974; Hengl, 2007; Li and Heap, 2008; Steimer, 2017). The deterministic spatial analysis comprises nearest neighbor, Inverse Distance weight, and spline techniques (Hengl, 2007; Sciarrettam and Trematerra, 2014). In this review, emphasis is given to inverse distance weight (IDW) as it is more advanced than the remaining techniques (Husanoviæ and Malviæ,2014). In the process of interpolation, the IDW assigns more weights to a point closer to the processing point than the points further away (Fortin and Dale, 2006). The IDW technique provides flexibility for a user to control the mathematical form of a weighting function and the number of points included in the estimation by indicating the radius of a circle around that location (Husanoviæ and Malviæ,2014). This implies the specified number of points within a given radius can determine the output value of each location (Paramasivam and Venkatramanan, 2019).

In the second category, the geostatistical technique as the branch of applied statistics has become an innovative tool to provide information on un-sampled locations predicting known data to simulate a surface map to enable better visualization of the spatial variability (Payna *et al*., 1999; Neves *et al*., 2010; Klobuar and Pernar, 2012; Kalivas *et al*., 2013). Geostatistics comprises semivariogram and kriging (Hengl, 2007; Olea, 2009). The semivariogram helps to characterize the spatial variabilities between paired points based on the theory of regionalized variables including the concept of spatial dependency (Rossi *et al*., 1992; Lesschen *et al*., 2005; Zawadzki *et al*., 2005). The concept of regionalized variable assumes that the relationship between paired random variables is stationary with constant mean and variance across separating distance and direction **(**Payna, *et al*., 1999; Baba *et al*., 2014; Klobuar and Pernar, 2012**;** Getis, 2009; Steimer, 2017). This means that data at unsampled locations can have a likelihood of being similar to data collected from the given sample locations (Husanoviæ and Malviæ,2014). Spatial dependency which is known as spatial autocorrelation states that closer objectives are more similar than those apart from each other (Egendre, 1993; Fortin *et al*., 2002; Cruz-Cárdenas *et al*., 2014). The absence of spatial dependency implies the rejection of the given data to not carry out the spatial analysis (Lesschen *et al*., 2005; Getis, 2009; Steimer, 2017).

With these all, the semivariogram technique estimates values between measured points considering a separation distance and direction between those points. Subsequently, it describes the autocorrelation distance that puts a radius of influence on measurement data at the given points **(**Ye, 2008; Samui and Sitharam, 2011; Klobuar and Pernar, 2012). The processes of semivariogram lead to the step of kriging to produce the spatial map of a given attribute (Husanoviæ and Malviæ,2014). Kriging is similar to the IDW in assigning more weight to the closer points (Fortin and Dale, 2006; Paramasivam and Venkatramanan, 2019). A prediction error of the kriging technique can be assessed using a cross-validation process (Relethford, 2008; Samui, and Sitharam 2011; Baba *et al*., 2014; Al-Mashagbah *et al*., 2017). In the process of cross-validation, one sample is removed from the dataset and a value in its location is predicted using information on the remaining observations. This process continues to the second, third, and other samples in the database and averaging a difference between predicted and observed values (Relethford, 2008; Kalivas e*t al*., 2013; Sciarrettam and Trematerra, 2014). The deterministic and geostatistical techniques in spatial analysis do not consider the impacts of environmental factors on biological organisms. It simply focuses on describing the spatial distribution of the organism without considering influencing factors while the gap can be addressed using ecological models. In light of this, the following section mainly emphasizes in description of the concept of models, the types of models, and how models can disentangle the interactions between organism and environmental factors.

2.3. Models and modeling in environmental research and resources management

2.3.1. Ecological Models

A model is defined as an abstraction of reality (Jeffers, 1988; Defries *et al*., 2005; Hadjibiros, 2014; Tenedório and Rocha, 2018; Wang, 2021); whereas the term modeling refers to the process of creating an abstraction of reality (Fedra,1993; Kumar, 2021; Legesse *et al*., 2022). Models have been widely applied in many fields such as ecology, agriculture, wildlife conservation, hydrology, oceanography, and climate change (Bennett *et al*., 2010; Prasad and Tiwa,2016; Wang, 2021). Models provide an opportunity for researchers to simulate ecological ideas that may not be possible to test in the field for reasons of logistic, political, ethical, or financial constraints (Jackson *et al*., 2010; Wang, 2021).

There are numerous complex interactions among ecosystem components ranging from the individual population to communities and even the entire ecosystem (Humphries and Baron, 2001). For this reason, ecological models are required to disentangle these complex interactions and to predict the outcomes of interactions between elements of an ecosystem (Tenedório and Rocha, 2018; Geary *et al*., 2019). This indicates that ecological models can produce the spatial distribution of biological organisms by analyzing relationships between biological and environmental variables (Moreno, 2007; Jopp *et al*., 2011; Meier, 2011; Tenedório and Rocha, 2018; Geary *et al*., 2019).

Ecological models can be broadly classified into two analytical and simulation-based models. The analytical model is known as the correlative or empirical model whereas simulation models are known as a numerical or process-based model (Wang, 2021). Analytical models examine the correlative relationships between dependent and independent variables to predict the outcomes of interactions (Haining, 2004; Zare, 2010; Pallaris, 1998; Fortunel *et al*., 2014). For instance, the prediction of species suitability can be done by associating the correlation between the known occurrence of species data with the suites of environmental variables (Soberón and Peterson, 2005; Pearson, 2007, Miller, 2010; Fournier *et al*., 2017). In line with this, most ecological models depend on the availability of measured values of dependent and independent variables (Meier, 2011; Wang, 2013). A dependent variable is a value of the given attribute subjected to the modeling process while the independent variables are factors that influence the state of the dependent variable (Jiang, 2012). The dependent variable can be also known as a response or predictor variable while the independent variables are known as explanatory (Jiang, 2012; Henderson *et al*., 2017).

Analytical models can be categorized into static and dynamic where the static models are constant over time but the dynamic models show changing conditions along the time horizon (Pearson, 2007). Models in the simulation category mainly involve simulating the physical or biological processes that explicitly describe the behavior of a system (Wang, 2021). For instance, the simulation models may simulate a process of how water, solar radiation, and temperature affect the rate of photosynthesis including how produced biomass can be allocated to different parts of the plant (Wang, 2021). However, it is challenging to obtain physiological responses of species to such environmental factors (Soberón and Peterson, 2005; Pearson, 2007).

The modeling process in ecology mainly passes through four steps that require a proper understanding (Peng *et al*., 2017). These four steps include (1) the collection of data on biological organisms which are dependent variables, (2) the identification of environmental factors or independent variables, (3) the selection of model types, and (4) the validation of model accuracy (Austin, 2007; Newbold, 2010). The collection of biological data in the first step is concerned with getting biological data such as species occurrence (Pearson, 2007); species abundance (Young, 2010); and carbon stock (Bedane *et al*., 2022) at an appropriate spatial extent and resolution (Vogiatzakis, 2003; Pearson, 2007; Getz *et al*., 2017). The terms extent and resolution are very important while an extent refers to the spatial and temporal scales at which ecosystem components can occur to produce realistic outputs (Chapin *et al*., 2011; Sing *et al*., 2015; Wulder *et al*., 2024). On the other hand, the term resolution refers to the size of the sample unit at which biological data can be collected (Austin, 2007; Pearson, 2007; Fournier *et al*., 2017). Organisms can perform at various spatial resolutions such as a resolution that fits the data collection of ants cannot be matched with data collection for elephants (Latimer, *et al*., 2007; Pearson, 2007).

The second step concerns the identification of independent variables that influence dependent variables (Nguyen *et al*., 2015; Hill *et al*., 2016; Mi *et al*., 2017; Rahman *et al*., 2021). A proper understanding of the nature of independent variables helps to select the best predictors at the appropriate scales to produce reliable model outputs. Explanatory variables in plant communities may include sunlight, water, and nutrients that may limit or enhance the growth and survival of plant species at different geographical scales (Getaneh *et al*., 2023). Temperature and moisture favor the growth of species abundance and species richness at a broader scale (Crowther *et al*., 2015; Rahman *et al*., 2021). The influences of topographic factors are more evident at a moderate scale (Rahman *et al*., 2021), whereas the impact of biotic factors is more profound locally at a stand level (Jafari *et al.*, 2013). Despite these, it is challenging to establish a distinct boundary between the impacts of direct and indirect predictors (Pearson, 2007). For instance, temperature and rainfall are considered the direct predictors as these variables can be consumed by plant species directly (Austin, 2007; Pearson, 2007), whereas elevation is an indirect predictor because the elevation is not directly consumed by plants but indirectly affects species distribution by modifying the condition of temperature and precipitation (Austin, 2007). It is also important to consider the impact of human activity as an explanatory variable because human activity can influence the distribution of biological organisms by destroying habitats or introducing new species to new locations (Zimmermann *et al*., 2010; Meier, 2011).

In the third step of the modeling process, the selection of an appropriate model is an important step among various models that have been developed over the past couple of decades in line with the proliferation of digital databases, innovation of GIS, and remote sensing data (Defries *et al*., 2005; Fischer, 2006; Skidmore *et al*., 2011; Hao, 2019). The Generalized Linear Model (GLM), Random Forest (RF), and Natural Neural Networks (ANNs) are the most common modeling techniques that have been widely used to model complex and multidimensional ecological data (Young, 2010; Wang, 2013; Aksu *et al*., 2019; Yudaputra *et al.*, 2019; Lof *et al.*, 2022). The GLM consists of three components while the first component includes a dependent variable that follows the distribution belonging to the family of exponential distribution functions such as binomial, Poisson, and gamma distributions (Newbold, 2010). GLMs deal with non-normally distributed predictors and overcome the assumption of regular linear regression models (Guisan *et al*., 2002). The second component is the independent variables that exert influence on dependent variables. The third is a link function that connects dependent and independent) variables (Newbold, 2010). GLM is more flexible and better suited to analyze ecological relationships which is poorly represented by the classical Gaussian distribution (Guisan *et al*., 2002). The outputs of the GLM can be also easily interpreted using a coefficient of determination to examine the impact of independent variables on a given dependent variable (Newbold, 2010).

Random Forest (RF) is an ensemble learning technique developed based on the combination of a large set of decision trees to conduct regression and classification modeling (Vincenzia *et al*., 2011; Zhang *et al*., 2019). The technique of regression trees can be used to model the continuous data type while the classification technique is applied to categorical data (Janitza and Hornung, 2018; Sahragard, *et al.*, 2018). The random forest algorithm performs well for ecological modeling for several reasons. First, it is non-parametric and flexible in handling explanatory or independent variables. Second, it can handle non-linear relationships between the dependent and independent variables (Henderson *et al*., 2017). Third, it does not assume the normal distribution of a dependent variable; and is efficient in processing multidimensional and complex ecological interactions (Cutler *et al*., 2007; Vincenzia, 2011). The random Forest algorithm can also help to identify the magnitude of the influence of independent variables on a dependent variable (Sahragard, 2018).

Artificial neural networks (ANNs) are another important machine-learning technique that imitates the learning system of the human brain (Williams, 2003; Kukreja *et al*., 2016; Aksu *et al*., 2019). The ANNs have been applied in ecology since the early 1990s (Williams, 2003). The architecture of the ANN model consists of three layers such as input, hidden, and output which are built of various neurons or nodes (Aksu *et al*., 2019; Chen *et al*., 2022). The input layer contains the input variables that influence the result of the model, while the output layer holds the results of a model (Aksu *et al*., 2019). The hidden layer lies in between the input and output layers and commences different complex computations (Kukreja *et al*., 2016; Chen *et al*., 2022). The ANNs learn patterns of the relationships between response and input data to produce a model under the process of a black box approach which is not somehow easier to understand the internal process of a modeling exercise (Williams, 2003). Apart from this limitation, the ANNs are useful for producing quality prediction outputs using both regression and classification techniques (Kukreja *et al*., 2016; Aksu *et al*., 2019; Yudaputra *et al*., 2019).

The fourth step concerns validating an accuracy of a model as spatial modeling cannot happen without errors (Pearson, 2007; Miller, 2010; Skidmore *et al*., 2011; Wang, 2021). Models never produce a perfect copy of reality rather than tend to approximate the reality (Holling *et al*., 1974). This is the reason why model validation is required to understand how much a model prediction approaches the given reality either to accept or reject an output of a model (Kidane *et al*., 2012; Wang, 2021). In line with this, understanding of causes of error can be helpful to minimize risks of error. The first source of error can occur as the spatial prediction is often done for larger areas using the sample data collected from relatively small locations. Secondly, heterogeneity of sampling intensity may cause biases where sampling is not evenly distributed. Thirdly, biases can be introduced when the data are collected only from easily accessible locations (Latimer, *et al*., 2007; Pearson, 2007; Wisz *et al.*, 2008). The fourth possible error might be related to sampling size. For instance, a limited sampling intensity in biological organisms can affect mainly the abundance of rare species leading to false absence while species is the area (Wang, 2013). Having a large sample size on the other hand can be constrained by finance, time, and human resources (Pallaris, 1998; Stockwell and Peterson, 2002; Rebelo and Jones, 2009; Wang, 2013). Recognizing the possibility of the happening of errors, researchers always specify a model accuracy to clarify a degree to how much-predicted value is closer to the real value of fostering trust in policymakers and end users (Pearson, 2007; Miller, 2010; Wang, 2021; Lof *et al.* 2022).

2.3.2. Soil erosion modeling

Soils support human life by providing diverse ecosystem services such as maintaining soil fertility, food production, and carbon storage (Mantel and Schul., 2014; Pierzynski *et al*., 2017; Rodrigues *et al*., 2021). Soil is considered a natural capital that is crucially required to maintain healthy conditions of ecosystem structures and functions to ensure a sustainable flow of ecosystem services (Adhikari and Hartemink, 2016; Pierzynski *et al*., 2017; Burkhard *et al*.,2019; Rodrigues *et al*., 2021). Nevertheless, soil erosion has become one of the most serious environmental problems in the world threatening agriculture productivity and ecological sustainability (Jahun *et al*., 2015; Prasad and Tiwa,2016; Igwe *et al*., 2017). More than one million ha of land has been globally affected by water erosion (Thomas *et al*., 2018) ending with a loss of 75 billion tons of fertile soil from the agricultural fields per annum (Gong *et al*., 2022). A loss of 25 to 40 billion tons of surface soil has globally resulted in an economic loss of $400 billion per year (Das *et al*., 2021). In Ethiopia, it has been reported that 1.9 billion metric tons of fertile soil have been lost annually from the highlands of the country (Tadesse *et al*., 2017). This soil loss has severely affected the state of soil productivity, habitat quality, food security, water availability, and biodiversity which implies negative consequences on environmental, economic, and social developments (Wang *et al*., 2016; Fayas *et al*., 2019; Gong *et al*.,2022).

Soil erosion mainly involves soil detachment, transport, and deposition stages which can take place at various spatiotemporal scales (Jahun *et al*., 2015; Burkhard *et al*.,2019). This process leads to the formation of splash, sheet, rill, and gully erosion types (Prasad and Tiwa,2016; Abdulkareem *et al*., 2021). The splash type of erosion is caused by the impact of rain droplets on the soil surface when raindrops fall on unprotected soil and displace soil particles (Bonthagorla *et al*., 2022). The sheet erosion is a separation of topsoil in the form of thin sheets and transported downward slope by overland flow or rain drop (Prasad and Tiwa,2016; Abdulkareem *et al*., 202; Bonthagorla *et al*., 2022). Sheet erosion by overland water flow can be developed into the form of small channels known as rills, though, the rill erosion does not have continuous patterns as the rills are formed in one storm and disappear before happing of another storm (Bonthagorla *et al*., 2022). Finally, gully erosion is the modified form of rill erosion and it occurs when runoff accumulates and flows rapidly and forcefully to detach and transfer soil particles by creating deep and wide gorges depending on the strength of soil parental materials (Prasad and Tiwa,2016; Bonthagorla *et al*., 2022).

The pressing problem of soil erosion has necessitated the estimation of the extent of soil loss and the mapping of critical erosion-prone areas using different modeling techniques (Kolli *et al*., 2021; Gong *et al*., 2022). The soil erosion models are useful for estimating soil loss from different ecosystems to quantify the impact of soil loss on social, economic, and environmental dimensions (Igwe *et al*., 2017; Abdulkareem *et al*., 2021), considering that the outputs of the erosion models are helpful for decision-makers to commence soil conservation measures (Fayas *et al*.,2019; Negese *et al*., 2020). Therefore, researchers have developed several soil-erosion models based on the premises of impacts of climate, soil characteristics, vegetation type, and topography on soil losses (Borrelli *et al*., 2021; Wagari and Tamiru, 2021).

Soil erosion models are broadly classified into three categories depending on the types of input, types of intended output, the scale of analysis, types of algorithms, and underlying principle of models (Santos *et al*., 1998; Jahun *et al*., 2015; Borrelli *et al*., 2021; Abdulkareem *et al*., 2021). The empirical soil erosion model comprises the Universal Soil Loss Equation (USLE), and its derivates such as the Modified Universal Soil Loss Equation (MUSLE), and (RUSLE) Revised Universal Soil Loss Equation (Igwe *et al*., 2017; Abdulkareem *et al*., 2021). Empirical models are the most widely used class of erosion models because of their simplicity and limited data requirement at the catchment scale (Santos *et al*., 1998; Prasad and Tiwa, 2016; Igwe *et al*., 2017). These empirical models operate based on data gathered from the field, and mostly standard runoff plots on uniform slopes (Santos *et a*l., 1998; Prasad and Tiwa, 2016). The main limitation of empirical models is limited to the area where they have been developed, and not applicability outside the boundary where it has been developed (Prasad and Tiwa, 2016; Igwe *et al*., 2017), while the adaptation of empirical models to a new environment is costly in terms of capital and time (Santos *et al*., 1998).

The Universal Soil Loss Equation (USLE) model is an empirical model developed by the United States Department of Agriculture (USDA) in the 1970s to estimate soil loss from agricultural fields (Wischmeier and Smith,1965) and it was improved later in the 1970s (Wischmeier & Smith, 1978). USLE is the most widely used model for predicting water erosion hazards as it is simple to use with low data requirements (Mantel and Schulp, 2013; Jahun *et al*., 2015; Burkhard *et al*.,2019). With a limitation to produce less reliable results with increasing the size of the study area under specific erosion threats such as gully erosion (Burkhard *et al*.,2019).

Progressively, USLE model was improved and replaced by the Revised Universal Soil Loss Equation (RUSLE) in the late 1970s (Renard *et al*., 1997; Kim, 2006) to estimate a mean annual soil loss using five soil erosion driving factors (Gong *et al*., 2022; Luvai *et al*., 2022); that includes rainfall erosivity, soil erodibility, land cover management, support practice, and LS value (Kayet *et al*., 2018; Phinzi *et al*., 2019). RUSLE model has been widely used in research for its well-established use of Geographic Information Systems (GIS), and data of remote sensing technologies (Jahun *et al*., 2015; Borrelli *et al*., 2021; Wagari and Tamiru, 2021). The integration of the RUSLE model with GIS tools is highly useful for quantifying soil losses and producing the soil erosion severity map for better understanding (Abera, 2014; Ganasri and Ramesh, 2016; Wagari and Tamiru,2021). The innovation of remote sensing technologies has provided a better opportunity to overcome the challenge of time-consuming and expensive ways of input data collection on soil erosion-causing factors (Ganasri and Ramesh, 2016; Tadesse *et al*., 2017; Fu *et al*., 2021; Wagari and Tamiru,2021). On the other hand, the RUSEL has two limitations. The first is that the RUSLE model estimates soil loss comes only from the sheet and rill erosions but cannot estimate a soil loss associated with gully erosion (Abera, 2014; Panagos *et al*., 2015; Prasad and Tiwa,2016; Phinzi *et al*., 2019). Second, the RUSLE model estimates a gross soil loss without excluding the amount of soil deposited in the catchment area (Thomas 2018; Alewell *et al*., 2019). However, the RUSLE model has been identified as a simple and robust model to estimate soil loss at different spatial scales (Thomas, 2018; Alewell *et al*., 2019; Fayas *et al*., 2019; Phinzi *et al*., 2019).

Physically-based models provide an understanding of fundamental sediment-producing processes with the capability to access the spatial and temporal variations of the sedimentation, transportation, and deposition processes in the landscape under a wide range of land use, soil, and climatic conditions (Prasad and Tiwa, 2016; Igwe *et al*., 2017). In this regard, the physical-based models are scientifically robust and flexible in handling input and output data with the proper understanding of the physical soil-causing processes (Igwe *et al*., 2017). For instance, the Water Erosion Prediction Project (WEPP) was developed in 1995 to predict soil erosion under various features of a landscape (Prasad and Tiwa,2016; Igwe *et al*., 2017). With this quality, it has been indicated in literature that soil erosion modeling has been shifted from empirical models towards the physically based model which is much more complex but provides good results (Santos *et al*., 1998). The limitation of the physical-based model is that it requires intensive input data with high-resolution spatial and temporal resolutions while these data are not often readily available (Prasad and Tiwa,2016).

The last type of soil erosion model is a conceptual model and it can be also known as the Parametric Model where AGNPS is a good example of this model (Prasad and Tiwa,2016). This model is based on the empirical and physical-based models to provide qualitative and quantitative processes in the catchment (Prasad and Tiwa,2016). In this, sediment-producing factors such as rainfall and runoff are treated as inputs in this model while the sediment yield is an output of the model (Igwe *et al.*, 2017). Its limitation is also related to its requirement for large meteorological and hydrological data which is changing to get those data (Prasad and Tiwa,2016). Having all these, the below heading depicts the roles of forest ecosystems in mitigating the effects of climate change and biodiversity conservation. This is to provide background on how forest attributes such as ACD and species attributes are important to characterize the condition of the forest ecosystem.

2.4. Forest Ecosystem Conditions in climate regulation and biodiversity Conservation

Forests are complex systems that provide various ecological benefits for the well-being of humankind (Szmyt, and Stoyan, 2014; Naidu and Kumary, 2016). Global forests can act both as a sink of carbon and carbon emitters (Chapin *et al*., 2011; Addi *et al*., 2019). Forests sequester carbon dioxide from the atmosphere and convert it to plant biomass (Chapin *et al*., 2011). The global forests further offset about 60% of carbon emissions that are emitted from the consumption of global fossil fuels (Zhang *et al*., 2016). FAOb (2010) has reported that the global forests are estimated to store about 289 Gt of carbon which is approximately 80% of the global terrestrial biomass. Of the global carbon storage, 44% is stored in the aboveground living biomass, 11% in the dead wood, and 45% in the forest soil (Addi *et al*., 2019). This shows how aboveground biomass is an important pool of carbon stock (Thokchom and Yadava, 2017). The tropical forest ecosystem specifically is estimated to store 460 billion tons of carbon in the forest biomass (Alvarez-Davila *et al*., 2017); and tropical forests account for 46% of the world's carbon storage (Addi *et al*., 2019).

Contrastingly, deforestation in tropical forests has resulted in the release of 1.7 billion tons of carbon dioxide emission to the atmosphere (Mwakisunga *et al*., 2012). Deforestation has globally emitted 5.9 GtCO2 in a year and become the second source of carbon emission next to fossil fuels (Gorte and Sheikh, 2010; Neba, 2013). Recognizing the role of forests in carbon regulation, the forest has become an important global agenda in international climate change negotiations such as reducing carbon emissions from deforestation and forest degradation (REDD) under the umbrella of the UNFCCC to create incentive mechanisms for developing nations to ensure sustainable forest management (Neba, 2013; Dissani *et al*., 2021). The global attention to forests has motivated researchers to quantify the dynamics of forest carbon stock because the effectiveness of the REDD mechanism depends on the availability of adequate knowledge and understanding (Nchimbi, 2021; Teferi *et al*., 2021).

Apart from the role of carbon regulation, forests are the richest biological organisms on the Earth and are considered a bank of biodiversity (Neves *et al*., 2010; Ahani and Jalilvand, 2013). Forests harbor more than half of the world's known terrestrial plant and animal species (Morales-Hidalgo *et al*., 2015; Pauli, 2010; Hofsvang, 2014). The tropical forest alone has been estimated to host 40,000 to 53,000 species (Labrière, *et al*., 2016). In this regard, tropical forest is assumed to serve as habitats for over half of the world's known terrestrial plant and animal species (Morales-Hidalgo *et al*., 2015; Pauli, 2010; Hofsvang, 2014); whereas the area of tropical forest accounts for 52% of the global forest (Ifo *et al*., 2016). Ethiopia is one of the tropical countries that has been identified as the origin of biodiversity and comprising 6500 and 7000 higher plant species with 12% endemic (Kflay and Kitessa, 214). Ethiopia is also one of the top 25 biodiversity-rich countries in the world and hosts two of 34 global biodiversity hotspot areas namely the Eastern Afromontane and the Horn of Africa hotspots (Amenu, 2016).

Despite that forest provides benefits of regulating forest carbon dynamics and biodiversity, human activities have induced profound impacts on the forest ecosystem (Neba, 2013; Kumari *et al*., 2021; Maes *et al*., 2015; Patarkalashvili, 2017). Deforestation has reduced the area of global forests from 4,128 million to 3,999 million hectares between 1990 and 2015 (FAO, 2015). Similarly, deforestation has resulted in a loss of forest cover and species extinction around the globe (Neves *et al*., 2010; Oindo,2011; Amenu, 2016). This alarming situation has received international attention to ratification of the Convention on Biological Diversity (CBD) in 1992 in Rio de Janeiro demanding to produce knowledge and information update on the protected areas to strengthen concerted global biodiversity conservation efforts (Scheller and Mladenoff, 2007; Neves *et al*., 2010; Reyers *et al*., 2010; Jafari *et al*., 2013).

Conversely, information on forest ecosytem has been characterized by a lack of spatial information (Pelissar *et al*., 2018; Cooper *et al.*, 2023); because research studies in the past have mainly focused on a statistical analysis that does not consider spatial information (Neves *et al.*, 2010; Kalivas *et al.*, 2013; Lichtenstern, 2013). The conventional statistics implicitly assume every un-sampled location is represented by the mean value of the sample locations (Kalivas *et al*., 2013; Szmyt, and Stoyan, 2014); but the likelihood of having an equal mean at every location cannot exist in nature (Ifo *et al.*, 2016; Thorson, 2016). This indicates how it has been challenging to understand the spatial distribution of forest attributes in geographical space (Redowan, 2015; Ifo *et al.*, 2016; Wulder *et al*., 2024).

Recognizing this limitation, there has been growing interest in how to measure the spatial distribution of forest attributes such as the above-ground carbon and species diversity (Amenu, 2016; Kumar and Mina, 2021). Ecologists have employed species diversity indices to provide quantitative measures of species in a given area to understand the condition of biodiversity (Kumar and Mina, 2021; Kitikidou *et al*., 2024); and to compare species diversity in different ecosystems (Help *et al.*, 2001; Gao *et al*., 2014; Amenu, 2016). The species diversity index is a mathematical expression that combines species richness and evenness (Mcdonald *et al*., 2010; Kumar and Mina, 2021). Species richness refers to the total number of species in the community (Help *et al*., 1998; Kent, 2011; Perng *et al*., 2024); whereas species evenness is a relative abundance of individuals among species in a given habitat (Kumar and Mina, 2021). Species evenness tends to increase when all species in a sample have equal abundance, otherwise, it becomes low as there is dominance by a few species (Help *et al*., 1998; Hamilton, 2005; Oindo,2011; Kumar and Mina, 2021).

The Shannon-Wiener Index (H) and Simpson Index (D) are among the non-parametric indices widely used in literature (Ozcelik *et al*., 2008; Faridah-Hanum *et al*., 2010; Morris *et al*., 2014; Feroz, *et al*., 2015). The Shannon-Wiener index gives more weight to rare species in the sample (Kent, 2011; Merganič *et al*., 2012; Kumar and Mina, 2021). Contrastingly, the Simpson index puts more weight on the common species (Merganič *et al*., 2012; Kumar and Mina, 2021). The index of the Shannon-Weiner increases with the number of species in the community and can reach a very large number theoretically but it does not seem to exceed five in practical cases of biological diversity (Faridah-Hanum, *et al*., 2010). A habitat with an index of four and above can be considered extraordinarily biodiversity-rich (Lakićević and Srđević, 2018). The species indices can be mapped using different modeling techniques to provide spatial distributions (Redowan, 2015). The next section provides a conceptual framework that guides how this research study has been conducted.

2.5. Conceptual framework of this study

The conceptual framework helps to organize steps, procedures, and assumptions to be considered in addressing the intended purposes of the research study (Jackson *et al*., 2010). It creates a clear understanding of the processes of research from the initiation to the completion stages (Pittroff and Pedersen, 2005). The conceptual framework is particularly helpful in guiding the study of ecosystem assessment. The ecosystem assessment in this study has focused on examining the structural and functional components of the ecosystem because the status of these components is important to reflect the conditions of ecosystems (Humphries and Baron, 2001). The assessment of these components can be conducted at different spatial scales with the understanding that ecosystems exhibit variation at various spatial scales (Hadjibiros, 2014; Czúcz *et al*., 2021). In line with this premise, Fig 1 shows that the three research topics have been covered at a broader scale of the Bale Mountains Ecoregion (BMER). These include valuation of ecosystem services, erosion modeling, and spatial analysis of ACD and woody species diversity. The remaining two research topics have been considered at the local scale of Harana Forest where the topics have included modeling of the impacts of biophysical factors on the ACD and abundances of the selected woody species.

The ecosystem assessment at the broader scale of this study has mainly focused on examining the transition of ecosystem area among different ecosystems and valuation of ecosystem services based on Landsat imagery data of the years 2010, 2015, and 2022. The use of Landsat image is fundamentally important for the reason that Landsat image provides quality data over large parts of the Earth (Maes *et al*., 2015; Ridwan *et al*., 2018; Gomez-Fern Mendez *et al*., 2024). The term extent refers to the surface area of an ecosystem that is derived from remote sensing data (Defries *et al*., 2005; Fetene, 2024). The extent is important because the capacity of ecosystems to provide ecosystem services depends on the surface areas of the ecosystem (Lof *et al.* 2022).

Transition analysis has been conducted using Tera software to determine the transition of areas among different ecosystems along time differences. The dynamics in the area can show a change in ecosystem structure that could bring negative implications on ecosystem function and ecosystem services as the functional roles rely on the stability of the structural component of the ecosystem (Sheate *et al*., 2012; Zulian *et al*., 2018). Followingly, ecosystem services valuation has been applied to differentiate the ecosystems while the valuation technique is important to describe the condition of a given ecosystem in monetary value (Maes *et al*., 2015; Losonci, 2012; Schröter, 2015; Sharma *et al*., 2021). Technically, the valuation of ecosystem services is done by multiplying the area of each ecosystem at a given year with a coefficient of specific ecosystem services (ESV) for the identified ecosystems in the periods of 2010, 2015, and 2022. The valuation has been done for each ecosystem type along four bundles of ecosystem services such as provisioning, regulatory, cultural, and provisioning services (MEA, 2005). The total ESV of each ecosystem is a sum of the ESV of specific ecosystem services in each ecosystem whereas a sum of ESVs of all ecosystems provides a total ESV in USD for the specified year. The difference in the total ESV between the two periods is important to show a gain or loss in ESV. Information on gain and loss is helpful for decision-makers to make informed decisions (Czúcz *et al*., 2021).

The impact of soil erosion on the identified ecosystems in the BMER has been examined at the broader scale of the BMER by integrating the RUSLE erosion model with the ArcGIS map to identify vulnerabilities of ecosystems to soil risks. The RUSEL model consists of five erosion-causing factors that are known as model inputs. These include rainfall erosivity, soil erodibility, land cover, land management practices, and LS which is the combined effect of the slope length and slope gradients. These factors could be accessed from publications and online open resources. The final outputs of the RUSEL model in this study have included average soil loss in tons/ha/year and maps to show the spatial distribution of soil erosion in 2010 and 2022.

In addition to Landsat imagery, field data collection can be required because a coarse resolution of Landsat images cannot be sufficient to capture the detailed attributes of the structural component of a given ecosystem (Franklin *et al*., 2003). Nevertheless, field data collection is often time-consuming, costly, and labor-intensive (Pittroff and Pedersen, 2005) and it is not often possible to collect data from all parts of ecosystems while the ecosystem is complex and often characterized by a mosaic of different ecosystems such as forests, woodland, wetlands, grassland, and farmland (Wang, 2021; Lof *et al*., 2022; Zhang *et al*., 2023). In light of this complexity, ecosystem assessment might be limited to a single element of an ecosystem or a holistic assessment depending on the availability of financial resources and time (Zhang *et al*., 2023). This indicates that the complex nature of ecosystems can force researchers to define the scope of ecosystem assessment (Lof *et al,* 2022). Keeping this in mind, data collection in this study is limited to forest ecosystems to conduct the spatial analysis of forest attributes at the broader scale and the modeling of forest attributes at the local scale. The selection of forest ecosystems could be justifiable as the forest ecosystem provides immense contributions to climate regulation and biodiversity conservation (Binder *et al*. 2017; Gomez-Fern Mendez *et al*., 2024).

Simultaneously, the forest ecosystem also consists of plenty of attributes but it can be challenging to deal with all attributes (Wang, 2021). Recognizing this challenge, the scope of spatial analysis has been limited to the ACD and species indices while producing their spatial distribution maps using semivariogram and Kriging techniques. In such cases, values of each map have been grouped into six classes using the techniques of ArcGIS to estimate areas of forest land associated with the given classes of ACD and species indices. Concerning the prediction errors, the kriging technique automatically generated the magnitude of errors using the crosstab.

Finally, Random forest modeling has been exercised to examine the impacts of biophysical factors on the spatial distributions of ACD because understanding the impacts of biophysical factors on ACD is important to strengthen sustainable management of forest carbon dynamics (Getaneh *et al*., 2023). Correspondingly, the interactions of the abundance of tree species with abiotic factors were subjected to modeling using the RF, GLM, and ANNs modeling techniques at the scale of the Harana Forest ecosystem. In these modeling processes, 70% of the dataset has been used for training while 30% for validation of the accuracy of each model. The RF is used to produce the spatial distribution map of the ACD and species diversity indices. Moreover, the RF has provided values that determine the strength of each independent factor in influencing the dependent variable. This strength is explained in terms of a percent increase in mean squared errors (%IncMSE) while increasing in %IncMSE shows a higher strength (Scarnati *et al*., 2009; Kapwata and Gebreslasie, 2016). The performance of the GLM model is assessed using a coefficient of determination (R^2) whereas a higher R^2 indicates that the given independent variable can better explain variation in a response variable (Kapwata and Gebreslasie, 2016; Chen *et al*., 2022). The strength of independent variables in the ANNs can be measured using the Olden values to identify the strengths of the independent variable on the dependent variable based on the magnitude and direction of the effects (Olden and Jackson, 2002).

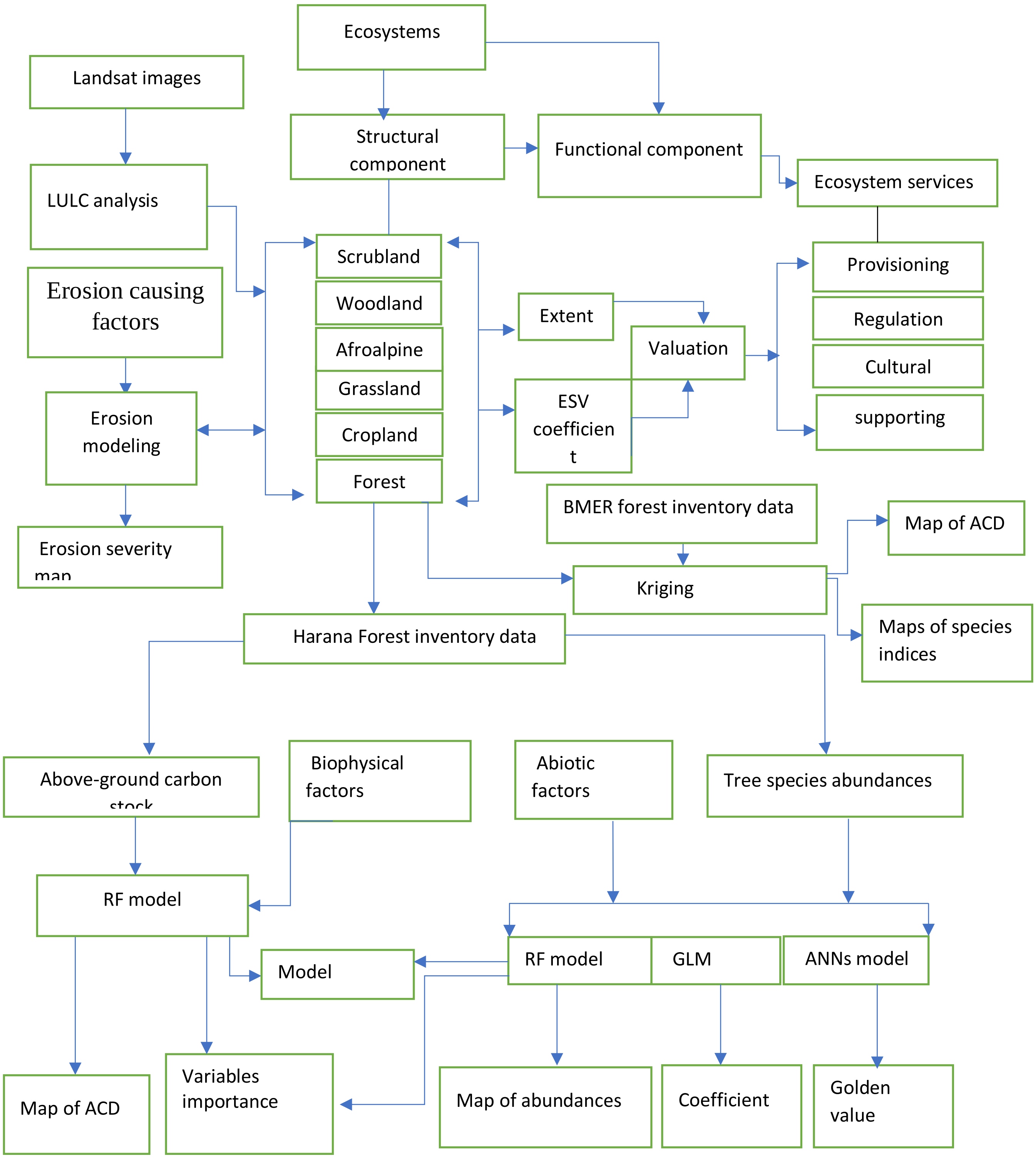

Figure 1: Own developed conceptual framework for assessing the conditions of the ecosystems

CHAPTERS 3: MATERIALS AND METHODS

3.1. Description of the study area

Bale Mountains Ecoregion (BMER) is geographically located between 5°30' 54'' N to 6° 52' 55''N and 39° 37' 52'' E to 40° 56' 00'' E (Fig 2). The BMER is administratively located in the Oromia National Regional State in Ethiopia. BMER comprises 16 administrative units known as Woredas: Adaba, Agarfa, Goba, Sinana, Berbere, Dinsho, Dodola, Gasera, Gololcha, Kokosa, Goro, Mada Walabu, Delo Mena, Harenna Bulluk, Nensebo, and Guradhamole with the total area of 37,674 km^2 (Hailemariam *et al*., 2015).

The central parts of the BMER cover a large plateau known as Senate that ranges with an elevation above 3000 m asl including (Tullu Dimtu) which is the second-highest peak in Ethiopia with 4377 m asl (OFWE *et al*., 2014). Senate is the largest Afro-alpine plateau in the continent of Africa (Kefale *et al*., 2021; Williams *et al*., 2005) where it is a habitat of Afro-alpine vegetation and also serves as a source of 40 springs that feed into five major rivers, Wabishebele, Genale, Dumel, Web, and Welmel (OFWE *et al*., 2014).

The elevation rapidly falls to the south of the plateau to the moist forest between 3700 m asl and 1500 m asl. The northern parts of the plateau comprise woodlands, grasslands, and wetlands, largely between 3000 m asl and 3500 m asl (Watson, 2007). The BMER is characterized by a bi-modal rainfall with an annual precipitation range of 600 to 1400 mm. The temperature varies along elevation with an average annual temperature of 7.5°C at Tullu Dimitu and reaches 27.5°C at in the elevation ranges between 500 to 1000 m asl (Hailemariam *et al*., 2015).

BMER comprises important conservation areas such as the Bale Mountains National Park (Kefale *et al*., 2021); and six national forest priority areas where these forest areas are the second forest block in Ethiopia (Williams *et al*., 2005). These areas are important habitats for several rare and endemic species (Kidane *et al*., 2012). By this virtue, the BMER is identified as one of 34 global biodiversity hotspot areas (Kidane *et al*., 2012; Williams *et al*., 2005). Harana forest is one of six national forest priority areas which is located between latitudes 6° 14' 40" N and 6° 38' 30" N, longitude 39° 22' 10" E and 39° 27' 50" E shown in (Fig 2). The Harana forest is situated in the northern parts of Delo Mena and Harana Buluk woredas within the BMER. The northern and northeastern parts of the Harana forest lie inside the boundary of the Bale Mountains National Park (BMNP) which has important conservation implications for the park.

The total area of the Harana forest covers 107,298.673 ha, with dimensions of 75 km from west to east and 115 km in the South-North direction. The rainfall follows a bimodal pattern, in which the first season starts in April and extends to June. The second rainy season begins in the middle of September and lasts around the beginning of November. The annual temperature in the area ranges from 14-22^{o}C, with a mean annual temperature of 18^{o}c (Ayele *et al*., 2019). Elevation ranges from 1270 to 3030 m a.s.l with increasing pattern from south to north and decreasing from west to east. Annual rainfall ranges from 765 to 1110 mm year^{-1}.

Concerning soil type, *Rendzic leptosols* occupy 63% of the Harana forest, *Chromic Luvisols* 35% while the remaining soil types accounted for 2% (FAO and ISRIC, 2012). The dominant tree species in the Harana forest include *Podocurpus falcatus*, *Warburgia ugandensis*, *Celtis africana*, *Syzygium guineense*, *Olea capensis*, *Diospyros abyssinica* and *Filicium decipiens* (Ayele *et al*., 2019; Kewessa *et al*., 2019).

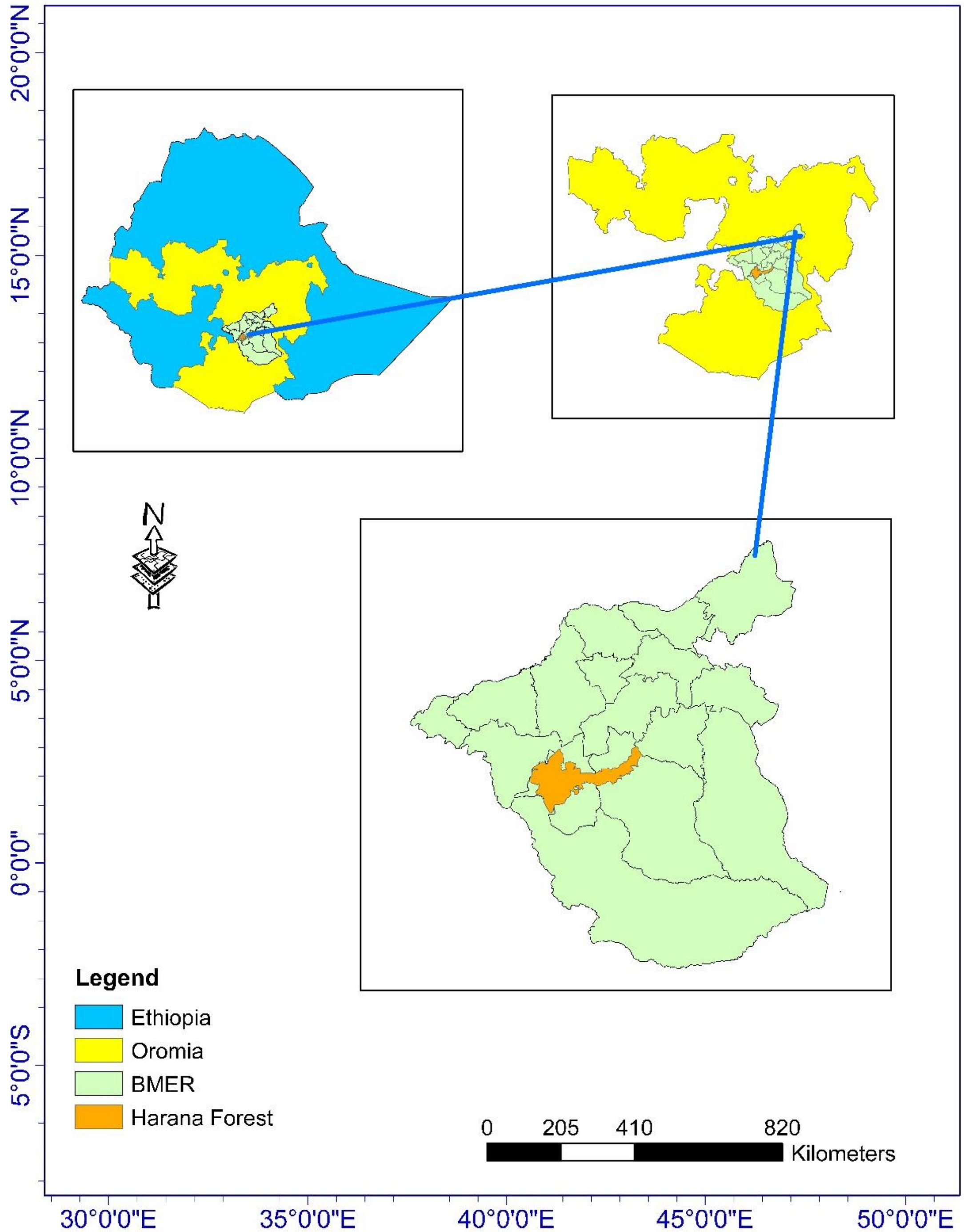

Figure 2: Map of the study area within broader geographical locations

3.2. Ecosystem services valuation in the Bale Mountains Ecoregion

3.2.1. Classification of land use and land cover types

The classification of ecosytem types in this study area was done using the differentiated land use and land cover classification established in the literature. There are six major LULC types: forest, woodland, scrubland, grassland, farmland, and other classes described. The descriptions of each are given in (Table

1) which was a base for conducting image classification processes indicated under section 3.2.2. This meant that the LULC was used as a proxy to identify the dynamics of ecosystems.

Table 1: Land use and land cover classification scheme in the study area

Ecoytem types	Descriptions of land uses and land-cover types
Forest	Forest refers to land with 0.5 ha and above, trees higher than 5 meters, and a canopy cover of more than 10% (FAOa, 2010). This comprises land dominated by evergreen and deciduous forests in the BMER.
Woodland	A woodland covers an area of open and closed woodland with dominant species of *Acacia-Commiphora* or *Combretum-Terminalia* (FAOa, 2010).
Scrubland	The scrubland area covers Erica species, afro-alpine vegetation (with some vegetation on the top of the Sanette plateau which includes *Lobelia rhynchopetalum* and *Helichrysum* species) including a small woody plant in the lowland part of the Ecoregion (Hailemariam *et al*., 2015).
Grassland	The land is mainly covered by a mixture of small plants, dominated by grass-like small plants, and shrubs less than 2 m (Mezgebu and Workineh, 2017).
Farmland	Farmland encompasses land mainly occupied by perennial and seasonal crops in rural areas (Mezgebu and Workineh, 2017).
Others	The other LULC types in this study cover rivers, small urban areas, and rocky materials.

3.2.2. Landsat imageries data access and analysis

It is a common practice to generate land use, and land cover (LULC) types using image classification techniques to differentiate various ecosytem types (Maes *et al*., 2015; Solomon *et al*., 2019). In this process of valuation of ecosystem services, the use of LULC types can be limited to assess trends of LULC types as the term ecosystems are more complex than LULC types (Maes *et al*., 2015). Keeping this in mind, a cloud-free Landsat 7 Enhanced Thematic Mapper (ETM+) of 2010 and Landsat 8 Operational Land Imager images (OLI) of 2015 and 2022 were downloaded from the United States Geological Survey (USGS) via earthexplorer.usgs.gov website using a parameter indicated in (Table 2). The ENVI 4.7 software was used to layer stack, mosaic, and clip the Landsat image of each year using a boundary shape file of the BMER. The training and testing data were generated from the image of each year using a polygon digitizing tool that is available in ENVI 4.7 based on the layer-stacked band numbers 2,3 & 4. The supervised maximum likelihood algorithm was used to classify the image of each year using the digitized training dataset. A supervised maximum likelihood algorithm has been widely used as it provides better accuracy (Yohanis and D'Huart, 2014; Ayele *et al*., 2019). The testing data were used to estimate the classification accuracy of images in terms of overall accuracy and Kappa values. The transition among different LULC types between two different periods was analyzed using the Terra set software.

Table 2: Descriptions of Landsat imagery and its parameters

Years	Satellite types	Resolutions	WRS (paths/rows	Sensor types	Date of acquisition
2010	Landsat 7	30m	167/055/056	ETM	1/10/2010
			168/055/056		
2015	Landsat 8	30m	167/055/056	OLI_TIRS	15/2/2015
			168/055/056		
2022	Landsat 8	30m	167/055/056	OLI_TIRS	1/25/2022
			168/055/056		

3.2.3. Estimation of ecosystem service values

The valuation of ecosytem services was initiated by identifying the ecosytem types that shared similar characteristics with ecosystems of the BMER indicated in (Table 3). Subsequently, the ecosystem service values (ESV) of each ecosytem service for each ecosytem type were adopted from other ecosytem that were identified in (Table 3). Those adopted ESVs were adjusted to a common price level of the year 2022 taking into account the effect of the price inflation (De Groot *et al*., 2020). The price adjustment was calculated using usinflationcalculator.com to avoid manual computation errors (Kankanamge and Jayantha, 2021). The adopted ESV for each ecosystem service was expressed in terms of US$ ha^{-1} yr^{-1} shown in (Annex 1). The adoption of such ESV is known as a benefit transfer approach that has been widely employed in literature (Sharma *et al*., 2019; De Groot *et al*., 2012; Fenta *et al*., 2020). Hence, the ESV of each ecosytem service within different ecosytem of the BMER was computed using (Eq 1) where ESV in US$ ha^{-1} yr^{-1} was multiplied by the area of each ecosytem type. Finally, a total ESV of the entire study area was quantified by summing the estimated ESV of each ecosytem type for each period.

$$ESV = \sum (A_K \times VC_{FK}) \quad \text{......} \quad Eq1$$

Whereas ESV: Ecosystem service values in US $ ha^{-1} yr^{-1}, A_k is the area in ha and VC_{fk} is a coefficient of each ecosystem service in US $ ha^{-1} yr^{-1} for land cover category k in each year.

Table 3: Landcover types and biome equivalents with the corresponding values

Ecoytem types of the BMER	Adopted similar ecosytem types *
Forest	Tropical forest
Woodlands	Woodland/rangeland
Scrubland	Tundra
Grassland	Grassland/rangeland
Farmland	Crops land

Source: * Adapted from Costanza *et al.* (2014)

3.3. Soil loss estimation in the Bale Mountains Ecoregion

3.3.1. Deriving factors of soil erosion in the RUSEL Model

3.3.1.1. Rainfall erosivity factor

Rainfall is used to estimate the soil erosivity factor while the rainfall erosivity factor (R) refers to the erosivity of rainfall at a particular location based on the rainfall amount, duration, and intensity (Kayet *et al*., 2018; Negese *et al*., 2022; Kolli *et al*., 2021; Luvai *et al*., 2022). The rainfall point data for this study were extracted from the EthioGIS database to produce rainfall patterns in raster formate using the kriging techniques in ArcGIS 10.4. A raster calculator in ArcGIS 10.4 was also used to create a layer of rainfall erosivity factor with 30-meter resolutions from the rainfall layer using Eq 2 which has been widely used in literature (Hurni, 1985; Negese *et al*., 2021; Moisa *et al*., 2022).

$R = -8.12 + (0.562 \times P)$ ……………………………………………………………………………Eq2

Where; R is the erosive factor in MJmm ha^{-1} h^{-1} yr^{-1}), and P is the mean annual rainfall in mm

3.3.1.2. Soil erodibility factor

The soil erodibility (K) factor shows the disintegration of soil particles from parent material under the actions of rainfall intensity, wind, and natural or human activities (Kayet *et al*.,2018; Fayas *et al*.,2019; Kolli *et al*., 2021). A determination of the K factor in this study was conducted by extracting the soil data of BMER from the Digital Soil Map of the World (DSMW) of FAO (2003). The K value of each soil type was computed using Eq3 which has been used by Kolli *et al*., (2021) while parameters of the equation such as silt, clay sand, and soil organic matter contents in percentage were derived from the DSMW (Pham *et al*., 2018). The calculated K values in Table 4 were assigned to each soil type in the attribute table of the BMER and those K values were rasterized with a resolution of 30 meters in ArcGIS version 10.4.

$K = (0.2 + 0.3 \times \exp(-0.0256 \times \mathrm{SILT} \times (1 - \mathrm{SILT}/100)) \times [\mathrm{SILT}/(\mathrm{CLAY} + \mathrm{SILT})]^{0.3} \times \{1 - 0.25\mathrm{X}\,\mathrm{SAND}/[\mathrm{SAND} + \exp(3.72 - 2.95\mathrm{X}\ \mathrm{SAND})]\} \times (1 - 0.7 \times (1 - \mathrm{SILT}/100)/(1 - \mathrm{SILT}/100) + \exp[-5.51 + 22.9 \times (1 - \mathrm{SILT}/100)$ ……………………………………………………………………………………….Eq3

Table 4: Soil types of the BMER and erodibility factor derived from Digital Soil Map of the World

Soil type name in BMER	Symbol	K factor
Ferric acrisols	Af	0.29
Eutric cambisols	Be	0.28
Plinthic ferralsols	Fp	0.25
Eutric nitosols	Ne	0.31
Calcaric regosols	Rc	0.32
Pellic vertisols	Vp	0.24
Haplic xerosols	Xh	0.31
Haplic yermosols	Yh	0.32

3.3.1.3. Land cover management factor (C) and management practices (P)

The land cover management (C factor) is commonly used to express the effect of the cropping system and crop management practices on the rate of erosion (Renard *et al.*, 1997). In this sense, the C factor is a ratio of soil loss from the land under specified conservation conditions to the soil loss of bare land (Casermeiroa *et al.*, 2004; Luvai *et al.*, 2022). The values of the C factor for different LULC classes for the study were adopted from Moisa *et al*. (2022) as shown in (Table 5). LULC classifications of the study area for the years 2010 and 2022 were conducted using the Landsat imagery data as per the method described under section 3.2.2. The classified LULC of each year was converted to a vector file. These values were assigned to the respective LULC types of each year in the attribute table of the vector layers. The C factor of the years 2010 and 2022 was similarly rasterized using Arc GIS ver. 10.4. On the other hand, the land management practice (P-factor) refers to the ratio of the amount of soil loss under a specific land management practice compared to the land without no management practice (Pham *et al.*, 2018; Luvai *et al.*, 2022). For this study purpose, values of the P factor in Table 5 were adopted from Moisa *et al.* (2022) and the layers of the P factor for LULC types of the years 2010 and 2022 were produced using the same procedure applied to the C factor that is described in this section.

Table 5: Soil types oThe C and P factors of different LULC categories in the study area

LULC	C factor		P factor	
Forest	0.01	Moise *et at*., 2022	0.53	Moise *et at*., 2022
Woodland	0.014	Moise *et at*., 2022	0.6	Moise *et at*., 2022
Scrubland	0.014	Moise *et at*., 2022	0.6	Moise *et at*., 2022
Grassland	0.05	Moise *et at*., 2022	0.63	Moise *et at*., 2022
Farmland	0.18	Moise *et at*., 2022	0.9	Moise *et at*., 2022
Unclassified	1	Feyes, 2019	0.8	Kayet *et al*., 2018

3.3.1.4. Slope length gradient factor (LS)

LS factor is a combined effect of slope length(L) and slope steepness (S) that affects soil erosion and it uses as one of the inputs in the RUSEL model to estimate the extent of soil loss (Wang *et al*., 2020; Kolli *et al*., 2021; Gong *et al*.,2022; Luvai et al., 2022). A slope length refers to cumulative distances from a point at which the runoff starts up to where the surface runoff reaches a well-defined channel (Ganasri and Ramesh, 2016; Luvai *et al*., 2022 Kolli *et al*., 2021). A slope steepness (S) on the other hand shows the effect of slope steepness on soil erosion (Luvai *et al*., 2022). Researchers have widely computed the LS factors from the Digital Elevation Model (DEM) using ArcGIS techniques (Pham *et al*., 2018; Fayas *et al*., 2019; Wagari and Tamiru, 2021; Gong *et al*., 2022).

For this study purpose, the DEM with 30 m resolutions was downloaded using earthexplorer.usgs.gov to produce the map of the LS factor. The hydrology tool in ArcGIS map version 10.4 was used to produce the flow length of the study area using the created layers of fill and flow directions. Additionally, a slope in percent was generated from the DEM. The layers of flow length and slope% were used to compute the LS factor with the 30-meter resolution. A raster calculator in Arc GIS map version 10.4 was used to produce the layer of LS factor using Eq 4 cited in (Moisa, 2022).

LS = power (flow length,0.3)/22.1 * power((slopein%/9),1.3) ……………...…………....……....Eq4

Whereas LS is the slope length gradient factor, 30 m refers to resolutions of DEM.

The value of m is 0.5 if the slope angle is greater than 5%, 0.4 on slopes of 3–5%, 0.3 on slopes of 1% to 3%, and 0.2 on slopes less than 1% (Das *et al*., 2021; Fu *et al*., 2021). The n value ranges between 1.0 and 1.3 (Zhang *et al*., 2017) where lower values of n are used for prevailing sheet flow and higher values for prevailing rill flow (Pham *et al*., 2018).

3.3.2. Annual mean soil loss estimation

The Revised Universal Soil Loss Equation Model (RUSLE) has been widely used to estimate the average annual soil loss using five soil loss driving forces (Gong *et al*., 2022; Luvai *et al*., 2022). These include rainfall erosivity (R), soil erodibility (K), cover management (C), support practice (P), and slope length (LS). The rasterized formats of five soil erosion driving factors were multiplied using a raster calculator in Arc GIS map version 10.4 to estimate the average annual soil in the study area using Eq 5 which has been widely used in literature (Kayet *et al*., 2018; Pham *et al*., 2018; Gong *et al*., 2022; Kolli *et al*., 2021; Luvai *et al*., 2022).

$$A = R * K * C * P * LS \ldots\ldots\ldots\ldots\ldots\ldots\ldots\ldots\ldots\ldots\ldots\ldots\ldots\ldots\ldots\ldots\ldots \textbf{Eq5}$$

where, A: average annual soil erosion (t^{-1} /ha^{-1}/$year^{-1}$), R: rainfall erosivity factor (MJ mm ha^{-1} h^{-1} $year^{1}$); K: soil erodibility factor (t MJ^{-1} ha $^{-1}$ mm^{-1}), C: vegetation cover (dimensionless); P, Erosion controlling practices (dimensionless); L: slope length, S: slope steepness (dimensionless).

3.3.3. Estimation of soil loss in different classes

Zonal statistics in the spatial analyst tools of ArcGIS map version 10.4 was used to compute the extent of soil loss severity within LULC types, slope classes, and soil categories. This was applied to each soil loss map for the years 2010 and 2022. The soil loss severity classes were classified into five classes such as Very slight <5, Slight 5 to 15, Moderate15-30, sever 30-50, and very sever > 50 in ton^{-1} $ha^{-1}year^{-1}$ where this classification approach was done based on what has been already established in the literature (Kayet *et al*. 2018; Thomas *et al*., 2018; Kolli *et al*., 2021). Additionally, the slope of the study area was classified into six classes in line with what Tsegaye and Bharti (2021) have used. These classes included <5 flat, 5-10 gentle,10-20 sloping, 20-40 strong sloping, and > 40 steep that was used to extract the soil loss in each slope class. Moreover, soil loss was estimated in eight-soil categories of the study area includes *Ferric acrisols, Eutric cambisols, Plinthic ferralsols, Eutric nitosols, Calcaric regosols, Pellic vertisols, Haplic xerosols* and *Haplic yermosols*.

3.4. Forest data assessment in the BMER and techniques of data analysis

3.4.1. Sampling size determination and forest data collection

Forest data assessment was conducted using a stratified random sampling design technique where forest areas were categorized into Dry and Moist forest strata based on topographic and climatic factors. This categorization has been established in the previous work reported by Asante *et al*., (2013). Each forest stratum was divided by 1000 ha to partition the forest area with a plot size of 1km by 1km. This was done to get a clue about the possible number of plots to occur in each stratum (Table 6). Parallelly, the preliminary survey of 15 sample plots with a radius of 15 meters was conducted in each stratum to estimate the variances which was used as input to calculate the required sample size. The required sample size was computed using the variance derived from the preliminary survey shown in (Table 6) along with a tolerable error of 10%, at a 90% confidence interval and the T value of 2. Finally, the sample size of 236 plots was calculated using Eq 6 cited in (Huy, 2013). The sample size of 236 was randomly distributed to the entire forest area using the ArcGIS technique. However, with the understanding that forest data collection within a 1000-ha plot size would be costly in terms of labor, finance, and time. Three concentric circular plots were alternatively used with a 15-meter radius for tree data collection while the remaining two circles were established with radii of 5, and 2 meters to collect data on tree saplings and seedlings, respectively. The collection of forest data was conducted with the aim of providing information for piloting sustiantable timber harvesting and attaining the purpose of this research when the author of this dissertation was a project manager that coordinated the field work to meet both objectives. The data collection was completed within one month.

During forest data collection, the coordinates of the center of each plot were fed into GPS and the data collection team searched for the center of a plot by pressing the “Go to” tab. Upon arrival at the center of the plot, the GPS sounded a tone and the team established three concentric circular plots. Within a quadrant size of 15 m for measuring trees DBH ≥ 5.0 cm using diameter tape and caliper. Counting of saplings with a diameter of 1.0 to 5.0 cm was conducted within a 5.0 m radius. Seedlings with less than 1.0 cm root collar were counted within a radius of 2 m. A circular plot in this study was chosen for its suitability in capturing irregularly distributed trees in natural forests while a rectangle plot is more useful to the manmade forest where planting rows are well defined (Huy, 2013; UNFCCC, 2015).

$$\boldsymbol{n} = \frac{(\sum_{i=1}^{L} \ N_i * s_i)^2}{\frac{N^{2*}E^2}{t^2} + (\sum_{i=1}^{L} \ N_i * s_i)^2} \ldots\ldots\ldots\ldots\ldots\ldots\ldots\ldots\ldots\ldots\ldots\ldots \mathbf{Eq}5$$

n= total number of sample plots required of (x); i= project strata number from 1 until L (2); L = total number of strata [dimensionless (2); Ni = maximum possible number of sample plots in the stratum; Si

= standard deviation for each stratum (xx); N= maximum possible number of sample plots in the project area; E= desired level of precision of 10% for this study; t= sample statistic from the t-distribution for the 90% confidence level and "T" value is set at 2, since the sample size is unknown.

Table 6: Statistical information to determine sample size to collect forest data

Strata (A)	Area in ha (B)	SD in t/ha (C)	Variances from the preliminary survey (D)	Sample frame (Ni) (E)	Sample size (n) (F)
(A)	(B)	(C)		(E)= B/1000ha	(F)
Moist	201856.28	215	46225	202	
Dry	57088.55	75	5625	57	
Total sample size (N)				259	235.54 ≈ 236

3.4.2. Analysis of above-ground carbon stock and species diversity

The above-ground biomass of each tree was calculated in Kg using allometric equations of Eq 7 and Eq 8 that were developed for Moist and Dry tropical forests, respectively (Chave *et al*., 2005; Asante *et al*., 2013). The estimated biomass of each tree was converted from kg to ton. The calculated biomass of each tree in tons was divided by two to estimate the above-ground carbon stock (ACD) of each tree with the understanding that half of tree biomass is assumed carbon content (Chave *et al*., 2009). A wood density of 0.65 was used in the equation which is the average value of all tree species established for tropical forests (Chave *et al*., 2009; Jeyanny *et al*., 2014). The ACD of all trees in each plot was summed and expressed as ACD per plot to produce the spatial distribution map of ACD using the geostatistical modeling techniques. Additionally, the ACD of each tree was multiplied by a coefficient of 3.67 to quantify the amount of carbon dioxide equivalent that would happen in the case of deforestation. SPSS version 20 was used to calculate the descriptive statistics of ACD and tree species while SPSS stands for Statistical Package for the Social Sciences.

$$Y = \left(\frac{\mathbf{0.65 * exp\left(-1.499 + (2.148 * ln(D)) + \left(0.207 * (ln(D))^2\right) - \left(0.0281 * (ln(D))^3\right)\right)}}{\mathbf{2}}\right) \ldots\ldots\ldots\ldots\ldots\ldots\ldots\ldots\ldots\ldots\ldots\ldots \mathbf{Eq}\ 6$$

$$\mathbf{Y = \frac{\left(0.65 * EXP\left(-0.667 + (1.784 * LN(D)) + \left(0.207 * (LN(D))^2\right) - \left(0.0281 * (LN(D))^3\right)\right)\right)}{2}} \ldots\ldots\ldots \mathbf{Eq7}$$

Where*:* 'Y' represents above-ground biomass (kg) per tree, D is DBH (cm), 0.06 is the average density of all tree species in a tropical area, and the number 2 is used to convert the biomass to carbon content.

3.4.3. Analysis of tree species richness and species diversity

The analysis of species richness was counted as the number of tree species in each plot while the Shannon Weiner diversity Index was calculated using Eq 9 which is widely used in literature (Ozcelik *et al*., 2008; Kent, 2011). The species evenness index was derived from the Shannon Weiner index using (Eq 10). Species evenness value ranges between zero and one, whereas a value closer to one could indicate a better evenness (Redowan *et al*., 2015).

$$\textbf{Shannon wiener diversity}(\mathbf{H}') = -\sum_{\mathbf{i=1}}^{\mathbf{s}} \boldsymbol{Pi} \ln \boldsymbol{Pi} \quad \text{Eq 9}$$

Where: ‘S’ is the number of species, Pi: is the proportion of individuals or the abundance of the ith species, and ln: log base n.

$$\textbf{Species evenness}(\mathbf{E}) = \frac{\mathbf{H}'}{(\mathbf{Ln}(\boldsymbol{S}))} \quad \textbf{Eq10}$$

Whereas H’ Shannon wiener index, Ln (log base n), and S is a sum of all species in each plot.

3.4.4. Mapping of forest attributes using semi-variogram and kriging techniques

A normality test was conducted for each dataset of species richness, Shannon Weiner index, species evenness, and ACD using SPSS ver 20. All data exhibited normal distribution patterns except the data of ACD. For this reason, the data of ACD was subjected to data transformation using the square root technique, and the transformed ACD data was referred to as Sqrt-ACD. Concurrently, the trend analysis was checked using spatial analysis tools in ArcGIS ver.10.4. A trend refers to a deviation from the assumption of geostatistics that states a mean of paired points is constant, otherwise, the presence of a trend leads to the absence of the spatial dependency which would not qualify for spatial analysis (Rossi *et al*., 1992; Relethford, 2008; Ye, 2008). In this study, the trend was not detected in all datasets, and the detrending technique was not required, implying that the given datasets were suitable for the spatial analysis using Semi-variogram and kriging techniques (Relethford, 2008; Ye, 2008). Semi-variogram $\gamma(h)$ is half of the average squared difference of values between points that are separated by a lag distance h. Mathematically, a Semi-variogram is given in Eq 11 (Payna *et al*. 1999; Hengl, 2007; Lichtenstern, 2013).

Having normality test and trend, Semi-variogram analysis of the species richness, Shannon Weiner index, species evenness, and Sqrt-ACD was conducted using Arc GIS by graphing semi-variogram clouds in which the semi-variances were plotted against a given separation distance between paired variables (Hengl, 2007; Lichtenstern, 2013). In the graphing process, an increased monotonical curve reaching a sill at the defined lag distance indicates the presence of spatial autocorrelation but if a straight horizontal line is presented it shows the absence of spatial autocorrelation (Maynou, 1998; Relethford, 2008). In this process, an experimental semi-variogram of the species richness, Shannon Weiner index, species evenness, and Sqrt-ACD was constructed after testing multiple times by adjusting parameters of the semi-variogram such as a lag width, lag size, sill, nugget, and ranges. This was repeatedly conducted until the graph of a scatter plot of each dataset was properly defined by a constructed experimental semi-variogram. Additionally, the variability of data patterns with directions of semi-variogram was checked using the geostatistical technique in the spatial analysis tool of ArcGIS vers10.4. The analysis showed that semi-variograms of all attributes appeared to exhibit a uniform pattern which is known as an omnidirectional variogram; while an anisotropic variogram shows variability of pattern along different directions (Fortin *et al.*, 2002; Akhavan and Kia-Daliri, 2010; Steimer, 2017). The experimental semi-variograms of species richness, species evenness, and the Sqrt-ACD were fitted into the exponential model whereas the Shannon Weiner diversity index was fitted to the Gaussian distribution model in Semi-variograme.

$$\gamma^{(h)} = \frac{1}{2N(h)} \sum_{i=1}^{N(h)} [z(x_i) - z(x_i + h)]^2, \ldots \ldots \ldots \ldots \ldots \ldots \ldots \ldots \ldots \ldots \ldots \ldots \ldots \ldots \ldots \ldots \ldots \ldots \ldots \ldots \text{Eq11}$$

Whereas (h): is the semivariance at a given distance h; z(xi) is the value of the variable Z at the location of x_i, h is the lag distance, and N(h) is the number of pairs of sample points separated by "h" distance**.**

Completing the process of semi-variogram, maps of species richness, species evenness, and Sqrt-ACD were produced using kriging where it is represented mathematically in (Eq 12) cited in **(**Fu *et al.*, 2014). The map of each attribute was clipped in ArcGIS using a shapefile of BMER to maintain spatial fit to the context of the BMER. Importantly, Kriging automatically can produce prediction errors using cross-validation technique (Baba *et al.*, 2014). The prediction error refers to difference between interpolated and the observed values (Baba *et al.*, 2014; Sciarrettam and Trematerra, 2014). Root-Mean-Square Standardized Error (RMSSE) has been commonly employed (Luo *et al.*,2007; Samui and Sitharam 2011: Kalivas *et al.*, 2013; Baba *et al.*, 2014).

$$\hat{z}\,(x_0) = \sum_{i=1}^{n} \lambda_i z(x_i), \ldots \ldots \ldots \ldots \ldots \ldots \ldots \ldots \ldots \ldots \ldots \ldots \ldots \ldots \ldots \ldots \ldots \ldots \ldots \ldots \ldots \ldots \ldots \ldots \ldots \ldots \ldots \ldots \ldots \ldots Eq\ 12$$

Where ˆz(x_0) is the value to be estimated at the location of x_0; z (xi) is the known value at the sampling site x*i*, and λ_i is a weighting coefficient.

3.4.5. Classifying spatial distribution maps of forest attributes into different classes

Maps of species richness, species diversity, species evenness, and ACD were reclassified into six classes for each using the equal interval classifier in Arc GIS ver. 10.4. The equal interval classifier was applied considering its advantage of dividing the values of attributes into equal sizes (Osaragi, 2008). The reclassification was required to estimate a forest area that could be associated with each class. This helps in understanding the contribution of different parts of forest areas in constituting various ACD, species richness, and diversity.

3.4.6. Analysis of relationships between deforestation area and tree species losses

The relationship between the area of deforestation and tree species indices was conducted by having different spatial maps. Primarily, the land use and land cover classification maps of the years 2010 and 2022 that are shown in section 3.2.2 were used to extract the forest map in each year. An extraction of forest maps for each year was conducted using a technique of raster calculator in ArcGis ver 10.4. Subsequently, the raster calculator was used to subtract the forest area of 2010 from the forest area of 2022 to produce a binary map that comprised both persistent forest area and deforested area between 2010 and 2022. This output was referred to as a deforestation map. Additionally, the maps of tree species richness, species diversity, and species evenness indices that were produced using the kriging under section 3.4.4 were reclassified into six classes using an equal classifier in Arc GIS. The reclassified map of each index was converted to a shapefile using ArcGIS techniques while the reclassified output maps were referred to as the species richness, species diversity and species evenness shapefiles. For estimating impacts of deforestation on species richness, the deforestation map and species richness shapefile were used as inputs in zonal histogram in ArcGIS map to relate an area of deforestation that was associated with different classes of species richness. This process was repeated for the species diversity index and species evenness to generate information how deforestation resulted in loss of tree species diversity and evenness within different classes.

3.5. Estimation of above-ground forest carbon in the Harana Forest

3.5.1. Sampling methods and data collection of woody tree species

Harana Forest is divided into different compartments to implement participatory forest management (PFM). Forest data are periodically collected from forest compartments to develop participatory forest management plans. In line with this purpose, the forest data collection was conducted in collaboration with Farm Africa and Oromia Forest and Wildlife Enterprise (OFWE) in such a way as to meet the purposes of this research and the objective of PFM where the data collection process took five months while the Author was the project coordinator in Farm Africa.

A systematic random sampling technique was used by dividing each forest compartment into square girds of 1km by 1km distance from directions of South-North and East-West using Arc GIS v 10.4. The coordinate points where the grids intersected were fed into the GPS tool to identify and mark the exact locations during the field data collection.

Each of the marked coordinate points on the ground was used as the center of a plot and three nested circular plots were established from the center. The radii of three circular plots included 15, 5, and 2 meters collect various data on woody species. These plots were established using a measuring tape, ropes, and ribbons. A circular plot was chosen for its less vulnerability to errors due to incorrect omissions or inclusions of trees around the plot boundary (UNFCCC, 2015; Mwakisunga *et al*., 2012).

Regarding data collection, the diameter of each tree was measured using diameter tape for all trees ≥ 5 cm at 1.3 m from the aboveground within a 15-meter radius. Tree stems that were forked below 1.3 m were considered as different trees and measured separately but in case stems were forked above 1.3 m from the ground they were considered as a single tree. Tree heights were measured using a digital hypsometer. Woody species saplings with a diameter of 1 to 5 cm were counted within the circular plot of a 5 m radius and seedlings below one cm root collar were counted within the circular plot of a 2 m radius. Meanwhile, the vernacular and botanical names of each tree species were recorded.

3.5.2. Data analysis of the above-ground forest carbon density of the Harana forest

A count of each species for saplings and seedlings with radii of 2 m and 5 m was converted to a size of 15 m radius which was 0.07065 ha. This was to make computational analysis on a standardized unit (Zhang *et al*., 2019). The ACD was estimated using an allometric equation (Eq 7) under section 3.4.2 .The estimated above-ground carbon of each tree was converted from kg to ton and summed at a plot level and the added value was expressed as the above-ground carbon density (ACD) per plot and it was also expressed in terms of ha. The plot level estimation of ACD was required for spatial modeling of the ACD in the Harana Forest versus the identified predictor variables (Table 7).

Statistical Package for Social Sciences (SPSS) Ver20.0 was used to compute the mean of ACD in the Harana Forest. This mean was used as a threshold to classify the ACD into low and high classes. Those plots with a mean value of above 31.27 tons were categorized as high-class while the remaining values were classified into the low class.

3.5.3. Determinants of the spatial distribution of the ACD

In addition to forest data collection, the identification of predictor variables was conducted based on an extensive review of relevant literature. The literature shows that spatial distribution of the ACD could be influenced by elevation, slope, aspect, soil texture, temperature, and precipitation (Merganič *et al*., 2012; Vayreda *et al*., 2012; Fibich *et al*., 2016; Sahragard *et al*., 2018 *et al*., 2018; Hofhans *et al*., 2020). The spatial distribution of ACD can be also influenced by biological factors such as the number of tree species richness and species diversity (Vayreda *et al*., 2012). Moreover, natural and human disturbances can affect the amount and distribution of ACD though, including the impact of human activity in the spatial modeling is challenging (Vayreda *et al.*, 2012).

Based on the in-depth review, a total of 38 environmental variables were collected from different data sources (Table 7). Of the total 19 variables were climatic factors that were downloaded from the Bioclim data portal which are indicated in Table 7. The Digital Elevation Model (DEM) with 30 resolutions was downloaded from the USGS data portal, whereas a slope and aspect were derived from the DEM using appropriate tools in ArcGIS v10.4. Soil physical and chemical characteristics were downloaded from the open-access soil grid database of the International Soil Reference and Information Centre (ISRIC). These included soil physical and chemical properties at the depths of 0 cm, 5 cm, 15 cm, 30 cm, 60 cm, 1m, and 2 m. The layer of each environmental variable was resampled to 30 m resolution and extracted using the polygon of the study area where the dataset was projected to the common project coordinate system (UTM zone 37N, WSG 84 datum, linear unit of meter). Apart from this, data of species diversity was computed using Eq 9 which is given under section 3.4.2 while species richness is referred to the total number of species counted in the Harana forest.

Table 7: Biophysical variables used to predict the spatial distribution of ACD

Variables	Short name	Resolution	Data sources
Temperature (^{O}c)	Temperature	10 arc-minute	Bioclim.www.org
Precipitation (mm)	Precipitation	10 arc-minute	Bioclim.www.org
Elevation (DEM) (m)	Elevation	30m	http://earthexplorer.usgs.gov
Slope (%)	Slope	30m	Derived from DEM
Aspect	Aspect	30m	Derived from DEM
Clay soil content at 0 cm (%)	Clay0	250m	https://soilgrids.org/SoilGrids
Clay soil content at 5 cm (%)	Clay05	250m	https://soilgrids.org/SoilGrids
Clay soil content at 15 cm (%)	Clay15	250m	https://soilgrids.org/SoilGrids
Silt content % at0cm depth (%)	Silt0	250m	https://soilgrids.org/SoilGrids
Silt content %5cm depth (%)	Silt105	250m	https://soilgrids.org/SoilGrids
Soil organic content % at 0 cm depth (%)	SOC0	250m	https://soilgrids.org/SoilGrids
Soil organic content % at 05cm depth (%)	SOC5	250m	https://soilgrids.org/SoilGrids
Soil cation exchange capacity % at 0cm depth	CEC0	250m	https://soilgrids.org/SoilGrids
Cation exchange capacity at 05cm depth	CEC05	250m	https://soilgrids.org/SoilGrids
Cation exchange capacity % at 15cm depth	CEC15	250m	https://soilgrids.org/SoilGrids
Species richness	SR	Count	Forest inventory data
Shannon-weiner index	H’	30m	Forest inventory data
Podocarpus falcatus	*P. falcatus*	30m	Forest inventory data
Szgium guinesses	*S. guinesses*	30m	Forest inventory data
Olea capensis	O. *capensis*	30m	Forest inventory data
Filicium decipiens	*F. decipiens*	30m	Forest inventory data

3.5.4. Spatial modeling of the above-ground carbon density

The spatial modeling of the ACD for the Harana forest was conducted using the Random Forest package in R-software version 3.1.6. The process of modeling the ACD began by conducting preliminary modeling using all 38 rasterized predicting variables (Table 8) to identify those variables with strong effects on the spatial distribution of the ACD. The strength of each predictor in terms of a mean decreased Gini was automatically generated by the Random forest. A higher value of the Gini index indicates the strength of the variable in the model, otherwise, it would be a weak variable (Scarnati *et al*., 2009). Accordingly, 21 variables with high Gini values were selected to run the final prediction of the ACD.

The model accuracy of the Random Forest was evaluated based on out-of-bag error (OOB) error. The OOB error is useful to control the overfitting of model output (Vincenzi, 2011; Sahragard *et al*., 2018, 2018; Zhang *et al*., 2019). The 'optimal' tuning parameters of the Random Forest model were determined by conducting the Random Search by applying a Random 3-fold equal proportion of cross-validation which was repeated six times with a tuned length of 15. The number of trees to grow per node was determined to 500, and the number of variables was randomly split at each node was set at 10 which is referred to as (mtry). In line with this, the model prediction was done with the OOB value of 28% was minimized by changing the model parameters. Finally, the overall accuracy of the model was computed based on values that were correctly and incorrectly classified in the confusion matrix. The values in a confusion matrix were used to compute the overall accuracy of the random forest model using (Eq 13). Similarly, the RF model automatically generated a partial effect graph which shows the effect of each predictor variable on the spatial distribution of the ACD.

$$\text{Overall accuracy }\% = \left[\frac{A + D}{A + B + C + D}\right] * 100 \ldots\ldots\ldots\ldots\ldots\ldots\ldots\ldots\ldots\ldots\ldots\ldots\ldots\ldots\ldots\ldots\ldots\ldots\ldots\ldots\ldots \quad \text{Eq 13}$$

Where: A=correctly classified low class of ACD; B= incorrectly classified low-class ACD; C= incorrectly classified high ACD; D= Correctly classified high classes of ACD

3.5.5. Spatial clustering analysis of the ACD

Spatial clustering could be analyzed using Moran's I statistic which comprises Global Moran's and local indicators of spatial association (LISA). The Global Moran's index helps to quantify the spatial autocorrelation as a whole but the Global Moran is weak in identifying places where clustering could occur (Jacquez, 2008; Fu *et al*., 2014). Alternatively, LISA describes the extent to which observations are similar or dissimilar to their neighbors (Bataineh, 2006; Fu *et al*., 2014). The types of spatial clustering of neighboring points can be described into four different distinct patterns: High cluster (HH), Low cluster (LL), High-outlier (HL), and Low outlier (LH). The high-clustering (HH) shows a similarity of ACD in neighboring locations, whereas LL represents a low clustering of ACD. High-outlier indicates locations where high ACD is surrounded by low values of ACD. The low-outlier shows locations where a low ACD is surrounded by a high value of ACD (Camarero *et al*., 2005; Fu *et al*., 2014). With this understanding, the ACD of 1122 plots was converted to a vector layer in ArcGIS v10.4 software to map the spatial clustering of ACD using the LISA statistics.

3.5.6. Pearson correlation and scatter plot analysis

Locations with high-high and low-low ACD were extracted using ArcGIS10.4. The extracted values were imported to SPSS ver. 20.0 to conduct Pearson correlation analysis against each corresponding biophysical predictor of the same locations. This was done to investigate how those biophysical factors contributed to the occurrences of high cluster areas.

3.6. Spatial distribution modeling of the abundances of woody species

3.6.1. Sampling method, species data collection and analysis

The woody species data of the Harana forest were collected using the method described under section 3.5.1 to predict the spatial distribution of abundances of the selected woody species. Of the total collected data, eight woody species were chosen considering their ecological roles of containing 45% of the above-ground carbon stock in the Harana Forest (Bedane *et al*., 2022). These species included *Podocarpus falcatus* (*P. falcatus*), *Croton macrostachyus* (*C. macrostachyus*), *Celtis africana (C. africana*), *Syzygium guineense* (*S. guineense*), *Olea capensis (O. capensis*), *Diospyros abyssinica* (*D. abyssinica*) and *Feliucium decipenses* (*F. decipenses*). Despite that, the lifeform of *Coffea arabica* (C. *arabica*) is not a tree but spatial modeling of its abundance was done considering that it shares a large proportion of the total density of the shrubs (Kewessa *et al*., 2019). The abundance of *Coffea arabica* (C. *arabica*) was included taking into account that the expansion of *C. arabica* induced a negative impact on the forest ecosystem (Kewessa *et al*., 2019). Therefore, understanding the spatial distribution of *C. arabic* could provide explicit spatial information on how forest conditions have been affected.

3.6.2. Selection of abiotic factors which influence abundances of species

The in-depth review helped to identify the most common abiotic factors that affect the abundance of woody species. These included elevation, annual precipitation, temperature, and edaphic factors (Jeyanny *et al*., 2014; Yu *et al.*, 2014; Thokchom and Yadava,2017; Rahman *et al*., 20211). For this study purpose, a digital elevation model (DEM) of 30 m resolution was downloaded from the USGS data portal to generate topographic factors (elevation, aspects, and slope). Annual mean temperature and precipitation data were downloaded from the Bioclim portal using Bioclim.www.org. The soil layer data were accessed from the GIS database of Farm Africa while those data consisted of soil pH, organic matter (OM), total nitrogen (N), carbon to nitrogen ratio (CN), available phosphorus (P), available potassium (K), magnesium, and calcium, including percentages of clay, silt, and sand contents. GPS coordinates of 1122 sample plots from where the data of species abundances were collected were used to extract the soil physical and chemical properties that correspond to each sample plot using multiple-point extraction techniques in ArcGIS map v10.4. The purpose of this extraction was to create a spatial correlation between the abundance of species and soil variables to conduct spatial modeling. Upon the completion of data collection of the abundances of woody species and predictor variables, the data exploration process was conducted to fit into the requirement of the assumption of different models where the description of the detailed process is presented under the subsequent heading.

3.6.3. Data exploration and transformation

Ecological data in nature do not often follow a normal distribution due to skewness (Feng *et al.*, 2014) while statistical procedures require variable data to be normally distributed (Osborne, 2016). In line with this requirement, the abundance data of each woody species that did not show normal distribution patterns were transformed using the logbase10 (abundance+1) transformation technique. The log transformation was used because the ANN model would require the transformed value of a response variable to make the computation of the complex ecological interactions (Sola and Sevilla,1997; Puheim and Madarász, 2014). The log transformation is selected as it has been widely used to convert skewed ecological data (Feng *et al.*, 2014), and any constant number is added to the original data before the data transformation to avoid undefined values for the log numbers below number one (Feng *et al.*, 2014; Osborne, 2016).

The ANN model also requires the normalized value of input variables to a similar scale, otherwise, predictors with different measurement scales can produce unrealistic outputs (Puheim and Madarász, 2014). For this reason, predictor variables in this study were normalized using Eq 15 cited in (Olden and Jackson, 2002).

$$\mathrm{N} = (\mathrm{Xi} - \mathrm{Minimum(X)})/(\mathrm{Maximum(X)} - \mathrm{minim(X)} \;\ldots\ldots\ldots\ldots\ldots\ldots\ldots\ldots\ldots\ldots\ldots\ldots\ldots\ldots\ldots\ldots\ldots\ldots\ldots\ldots\ldots\; \mathrm{Eq15}$$

whereas; N refers to a normalized value for observation X_i, X_i is the list of observations

3.6.4. Random Forest modelling

The random forest regression model in the R software ver. 4.1.0 was used to examine relationships between the log abundance of each species and abiotic factors. In this process, a total of 1122 samples were classified into 80% training and 20% testing. This was done for the reason that the RF model does not require any independent data set to run a model validation (Kapwata and Gebreslasie, 2016). The RF model was run for each species using three steps that are commonly described in the literature (Kapwata and Gebreslasie, 2016). First, setting (ntree=500) which was the number of trees to grow in a model depending on bootstrap sampling. Second, (mtry=5) was set where several predictor variables were to perform splitting of the data at each node to grow un-pruned regression trees with the identified independent variables. Third, estimated values of regression trees were added and averaged to predict outputs of the log abundance of each woody species.

The RF model was further used to predict the spatial distribution map of the log abundance of each species using raster layers of 16 predictor variables while data on the log abundance of species were available in the shapefile. The RF model was selected to produce the prediction maps because it achieved a smaller prediction error for many species as compared to the ANN and GLM models. The accuracy of the RF model was assessed using (MSE) mean squared error and (R^2) coefficient of determination (Scarnati *et al*., 2009). The RF model identified the variable importance using a percent increase in mean squared errors (%IncMSE). A large %IncMSE value shows a high degree of variable importance in predicting a given response variable (Scarnati *et al*., 2009; Kapwata and Gebreslasie, 2016).

3.6.5. Artificial neural network modeling

ANNs were constructed using a neural net package in the R Software ver. 4.1.0 in a way consisted of one input layer, one hidden layer, and one output layer. The number of hidden layers was determined to be one as increasing the number of hidden layers could lead to overfitting of the model (Chen *et al.*, 2022). A total of 1122 sample locations was split into 80% training and 20% testing data to run the model for each of the eight woody species. A supervised backpropagation algorithm (BPN) was used to train the model using the forward and backward processes. During the forwarding learning process, 16 input variables were propagated from the input layer to the hidden layer where weights and bias values were assigned to neuron connection in the ANN model (Chen *et al*., 2022). Weights are multiplied by the corresponding input variable to determine the contribution of input variables in the model (Kukreja *et al*., 2016; Aksu *et al*., 2019; Chen *et al*., 2022). The sigmoid activation function was used to decide whether a sum weight would be transferred into the output layer or not (Chen *et al*., 2022). The sigmoid activation function was used for its advantage of handling data that are characterized by non-linear features (Kukreja *et al*., 2016; Aksu *et al*., 2019). Back-propagation learning was conducted to adjust weights and biases to minimize prediction errors between the actual and prediction values (Ahmadzadeh *et al*., 2017; Aksu *et al*., 2019; Chen *et al*., 2022).

The accuracy of the ANN model was determined using a coefficient of determination (R^2) and (MSE) mean squared error (Chen *et al*., 2022). The Olden algorithm was further used to identify variable importance based on the quantified magnitude and direction of the effects of input variables on the response variable (Olden and Jackson, 2002). The Olden variable importance in this study was standardized using Eq 16 as proposed by Olden and Jackson, (2002). This standardization process was required to display the variable importance graphically to provide a clear illustration for better visualization.

$$\mathrm{Zn} = \frac{(x_n - \bar{X})}{\delta_x} \ldots\ldots\ldots\ldots\ldots\ldots\ldots\ldots\ldots\ldots\ldots\ldots\ldots\ldots\ldots\ldots\ldots\ldots\ldots\ldots\ldots\ldots\ldots Eq16$$

Where: Z_n is the standardized value of observation n, X_n is the original value of observation n, $\bar{x}$ is the mean; while δ_X is the standard deviation of the variable X.

3.6.6. Generalized learner modelling

A generalized linear model in R software version 4.1.0 was used to quantify the impact of predictor variables on the log abundance of each woody species. The total sample data was divided into 80% training and 20 testing data. The GLM model was run by specifying the identity link function to compute the linear relationship between predictor variables and response variables (Lopatin *et al*., 2016; Goldburd *et al*., 2020). The identity link is used to create a linear relationship between response and predictor variables (Dunn and Smyth, 2018; Goldburd *et al*., 2020). The effects of identified abiotic factors on the log abundances of species were interpreted using parameter estimates at the given significance level. The performance of the GLM model was assessed using the coefficient of determination (R^2) and the (AIC) Akaike information criterion (Rion, 2010; Sakate and Kashid, 2016). A higher R^2 indicates the selected environmental predictors could better explain variation in the response variable (Kapwata and Gebreslasie, 2016; Chen *et al*., 2022).

CHAPTERS 4: RESULTS

4.1. Dynamics in areas of ecosystems and monetary values of ecosystem services

4.1.1. Types and state of land use and land cover in the study area

Six land uses and land cover types were identified such as forest, woodland, scrubland, grassland, farmland, and another class (Table 8 and Fig 3). The first five LULC types were referred to as ecosystems in the processes of valuation of ecosytem services. The accuracy of the image classification of 2010 was achieved with an overall accuracy of 92.22% and a kappa value of 0.90 whereas the accuracies of the images of 2015 and 2022 were achieved with overall accuracies of 70.88% and 80.16%, respectively, while the corresponding Kappa scores were 90.62 and 0.75. The result showed that the area of the forest was 689,673 ha covering 18% of the total area of the BMER in 2010 but declined to 599,732 ha in 2022 with a proportion of 16% of the total area in the year 2022 (Table 8). The woodland ecosystem was the largest area accounting for 45% of the total area in 2010 and its proportion increased to 48% in 2015 and 2022. The area of farmland was 521,332 ha in 2010 with 14% of the total area but sharply increased to 771,365 ha in 2022 covering 20% of the total area in 2022. The proportion of grassland ecosystems dramatically dropped from 9% to 3% between 2010 and 2022 (Table 8).

Table 8: LULC dynmaics of the BMER at different periods

Ecosystem types	Years					
	2010		2015		2022	
	Ha	Percent	Ha	Percent	Ha	Percent
Forest	689,673	18	632,070	17	599,732	16
Woodland	1,680,723	45	1,800,295	48	1,790,134	48
Scrubland	526,962	14	397,120	11	490,407	13
Grassland	335,590	9	302,966	8	105,907	3
Farmland	521,332	14	593,505	16	771,364	20
Others	13,144	0.004	41,468	0.01	9,880	0.003
Total	3,767,424	100	3,767,424	100	3,767,424	100

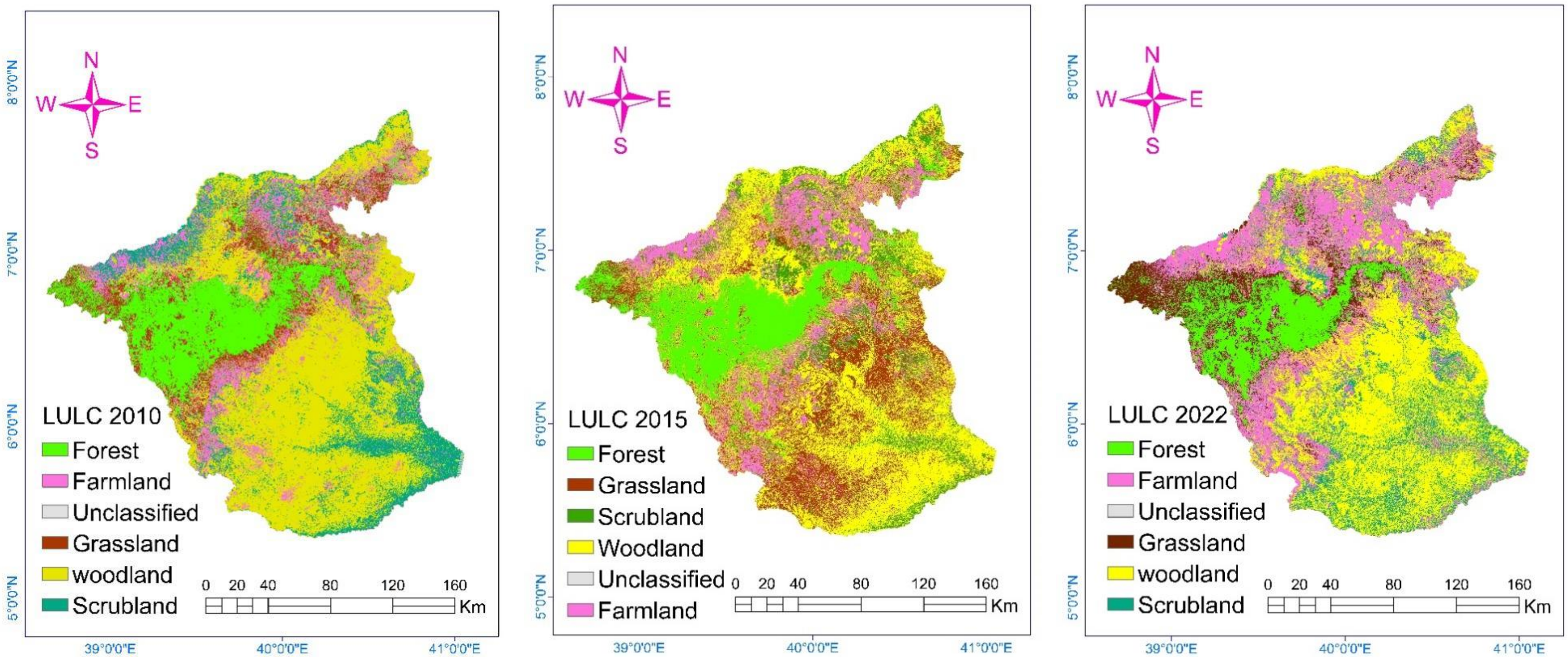

Figure 3: Maps of different ecosystems derived from LULC classifications

4.1.2. Transitions of surface areas among different ecosystems

The forest ecosystem in the BMER lost 59,650 ha of its area to farmland, 62,000 ha to grassland, and 37,802 ha to woodland, including 18,737 ha to scrubland (Fig. 4). The grassland ecosystem lost 1,700 ha to farmland and 1481 ha to the scrubland. About 42,558 ha of scrubland was converted to farmland while 26,671 ha was transformed to a woodland ecosystem. The woodland ecosystem received 37,802 ha from forestland and 26,671 ha from scrubland. The farmland ecosystem mainly gained 103,639 ha from woodland, and 59650 from forest between 2010 and 2022 (Fig. 4).

Figure 4: The net contributions of each ecosystem to other categories between 2010 & 2022

4.1.3. Overall ecosystem services of the BMER in monetary values

The total ESV was estimated at US$ 103 billion in 2010, US$ 95.8 billion in 2015, and US$ 92.5 billion in 2022 (Table 9). Specifically, the ESV of the forest ecosystem was estimated at US$ 94.5 billion in 2010 accounting for 91% of the total ESV in 2010. However, this ESV declined to US$ 86.6 billion in 2015 and US$ 82.2 billion in 2022. Conversely, the ESV of the farmland showed increasing from US$ 4.81 billion in 2010 to US$ 5.48 billion in 2015 and US$ 7.12 billion in 2022 (Table 9). The ESV of the grassland was the smallest with US$ 1.22 billion in 2010 but sharply declined to US$ 385 million in 2022 (Table 9).

Table 9: Monetary values of ecosystem services (US$) under different ecosystems in different periods

Ecosystem types	Year					
	2010		2015		2022	
	US$	Percent	US$	Percent	US$	Percent
Forestland	9.45E+10	91%	8.66E+10	90%	8.22E+10	89%
Woodland	1.61E+09	2%	1.73E+09	2%	1.72E+09	2%
Scrubland	1.21E+09	1%	9.12E+08	1%	1.13E+09	1%
Grassland	1.22E+09	1%	1.10E+09	1%	3.85E+08	0.4%
Farmland	4.81E+09	5%	5.48E+09	6%	7.12E+09	8%
Total	1.03E+11	100%	9.58E+10	100%	9.25E+10	100%

Source: Computed value based on data in Annexes 2,3 and 4

4.1.4. Status of the bundle of ecosystem services under different ecosystems

ESV of provisioning services in the BMER was estimated at US$ 49.1 billion in 2010 but decreased to US$ 45.1 in 2015, and US$ 42.9 billion in 2022. The value of regulation services reduced from US$ 6.32 billion in 2010 to US$ 6.23 billion in 2015, but it was increased to US$ 6.54 billion in 2022. The ESV of cultural services was the highest of all groups of ecosystem services having US$ 47.9 billion in 2010, US$ 44.5 billion in 2015, and US$ 43.0 billion in 2022, though it showed a decreasing trend. The ESV of supportive services was the smallest of all ESVs at different periods (Table 10).

Table 10: Dynamics of ESVs of categorized ecosystem services under different ecosystems

Years	ES categories	ESVs of different categories of ecosystems in USD in different ecosystems						
		Forest	Woodland	Grassland	Farmland	Scrubland	Sum	% of ESV
2010	Provisioning	4.78E+10	1.73E+07	3.66E+08	6.71E+08	2.90E+08	4.91E+10	48%
	Regulation	2.40E+09	6.27E+08	6.52E+08	2.04E+09	6.10E+08	6.32E+09	6%
	Supportive	5.52E+06	0.00E+00	0.00E+00	0.00E+00	0.00E+00	5.52E+06	0%
	Cultural	4.43E+10	9.69E+08	2.01E+08	2.11E+09	3.10E+08	4.79E+10	46%
	Total	9.45E+10	1.61E+09	1.22E+09	4.81E+09	1.21E+09	1.03E+11	100%
2015	Provisioning	4.38E+10	1.85E+07	3.31E+08	7.64E+08	2.19E+08	4.51E+10	47%
	Regulation	2.20E+09	6.72E+08	5.88E+08	2.32E+09	4.60E+08	6.23E+09	7%
	Supportive	5.06E+06	0.00E+00	0.00E+00	0.00E+00	0.00E+00	5.06E+06	0%
	Cultural	4.06E+10	1.04E+09	1.82E+08	2.40E+09	2.34E+08	4.45E+10	46%
	Total	8.66E+10	1.73E+09	1.10E+09	5.48E+09	9.12E+08	9.58E+10	100%
2022	Provisioning	4.15E+10	1.84E+07	1.16E+08	9.93E+08	2.70E+08	4.29E+10	46%
	Regulation	2.09E+09	6.68E+08	2.06E+08	3.01E+09	5.68E+08	6.54E+09	7%
	Supportive	4.80E+06	0.00E+00	0.00E+00	0.00E+00	0.00E+00	4.80E+06	0%
	Cultural	3.85E+10	1.03E+09	6.35E+07	3.12E+09	2.88E+08	4.30E+10	47%
	Total	8.22E+10	1.72E+09	3.85E+08	7.12E+09	1.13E+09	9.25E+10	100%

Source: Computed based on data in Annexes 2,3 and 4

4.1.5. Losses and gains of ESVs of the batch of ecosystem services in different ecosystem types

A total net loss of US$ 10.8 billion ESV was estimated between 2010 and 2022 in the BMER in association with the losses of ESVs in forest, scrubland, and grassland ecosystems (Table 11). A large net loss in the ESV was detected in provisioning services with a value of US$ 6.18 billion while the net loss in cultural ecosystem services was US$ 4.86 billion. The net gain of ESVs of regulation was US$ 216 million and the net loss in supporting services was US$ 720,000 million, respectively (Table 11). Specifically, the total net loss of ESV in the forest ecosystem was US$ 12.3 billion which was higher than the overall net loss of 10.8 billion in all ecosystems during 2010 and 2022 (Table 12). Of the total loss of ESV of US$ 12.3 billion in the forest ecosystem, a loss of provision service was US$ 6.23 billion, while the loss of cultural service in the forest ecosystem was US$ 5.78 billion (Table 12). Scrubland lost US$ 84 million ESV between 2010 and 2022 across four categories of ecosystem services. Grassland lost US$ 835 million in the same period. Woodland showed a net gain of USD 105 million while the farmland ecosystem showed a net gain of US$ 2.31 billion between 2010 and 2022 (Table 11). The contribution of cultural services in farmland ESV was US$ 1.01 billion, followed by regulation and provisioning services with net gains of US$ 976 million and US$ 322 million, respectively (Table 11).

Table 11: Losses and gains of ESVs under different ecosystem types between 2010 and 2022

Categories of ES	Ecosystem type					
	Forest	Woodland	Grassland	Farmland	Scrubland	Net change
Provision	-6.23E+09	1.13E+06	-2.51E+08	3.22E+08	-2.01E+07	-6.18E+09
Regulation	-3.13E+08	4.08E+07	-4.46E+08	9.76E+08	-4.23E+07	2.16E+08
Supportive	-7.20E+05	0	0	0	0	-7.20E+05
Cultural	-5.78E+09	6.31E+07	-1.38E+08	1.01E+09	-2.15E+07	-4.86E+09
Net change	-1.23E+10	1.05E+08	-8.35E+08	2.31E+09	-8.40E+07	-1.08E+10

Source: Computed based on data in Annexes 2,3 and 4

4.1.6. Implications of dynamics of ecosystems on specific ecosystem services

The ESV of food service was increased from US$ 798 million in 2010 to US$ 883 million in 2022. Showing a gain of US$ 85 million (Table 12). The ESV of water services was estimated at US$38.6 billion in 2010 but decreased to US$ 35.4 billion in 2022 by losing US$ 4.87 billion. Similarly, the service of regulating water flow was US$ 502 million in 2010 and declined to US$ 462 million in 2022 by losing US$ 39.8 million between the two periods. The ESV of raw materials was declined from US$ 9.75 billion in 2010 to US$ 8.36 billion in 2022 losing US$1.39 billion. The ESV of climatic regulation was estimated at US$775 million in 2010 but decreased to US$ 699 million in 2022 by losing US$ 7.64 million. The ESV of air quality regulation declined from US$ 272 to US$ 242 million between 2010 and 2022. The value of soil erosion prevention was estimated at US$ 123 million in 2010 but decreased to US$ 118 million in 2022 showing a loss of US$ 4.55 million. The loss of ESV of soil fertility maintenance was estimated at US$ 182 million between 2010 and 2022 (Table 12).

Table 12: Trend of the selected ecosystem services within different ecosystems at different periods

Ecosystem services	ESV of ecosystem services in US$ at different periods			
	2010	2015	2022	Change between 2010 and 2022
Food	7.98E+08	8.01E+08	8.83E+08	8.50E+07
Water service	3.86E+10	3.54E+10	3.37E+10	-4.87E+09
Raw materials	9.75E+09	8.91E+09	8.36E+09	-1.39E+09
Air quality regulation	2.72E+08	2.52E+08	2.42E+08	-3.08E+07
Climate regulation	7.75E+08	7.30E+08	6.99E+08	-7.64E+07
Regulation of water flows	5.02E+08	4.77E+08	4.62E+08	-3.98E+07
Maintenance of soil fertility	1.06E+09	9.71E+08	8.81E+08	-1.82E+08
Erosion prevention	1.23E+08	1.20E+08	1.18E+08	-4.55E+06
Maintenance of life genetic diversity	5.52E+06	5.06E+06	4.80E+06	-7.20E+05

Source: Computed based on data in Annexes 2,3 and 4

4.2. Soil loss estimation in the Bale Mountains Ecoregion

The below subheadings provide spatial distribution patterns of erosion-causing factors that determine the extent of soil loss using the RUSEL model.

4.2.1. Spatial characteristics of soil erosion factors

4.2.1.1. Rainfall erosivity factor

The annual rainfall in the BMER appeared to range between 125 and 1216 mm (Fig 5a) whereas the rainfall erosivity R-factor varied from 62 to 675 MJ mm ha^{-1} h^{-1} $year^{1}$ (Fig 5b). A strong erosivity factor was observed in the western parts with a decreasing pattern towards the central part of the BMER. The southern parts were mainly characterized by a small erosivity factor closer to 62 mm $ha^{-1}h^{-1}year^{-1}$ (Fig 5b).

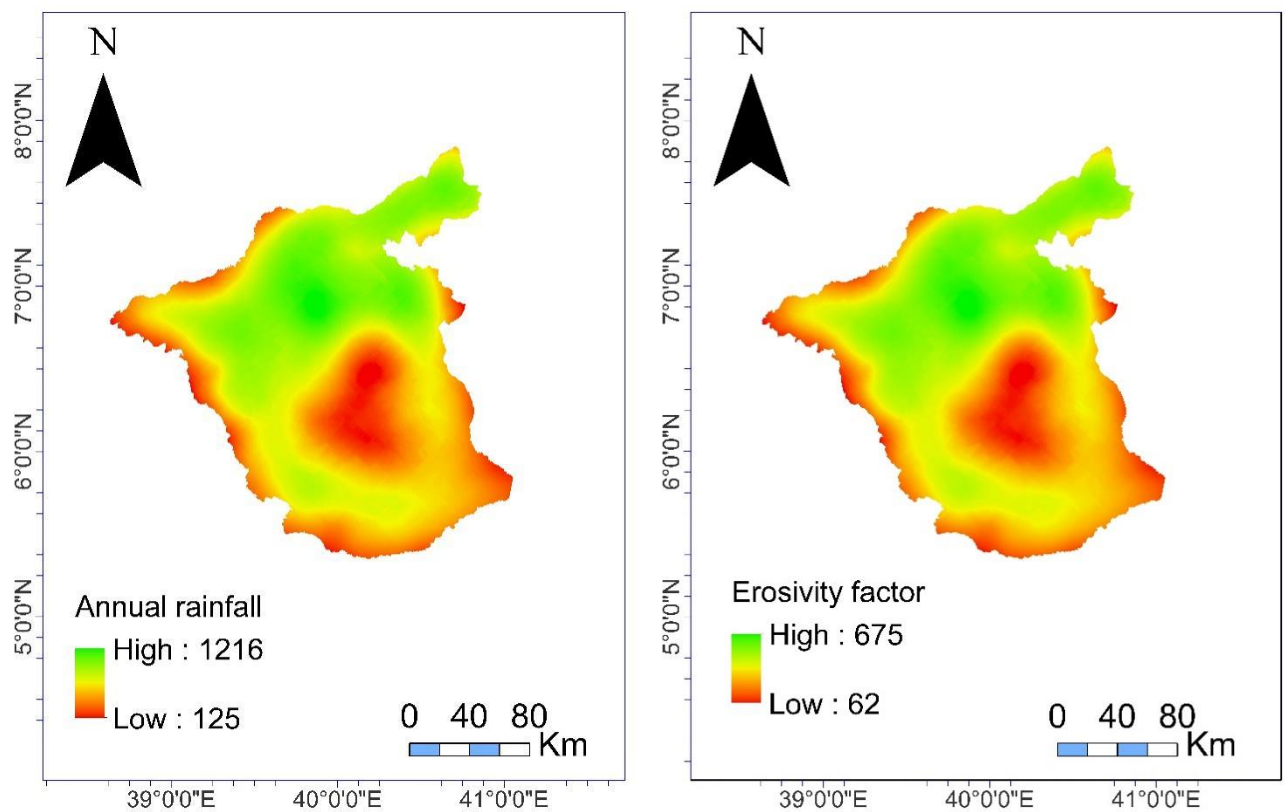

(A) **(B)**

Figure 5: Maps of rainfall in the study area (A) annual rainfall and (B) rainfall erosivity factor

4.2.1.2. Crop management cover (C) factor

The value of the C-factor varied from 0.14 to 0.65 and a higher C-factor value in the year 2010 was observed in the northwest and northeast including the elongated area in the middle of the study area (Fig

6a). Similarly, a higher value of the C factor in the year 2022 was increased to the entire northern parts that broadly extended from west to east (Fig 6b).

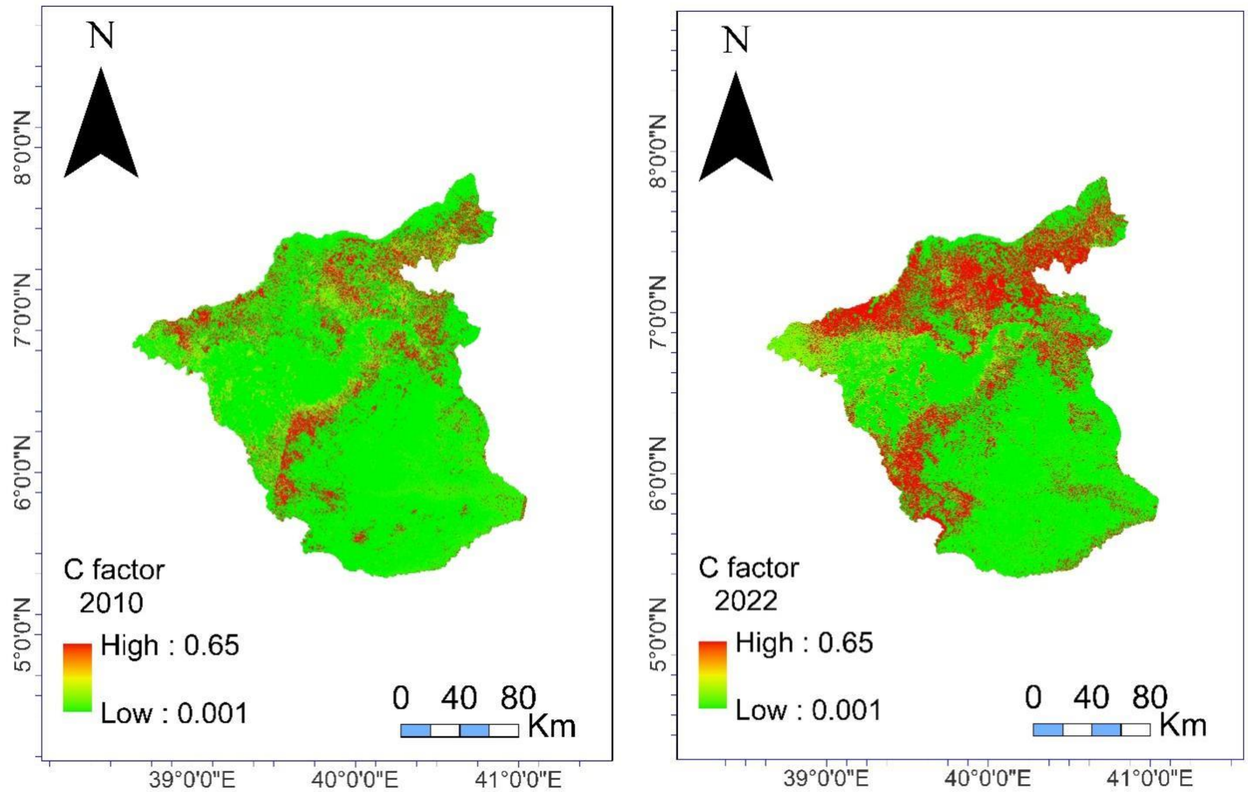

A B

Figure 6: Maps of soil cover management factor (A) in 2010 and (B) C-factor in 2022

4.2.1.3. Conservation practices (P) factor

A higher value of the P factor was observed in the northwest, and northeast including the elongated locations in the central part of the study area on the map of the year 2010 (Fig 7a). Similarly, those areas appeared to show the extended P value on the map of the year 2022 with a considerable increase in a size as compared to its area in the year 2010. The southern and western parts were identified to show somehow a smaller P value in both periods (Fig 7a & b).

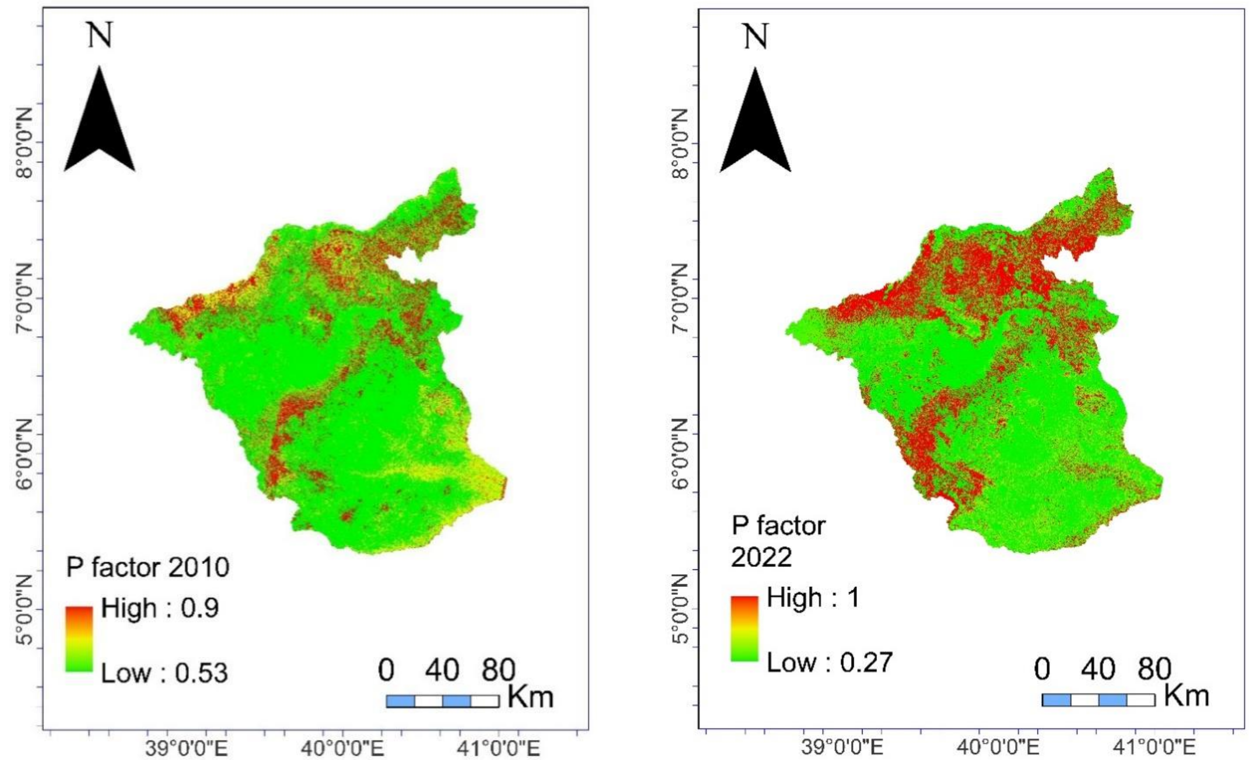

A B

Figure 7: Maps of soil conservation practices (A) P-factor in 2010 and (B) P-factor in 2022

4.2.1.4. Soil erodibility factor

The soil erodibility factor (K) in the BMER varied from 0.24 to 0.32 where a maximum value of 0.32 was associated with *Calcaric regosols* (*Ne*) and *Haplic yermosols* (*Yh*) soil types (Table 13). *Eutric nitosols* (*Ne*) and *Haplic yermosols* soil types showed the same value of the k factor which was 0.31. The most dominant soil types in the BMER were *Eutric nitosols*, *Calcaric regosols*, and *Haplic yermosols* with proportions of 35.3%, 29.5%, and 18.6%, respectively (Table 13). The *Eutric nitosols* were spatially distributed over a large area in the northwest and extended to the central parts of the BMER (Fig 8a). *Calcaric regosols* (*Rc*) soil type was narrowly distributed around the border towards the northeast of the study area. It also occupied the south, southeast, and around central parts (Fig 8a). *Haplic yermosols* (Yh) were distributed around a border in the southwest and expanded inwards to the center from the western parts of the study area (Fig 8a).

Table 13: Soil erodibility factor and its extent in the study area

Soil type	K values	Area in ha	Area in percent
Calcaric regosols (Rc)	0.32	1112192	29.50%
Eutric cambisols (Be)	0.28	142633	3.80%
Eutric nitosols (Ne)	0.31	1333644	35.30%
Ferric acrisols (Af)	0.29	14202	0.40%
Haplic xerosols (Xh)	0.31	120609	3.20%
Haplic yermosols (Yh)	0.32	701279	18.60%
Pellic vertisols(VP)	0.24	30	0.00%
Plinthic ferralsols (Fp)	0.25	350463	9.30%
Sum		3,775,051	100.00%

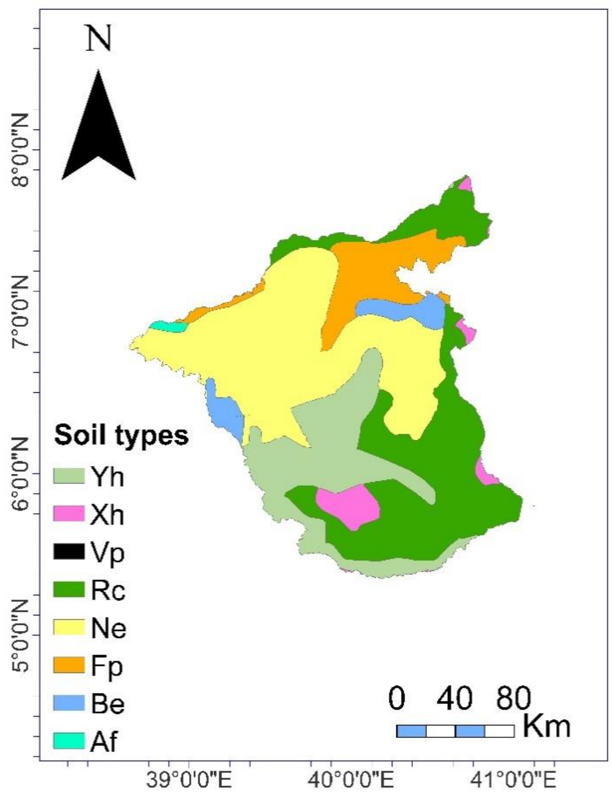

A

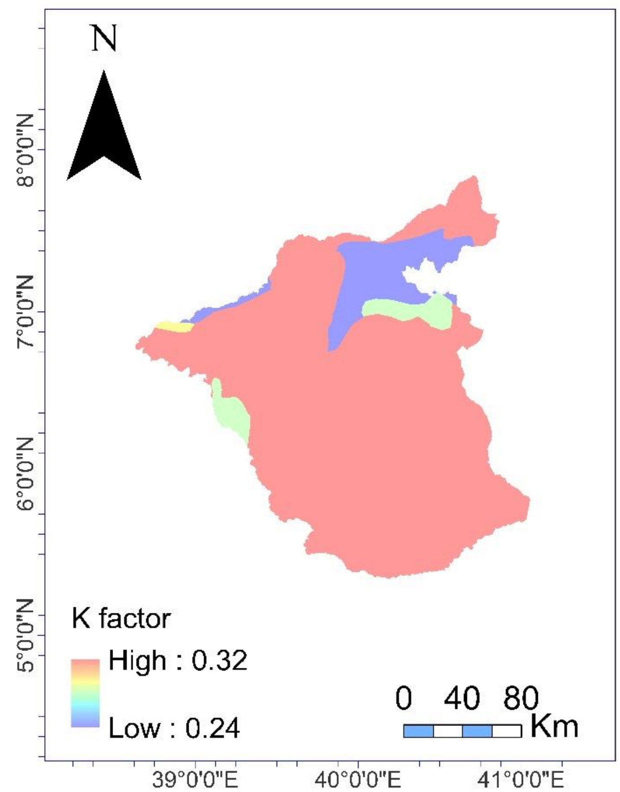

B

Figure 8: Maps of Soil type (A); Soil type and (B) K factor

4.2.1.5. Spatial distribution of slope and LS factors

Figure 9a shows that the central and southern parts of the study area are characterized by a slope below 10%. However, the slope above 40% is mainly confined to the north and northwest parts. The LS factor in the study area was estimated to range from 0 to 3.45 (Fig 9b). Higher LS values appeared to cover areas with a higher slope gradient. A higher LS value was mainly observed around the central parts of the study area (Fig 9b).

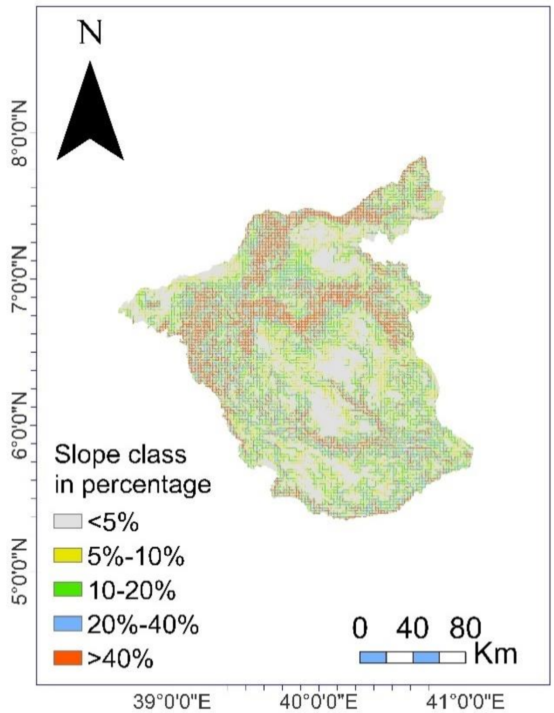

(A)

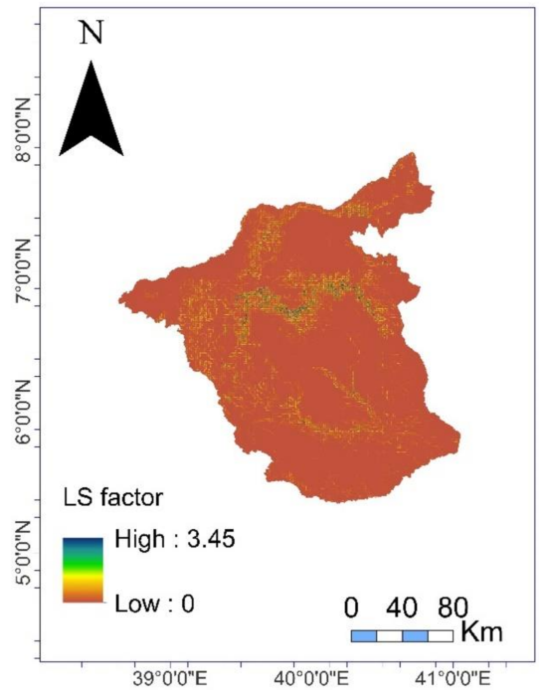

(B)

Figure 9: Maps of topographic features: (A) slope class in percent and (B) LS factor

4.2.1. Soil loss in different severity classes in 2010 and 2022

The total soil loss of the BMER in 2010 was estimated at 4.5 million tons and increased to 7.5 million tons in 2022 (Table 14). The annual mean soil loss varied from 0 to 306 $t^{-1}ha^{-1}yr^{-1}$ in 2010 and slightly increased to 391 $t^{-1}ha^{-1}yr^{-1}$ in 2022 (Table 14, Fig 10a &b). A very slight soil intensity below <5 $t^{-1}ha^{-1}yr^{-1}$ accounted for 61% of the total soil loss in 2010 and 63% in 2022, whereas its area coverage was about 99% of the total area in each period. The spatial distribution maps of soil loss in (Fig 10a &b) showed that the BMER mainly experienced a very slight soil loss with an intensity below 5 $t^{-1}ha^{-1}yr^{-1}$ (Fig 10a &b).

Table 14: Soil loss intensity within different soil loss severity classes in the BMER

Soil loss severity classes		2010				2022			
		Total soil loss		Area coverage		Total soil loss		Area coverage	
Category	t/ha/yr	t/yr	Percent	ha	Percent	t/yr	Percent	Ha	Percent
Very slight	<5	268,781	61%	3,751,351	99.70%	4750636	63%	3,742,912	99.35%
Slight	5-15	873591	19%	9,847	0.30%	1865536	25%	21,250	0.56%
Moderate	15-30	406972	9%	1,778	0.00%	597782	8%	2,669	0.07%
Sever	30-50	235310	5%	559	0.00%	194256	3%	468	0.01%
Very sever	>50	240875	5%	294	0.00%	130905	2%	167	0.00%
Total		4525529	100%	3,763,828	100%	7539113	100%	3,767,467	100%

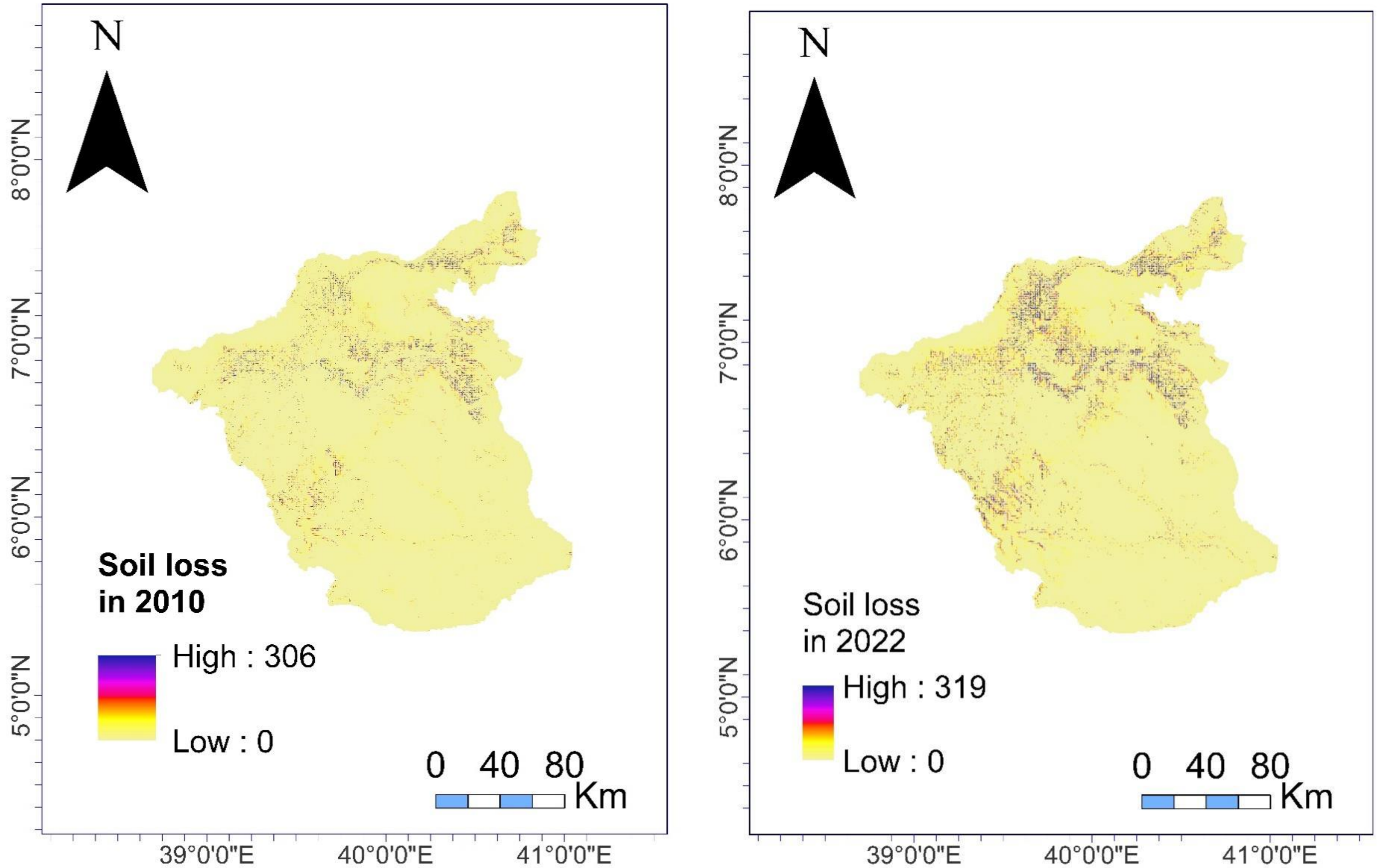

(A) (B)

Figure 10: Maps of spatial distribution patterns of soil loss intensity (A) in 2010 and (B) in 2022

4.2.2. Soil loss intensity within different ecosystems

Soil loss on a farmland accounted for 56.06% of the total soil loss in 2010 with an area coverage of 14% of the total area of the BMER. However, soil loss in farmland increased to 68.9% of the total loss in 2022 covering 25% of the total area. The grassland ecosystem accounted for 10.34% of total soil loss in 2010 but declined to 9.3% in 2022, though, the volume of soil loss was still increasing (Table 15).

Table 15: Soil loss intensity within different LULC classes in the BMER in years 2010 and 2022

Ecosytem types	2010				2022			
	Total soil loss		Area coverage		Total soil loss		Area coverage	
	Tons/yr	Percent	Ha	Percent	Tons/yr	Percent	ha	Percent
Forest	29,923	0.66%	685,459	18	20,557	0.30%	420,994	11
Farmland	2,536,881	56.06%	520,307	14	5,195,401	68.90%	932,390	25
Grassland	467,846	10.34%	333,635	9	699,196	9.30%	366,650	10
Woodland	329,801	7.29%	1,682,474	45	257,205	3.40%	1,468,395	39
Scrubland	131,808	2.91%	526,771	14	163,836	2.20%	533,018	14
Others	1,029,270	22.74%	15,183	0%	1,202,918	16.00%	46,019	1
Sum	4,525,529	100.00%	3,763,828	100	7,539,113	100.00%	3,767,467	100

4.2.3. Soil loss intensities within different slope classes

The steep slope > 40% accounted for 58% of the total soil loss with an area coverage of 270,242 ha in 2010 but its proportion was reduced to 57% in the year 2022 while the area coverage was 270,503 ha. A slope class between 20-40% accounted for 16% of the total soil loss in 2010 and 18% in 2022. A flat slope below 5% showed a total soil loss of 521,974 tons/year in 2010 which accounted for 12% of the total soil loss. However, the total soil loss in the flat slope increased to 814,898 tons/year in 2022 with a proportion of 11% of the total soil loss in 2022 (Table 16).

Table 16: Soil loss intensities within different slope classes

Slope class		Area coverage of slope		2010		2022	
Labeling of slope	Slope class in percent	Ha	%	Total soil loss		Total soil loss	
				t/yr	%	t/yr	%
Flat	<5	2481830	66%	521974	12%	814898	11%
Gentle	5-10	346598	9%	190939	4%	311999	4%
Sloping	10-20	368100	10%	427302	9%	751483	10%
Strong sloping	20-40	296302	8%	737922	16%	1340287	18%
Steep	>40	270242	7%	2645087	58%	4315247	57%
Total		3763073	100%	4523223	100%	7533914	100%

4.2.4. Soil loss intensity within different soil types

The total soil loss in *Eutric nitosols* was estimated at 2,608,622 $t^{-1}ha^{-1}yr^{-1}$ in 2010 and 4,540,856 $t^{-1}ha^{-1}yr^{-1}$ in 2022 accounting for 58% and 60% of the total soil loss, respective (Table 17). *Plinthic ferralsols* (Fp) lost 615,954 tons in 2010 but the total soil loss increased to 925,840 tons in 2022. The total soil loss in *Calcaric regosols* (Rc) was estimated at 533,222 tons in 2010 and 843,055 tons in 2022 while the proportion appeared to decrease from 12% to 11% (Table 17).

Table 17: Soil loss intensities within different soil types in the BMER

Soil type	Area coverage of soil type		2010		2022	
			Total soil loss		Total soil loss	
	Ha	Percent	t/yr	Percent	t/yr	Percent
Eutric nitosols (Ne)	1,327,569	35%	2608622	58%	4540856	60%
Haplic yermosols (Yh)	700,059	19%	503367	11%	860831	11%
Haplic xerosols (Xh)	120,170	3%	33123	1%	56167	1%
Calcaric regosols (Rc)	1,109,608	29%	533222	12%	843055	11%
Pellic vertisols(VP)	27	0%	0	0%	1	0%
Plinthic ferralsols (Fp)	349,776	9%	615954	14%	925840	12%
Ferric acrisols (Af)	14,162	0%	2629	0%	3192	0%
Eutric cambisols (Be)	142,444	4%	228608	5%	309171	4%
Total	3,763,815	100%	4525526	100%	7539113	100%

4.3. Status of ACD and species diversity in the forest of the BMER

4.3.1. Descriptive statistics of above-ground carbon stock and species diversity

The mean above-ground carbon stock (ACD) was estimated at 97.66 $\pm$ 10.129 $t^{-1}ha^{-1}$ in the Dry forest of the BMER, while it was 207.19$\pm$ 16.946 $t^{-1}ha^{-1}$ in the moist forest. The overall mean ACD in both strata was estimated at 173.31 $t^{-1}ha^{-1}$ (Table 18). The mean emission of carbon dioxide equivalent was estimated at 357.51t/ha in Dry forests and 758.40 t/ha in moist forests whereas the overall mean value was 634.39 t/ha (Table 18).

The overall mean species richness (S) was estimated at 10.69 $\pm$0.396 with a maximum mean of 34 species in both strata. The overall mean values of the Shann Weiner index (H') and species evenness (E) were estimated at 1.74$\pm$0.055 and 0.52 $\pm$ 0.033, respectively (Table 18). The mean species richness in the Dry forest was 6.53 which was lower than the mean value of 12.56 species in the moist forest (Table 18). The mean values of the H' and E in the moist forest were 1.98 and 0.61, respectively which were higher than the mean values of 1.22 for the H' and 0.33 for E in the Dry forest ecosystem (Table 18).

Table 18: Descriptive statistics of forest structural attributes in the forest of the BMER

Forest types	Statistical parameters	ACD in t/ha	Co2 equivalent t/ha	S	H'	E
Dry forest	Minimum	0	0	1	0	0
	Maximum	391	1433	26	3	1
	Range	391	1433	25	3	1
	Mean	97.66	357.51	6.53	1.22	0.33
	Std. Error of Mean	10.129	37.082	0.614	0.094	0.057
Moist forest	Minimum	0	0	3	0	0
	Maximum	1468	5373	35	5	1
	Range	1468	5373	32	5	1
	Mean	207.19	758.4	12.56	1.98	0.61
	Std. Error of Mean	16.946	62.015	0.43	0.059	0.038
Both strata	Minimum	0	0	1	0	0
	Maximum	1468	5373	35	5	1
	Range	1468	5373	34	5	1
	Mean	173.31	634.39	10.69	1.74	0.52
	Std. Error of Mean	12.544	45.908	0.396	0.055	0.033

4.3.2. Spatial Dependency of Forest Attributes in a Forest ecosytem

The data of Sqrt-ACD in semi-variogram analysis was fitted to an exponential model with a lag size of 12 and a lag distance of 2620 m at a range of 31,440 meters, where a still-was attained at 43 (Table 19). The Sqrt-ACD exhibited a strong spatial dependency showing a nugget-to-sill ratio of 23% (Table 19). The Shannon wiener index exhibited the spatial autocorrelation over a range of 67,712 meters having a moderate spatial dependency of 45% for a nugget-to-sill ratio. A weak spatial dependency was detected in the data of species evenness having a nugget-to-sill ratio of 64% (Table 19). The semi-variogram for species richness was fitted to an exponential model with a lag size of 12 and a lag distance of 3881 m at a range of 34,446 m, while its still value was attained at 35, with the nugget-to-sill ratio of 28% (Table 19). Fulfilling the requirements of semi-variogram analysis, the spatial distribution maps of species richness, evenness, and Shannon Weiner index were produced using kriging techniques with an acceptable range of prediction errors such as a Root-Mean-Square Standardized Error (RMSSE) of 1.06 for the species evenness and 1.014 for the Shannon-Weiner index. The RMSSE of 1.07 for Sqrt-ACD and 0.29 for species richness (Table 20).

Table 19: Spatial dependency of forest attributes in semi-variogram

Values of forest attributes				
Parameters	S	H’	E	Sqrt-ACD
Model type	Exponential	Gaussian	Exponential	Exponential
number of lags	12	8	10	12
Lag size	3881	9122	6244	2620
Range	34,446	67,712	62,446	31,440
Nugget	5	0.34	0.028	10
Partial sill	30	0.41	0.016	33
Sill (nugget + partial sill)	35	0.75	0.044	43
Nugget-to-sill ratio	28%	45%	64%	23%

Table 20: Prediction accuracy of forest structural attributes

List of attributes of forest ecosystem	RMSSE
S	0.29
H'	1.01
E	1.06
Sqrt-ACD	1.07

4.3.3. Spatial distribution of above-ground carbon stock and species richness

The ACD between a range of 63 to 118 t/ha occupied 570,614 ha of forest area accounting for 54% of the total forest area in the BMER (Table 21). This range of ACD class occupied the northern, northeast, and northwestern parts of the forest of the BMER (Fig 11a). The highest ACD class with a range of 283 to 336 t/ha covering 3,218 ha accounting only for 0.3% of the total forest area (Table 21). Spatially, this class of ACD was observed in a very localized area in the Mena Angetu forest to the south of the BMNP (Fig 11a). The ACD class in the range of 118 to 172 t/ha occupied 321,357 ha with a proportion of 30% of the total forest area (Table 21). This class was spatially distributed in the south and southwestern parts of the forest in Mana Anagetu, Harana Kokosa forests, and in southern parts of the Bale Mountains National Park (BMNP) shown in (Fig 11a).

Species richness class between 6.84 to 11.13 occupied 36,7362 ha with a proportion of 35% of the total forest area (Table 21). This class was mainly distributed in the Harana Kokosa, and Goro Bele forests including in the BMNP closer to the southern border of the park (Fig 11b). The highest species richness class of 24.00 to 28.29 occupied 877 ha of forest land having a proportion of 0.1% (Table 21); and spatially was confined to the southwestern parts of Mana Angetu forest (Fig 11b). The lowest species richness class with a range of 2.55 to 6.84 occupied 32% of the total forest area showing spatial distribution in Adaba Dodola, Aloshie Batu, and Kubyu forests (Fig 11b). Species richness class of 6.84 to 11.13 occupied 1,058,329 ha with 35% of the total forest area and spatially distributed in Goro Bele, Harana Kokosa forests, and in some parts of the BMNP (Fig 11b).

Table 21: Distribution of ACD and species richness in high forest areas of the BMER

ACD in ton /ha	Area in ha	Percentage	Species richness (S)	Area in ha	Percent of area
11 – 63	76171	7%	2.55 - 6.84	342096	32%
63 – 118	570614	54%	6.84 - 11.13	367362	35%
118 – 172	321357	30%	11.13 - 15.42	245618	23%
172 -227	75227	7%	15.42 - 19.71	59871	6%
227 – 282	11741	1%	19.71-24.00	42506	4%
282 – 336	3218	0.30%	24.00- 28.29	877	0.10%
Sum	1058329	100%	Sum	1058329	100%

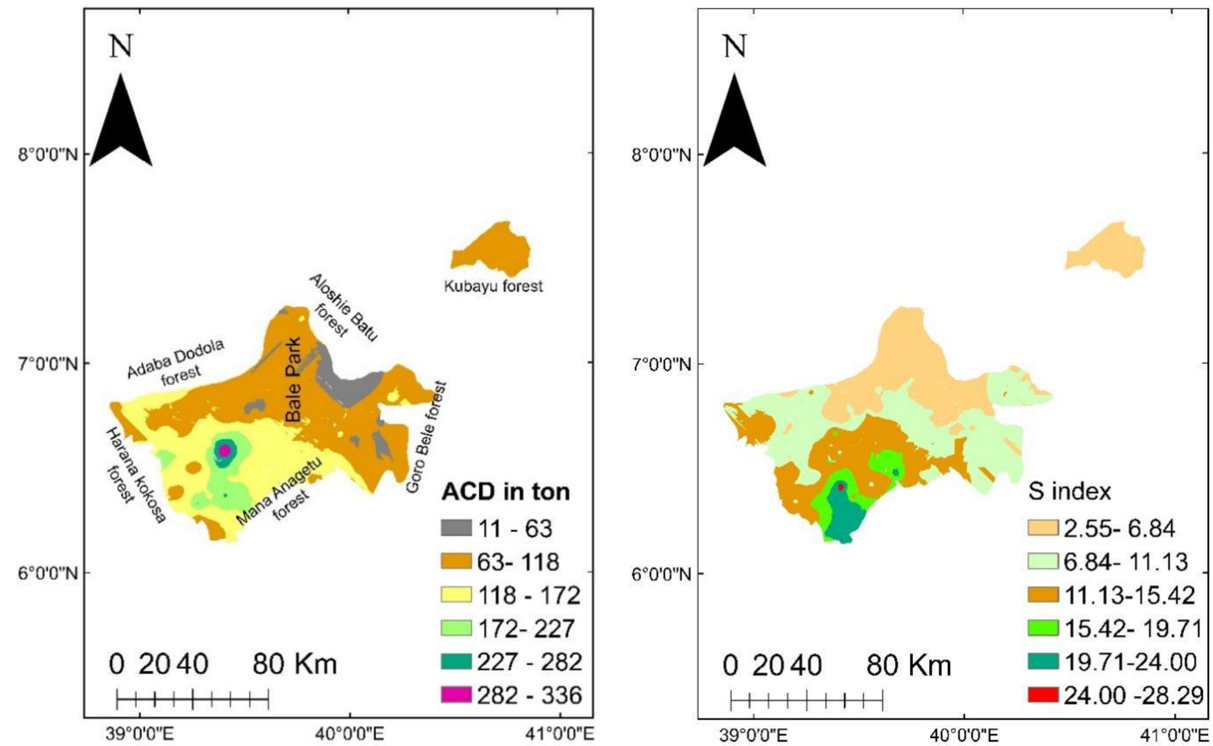

(A) Map of ACD per ha (B) Map of species richness index

Figure 11: Spatial distribution maps of ACD and species richness

4.3.4. Spatial distributions of species diversity indices

The Shannon Weiner index in a range of 1.67 to 2.97 distributed over a total forest area of 204,982 ha that accounted for 19% of the total forest area (Table 22) and its spatial distribution narrowly elongated from Goro Bele to Harana Kokosa forest crossing the southern parts of the BMNP (Fig 12a). The highest Shannon Weiner index class of 2.33 to 3.11 occupied 101,557 ha with a proportion of 10% of the total forest area (Table 22). This highest class was mainly distributed in the southern parts of the Mana Angetu forest closer to the edge of the forest boundary in the southern parts of (Fig 12a). The lowest Shannon Weiner diversity class of 0.57 to 1.02 was detected in the eastern parts of Adaba Dodola forest adjacent to Aloshie Batu forest including its northern part (Fig 12a). The Shannon Wiener index in the class of 1.33 to 1.67 occupied a large coverage with 27% of the total area (Table 22). This class looks to be elongated narrowly from east to western parts crossing the middle parts of the forest in the BMER (Fig 12a).

The species evenness class from 0.44 to 0.57 occupied 562,656 ha with a proportion of 53% of the total forest ecosystem (Table 22). This class was entirely distributed in Harana Kokosa, Goro Bele, and

BMNP (Fig 12b). The species evenness index class of 0.3 to 0.44 occupied 32% of the total forest area covering 342,770 ha (Table 22) with abundant spatial concentration in Adaba Dodola and Aloshe Batu forests. The highest species evenness class with a range of 0.70 to 0.84 was observed in southwest parts of the Mana Angetu forest. The species evenness class of 0.44 to 0.57 covered large parts of forests in the Harana kokosa, Goro Bele, and western parts of BMNP (Fig 12b). The entire forest parts of Adaba Dodola were associated with the species evenness index of 0.30 and 0.44 (Fig 12b).

Table 22:Tree species indices class and area coverage in the forest priority areas of the BMER

H' class	Shannon Weiner		Evenness index (E)		Percent of area coverage
	Area in ha	Percent of area coverage	Class of E	Area in ha	
0.57 -1.02	152178	14%	0	0.09	0.00%
1.02- 1.36	184394	17%	0.17 -0.30	23648	2%
1.36 -1.67	281210	27%	0.3- 0.44	342770	32%
1.67- 2.97	204982	19%	0.44- 0.57	562656	53%
2.97- 2.33	134008	13%	0.57- 0.70	129173	12%
2.33-3.11	101557	10%	0.70 - 0.84	82	0.01%
Sum	1,058,329	100%		1,058,329	100%

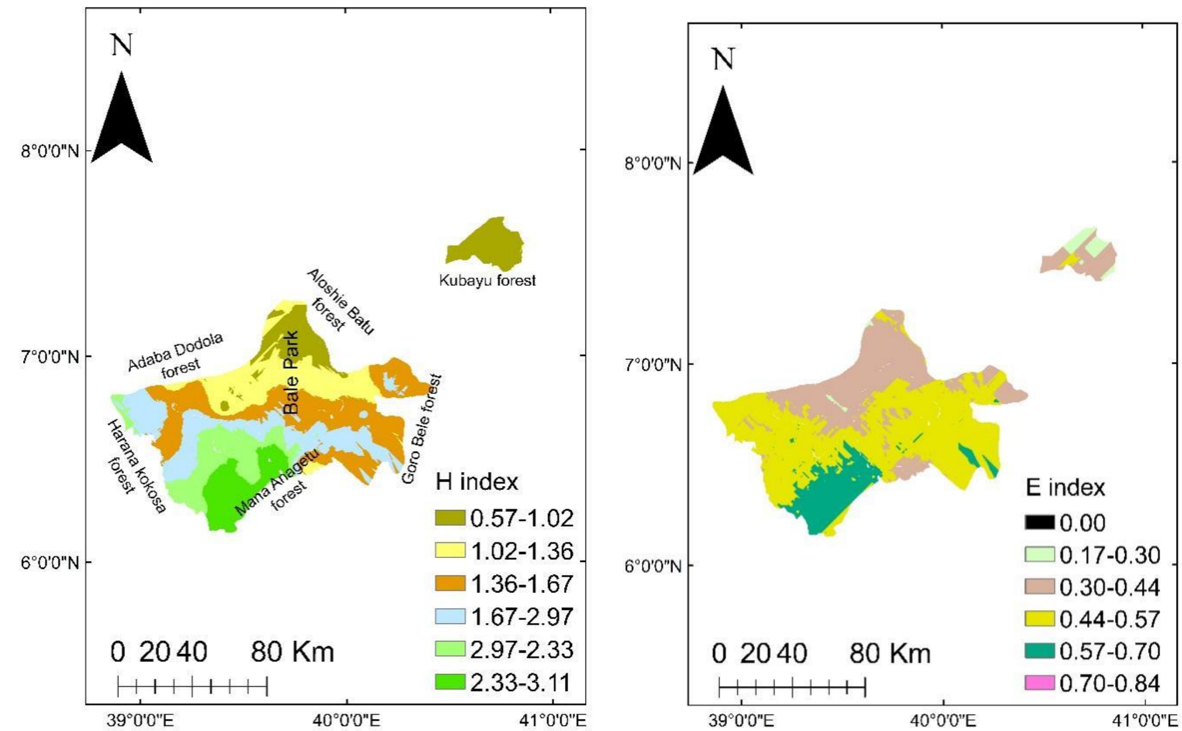

(A) Map of Shannon Weiner index (B) Map of species evenness index

Figure 12: Spatial distribution maps of Shannon Weiner diversity and species evenness

4.3.5. Impact of deforestation on tree species richness, species diversity, and evenness

A deforestation of 17,384 ha occurred in the forest area of the BMER between 2010 and 2022 (Table 23 and Fig 13). The zonal statistical analysis in the ArcGIS map revealed that deforestation of 10,356 ha (60%) of total deforestation resulted in a loss of species richness class of (6.84 to 11.13). between 2010 and 2022. Similarly, the deforestation of 3,759 ha of forest resulted in the loss of richness class of (2.55 to 6.88) as shown in (Table 23). The conversion of 7,745.76 ha of forest area ended with the loss of Shannon Weiner's diversity index in the range of (1.36 to 1.67); whereas the destruction of 4,978.08 ha caused a loss of the species evenness class of (0.44 to 0.57).

Table 23: Extents of species diversity losses due to deforestation between 2010 and 2022

Species richness (S)			Shannon Weiner index (H')			Species evenness index (E)		
S classes	Deforested area in ha	Percent	H' class	Deforested area in ha	Percent	E Class	Deforested area in ha	Percent
2.55- 6.84	3759	22%	0.57 -1.02	1129.95	7%	0	0	0
6.84- 11.13	10356	60%	1.02- 1.36	2212.11	13%	0.17-0.30	1496.7	1%
11.13- 15.42	2970	17%	1.36 -1.67	7745.76	45%	0.3- 0.44	49605.3	29%
15.42 - 19.71	230	1.30%	1.67- 2.97	4978.08	29%	0.44-0.57	118243.8	68%
19.71-24.00	67	0.40%	2.97- 2.33	1082.07	6%	0.57-0.70	4488.3	3%
24.00- 28.29	2	0.00%	2.33-3.11	235.71	1%	0.70 -0.84	2.7	0%
Sum	17384	100%		17384	100%		17384	100%

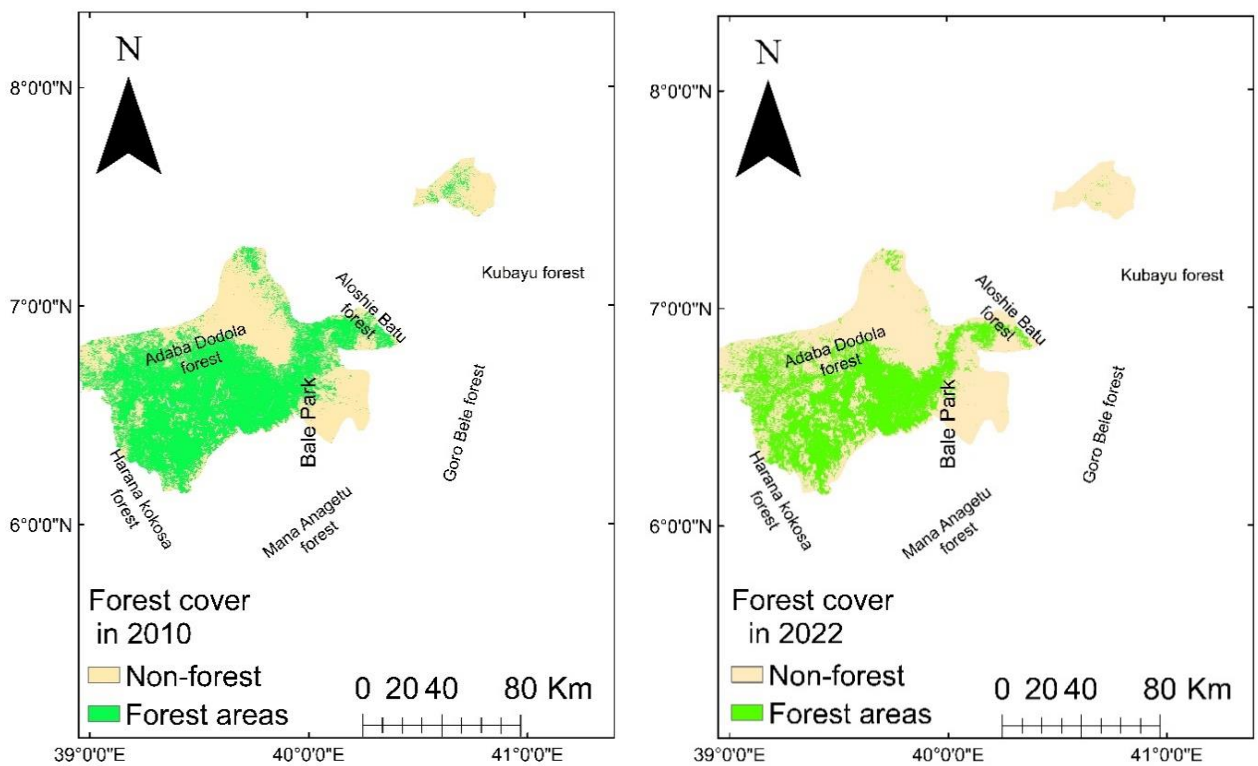

(A) Forest cover in 2010 (B) Forest cover in 2022

Figure 13: Spatial extents of forest cover in BMER at different periods

4.4. Spatial distribution of above-ground carbon stock in the Harana Forest

4.4.1. Description of the Biophysical Predictors of the ACD

The mean values of species richness and Shannon Weiner diversity index per plot were estimated at 9.7 and 1.14, respectively (Table 24). The mean proportion of clay content ranged from 37% to 40% while the mean soil organic content varied from 51.92% to 59.26%.

Table 24: Descriptive statistics of predictor variables based on the data of 1122 sample plot

Predictors	Mean	Std. Error	Minimum	Maximum
Species richness(SR)	9.7	0.16	1	29
Shannon index (H)	1.14	0.02	0.00	3.96
Elevation in m a.s	172.65	0.84	130	289
Slope in %	4.12	0.17	0	74
Temperature C^0	20.36	0.09	17	31
Precipitation in mm	1000	2.62	765	1127
Clay0 in%	37.19	0.12	24	47
Clay05 in%	37.44	0.11	24	47
Clay15 in%	40.62	0.12	25	51
Silt0 in%	26.51	0.08	20	35
Silt0 in%	26.2	0.08	19	34
CEC0 in%	38.38	0.23	25	70
CEC05 in%	33.37	0.11	24	54
CEC15 in%	31.74	0.1	22	51
SOC0 in%	59.26	0.55	22	122
SOC05 in%	51.92	0.38	29	100

4.4.2. Descriptive statistics of ACD in Harana forest

The mean ACD in the Harana forest was estimated at 131.505 t ha^{-1} ha while the carbon emission was estimated at 482.613_CO_2 equivalent in t ha^{-1} (Table 25).

Table 25: Descriptive statistics of the Biomass, ACD, and CO_2 equivalent

Parameters	Mean in ton ha^{-1}	Std. Error
Biomass	263.004	8.83
ACD	131.505	4.415
CO_2 equivalent	482.613	16.203

4.4.3. Contributions of dominant tree species in carbon storage

The analysis of ACD in each tree species showed that 65% of the total ACD in the Harana forest was occupied by 11 dominant forest tree species (Table 26). *Podocurpus falcatus* and *Szygium guinesses* alone occupied 22 % of the total ACD, with an equal proportion of 11% (Table 26).

Table 26: Quantity of different parameters in dominant tree species of all sample plots

Species	Biomass (ton ha^{-1})	ACD (ton ha^{-1})	Percentage of all species ACD
Podocarpus falcatus	1646.61	823.31	11%
Szgium guinesses	1593.87	796.93	11%
Croton macrostachyus	969.47	484.74	7%
Vepris dainellii	844.98	422.49	6%
Pouteria adolfi-friedericii	831.78	415.89	6%
Feliucium decipenses	675	337.5	5%
Octea gunieses	650.42	325.21	4%
Diospyros abyssinica	622.72	311.36	4%
Celtis africana	549.25	274.63	4%
Warburgia ugandensis	536.08	268.04	4%
Millettia ferruginea	398.69	199.35	3%

4.4.4. Spatial distribution pattern of ACD in the Harana forest ecosystem

The spatial distribution map of ACD with high and low density was produced using the RF model achieving an overall accuracy of 72%. A high class of ACD was confined to the eastern part of the Harana Forest Ecosystem (Fig 14a). A high-high clustering of ACD was observed in the eastern and southwestern parts of the Harana forest. Conversely, the central and northwest parts were characterized by a low-low clustering (Fig 14b).

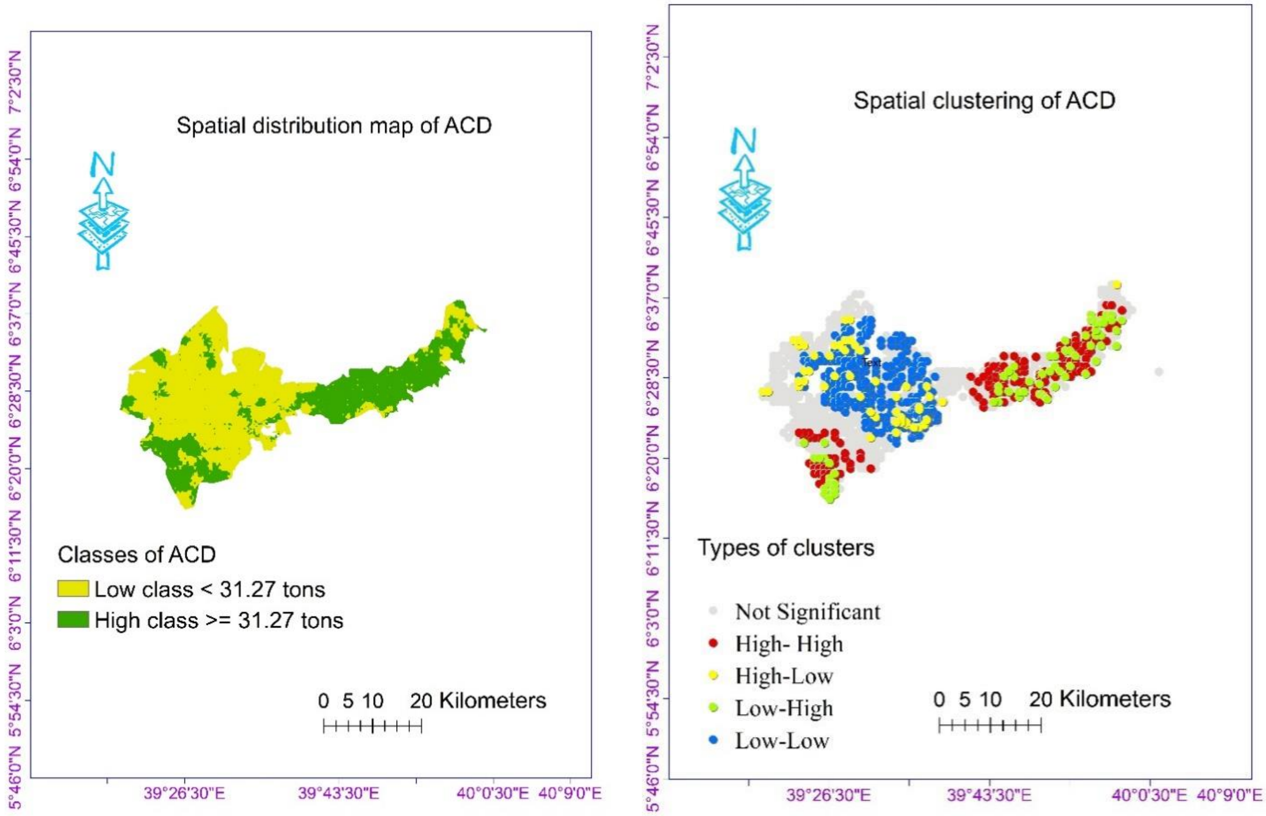

(A) (B)

Figure 14: Map showing (A) spatial prediction of ACD, and (B) Spatial clustering of the ACD

4.4.5. Importance of predictor variables in influencing above-ground carbon density

The importance of each biophysical predictor in the Random Forest model was identified using Mean-Decreased-Gini values. The most important variables that influenced the spatial distribution of ACD were identified to include the species richness, Shannon-Weiner index, *Filicium decipiens*, *Olea Capensis, SOC05, Podocarpus falcatus, and CEC15*. On the other hand, elevation, precipitation, temperature, slope, and slope aspects exhibited less impact on the spatial distribution of ACD having the ranks of 16^{th}, $17^{th,}$ 19^{th}, 20^{th}, and 21^{st}, respectively (Table 27).

Table 27: Importance of predictor variables in predicting the spatial distribution of ACD

Predictors	Designation	Gini value	Rank
Species richness	S	46	1
Shannon-Weiner index	H’	43	2
Filicium decipiens	*F. decipiens*	33	3
Olea capensis	O. capensis	27	4
Soil organic content % at 05cm depth (%)	SOC05	26	5
Podocarpus falcatus	*P. falcatus*	26	6
Cation exchange capacity % at 15cm depth	CEC15	24	7
Soil organic content % at 0 cm depth (%)	SOC0	24	8
Soil cation exchange capacity % at 0cm depth	CEC0	23	9
Silt content % at0cm depth (%)	Silt0	23	10
Clay soil content at 5 cm (%)	Clay05	22	11
Szgium guinesses	*S. guinesses*	22	12
Cation exchange capacity (%) at 05cm depth	CEC05	22	13
Silt content %5cm depth (%)	Silt05	21	14
Clay soil content at 15 cm (%)	Clay15	21	15
Elevation	Elevation	20	16
Precipitation	Precipitation	20	17
Clay soil content at 0 cm (%)	Clay0	19	18
Temperature	Temperature	18	19
Slope in %	Slope in %	17	20
Aspect	Aspect	14	21

4.4.6. Association between ACD clustering area and biophysical variables

The species richness and species diversity in this study showed a strong positive correlation with the high-high cluster of ACD at ($p < 0.01$) in (Table 28). Tree height, DBH, and tree density were positively correlated with the high-high clustering areas of ACD at ($p < 0.01$). The clay soil and organic contents at various soil depths were positively correlated with the high-high clustering areas of ACD ($p < 0.01$). Silt content and CEC showed negative correlations with the high-high clustering areas of ACD at ($p < 0.01$).

Table 28: Pearson correlation coefficient between clustering of ACD and each biophysical variable

Biophysical variable	Pearson correlation		Biophysical variable	Pearson Correlation
Species richness	0.625**		Silt15	-0.204**
Species diversity	0.530**		Silt30	-0.163*
DBH	0.750**		Silt60	-0.172*
Tree height	0.659**		Silt 1	-0.212**
Coffee density	0.215**		Silt2	-0.207**
Tree density	0.500**		Sand2	0.180*
Elevation	-0.015		CEC0	-0.365**
Slope	0.044		CEC05	-0.442**
Temp	0.119		CEC15	-0.466**
Precipitation	-.180*		CEC15	-0.484**
Clay0	0.201*		CEC1	-0.432**
Clay05	.220**		SOC0	0.164*
Clay15	0.234**		SOC05	0.490**
Silt0	-0.216**		SOC15	0.257**
Silt05	-0.204*		SOC1	0.187*

***significant at $p < 0.01$, * significant at $p < 0.05$*

4.4.7. Ecological response of above-ground carbon density to biophysical factors

The scatter plot analysis in this study indicates that an increase in species richness and Shannon Weiner indices positively contribute to more ACD (Fig 15a & b). The ACD decreased beyond an elevation of 1400 m asl but with abrupt oscillation, it exhibited a peak around 2490 m asl (Fig 15c). The increase in annual precipitation appeared to reduce the quantity of ACD (Fig 15 E). Regarding temperature, ACD showed increasing at a temperature of 19°C and followed a uniform pattern beyond a temperature of 19.5^{0}c (Fig 15 F).

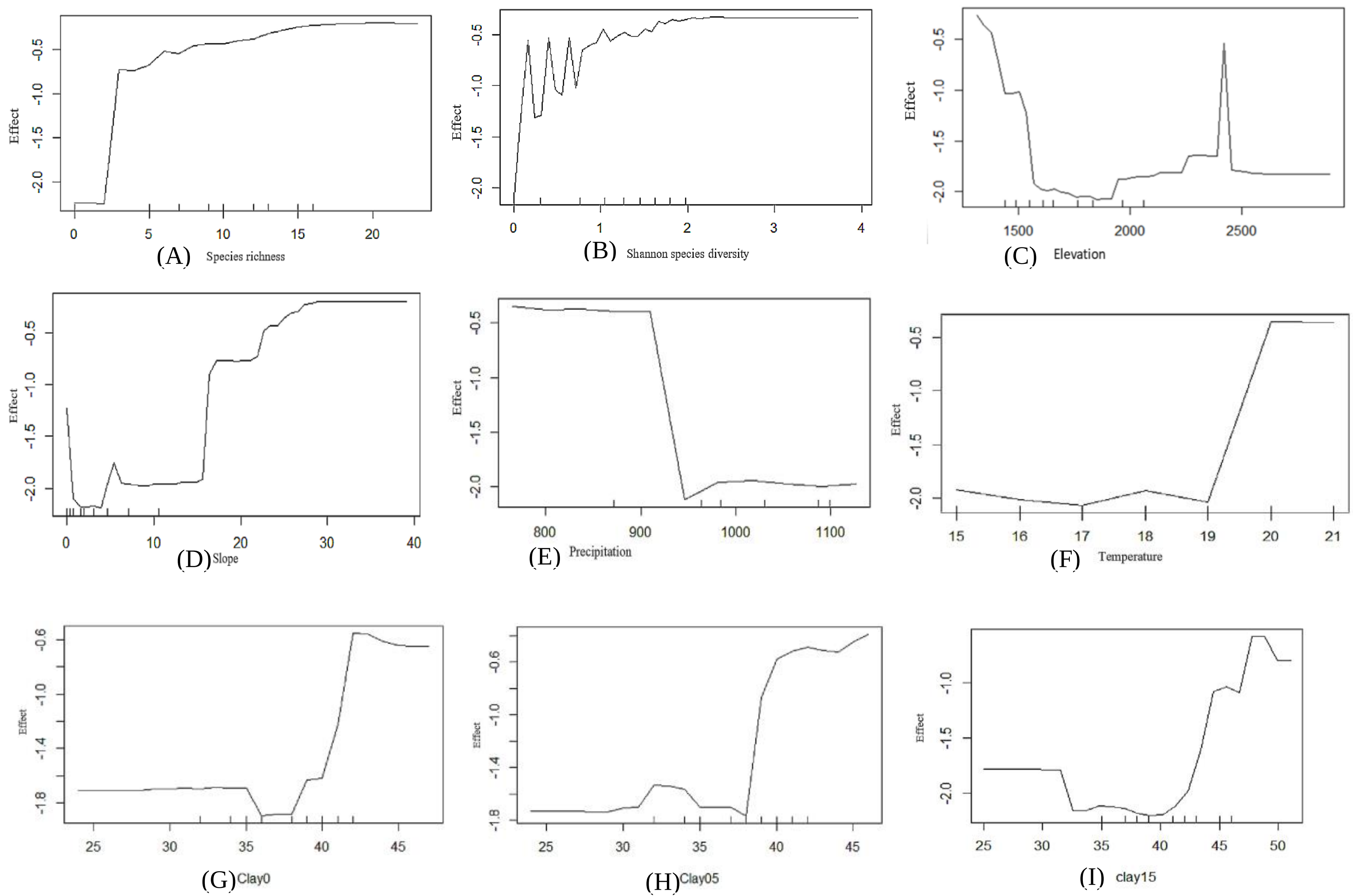
(A) Species richness
(B) Shannon species diversity
(C) Elevation
(D) Slope
(E) Precipitation
(F) Temperature
(G) Clay0
(H) Clay05
(I) clay15
Effect

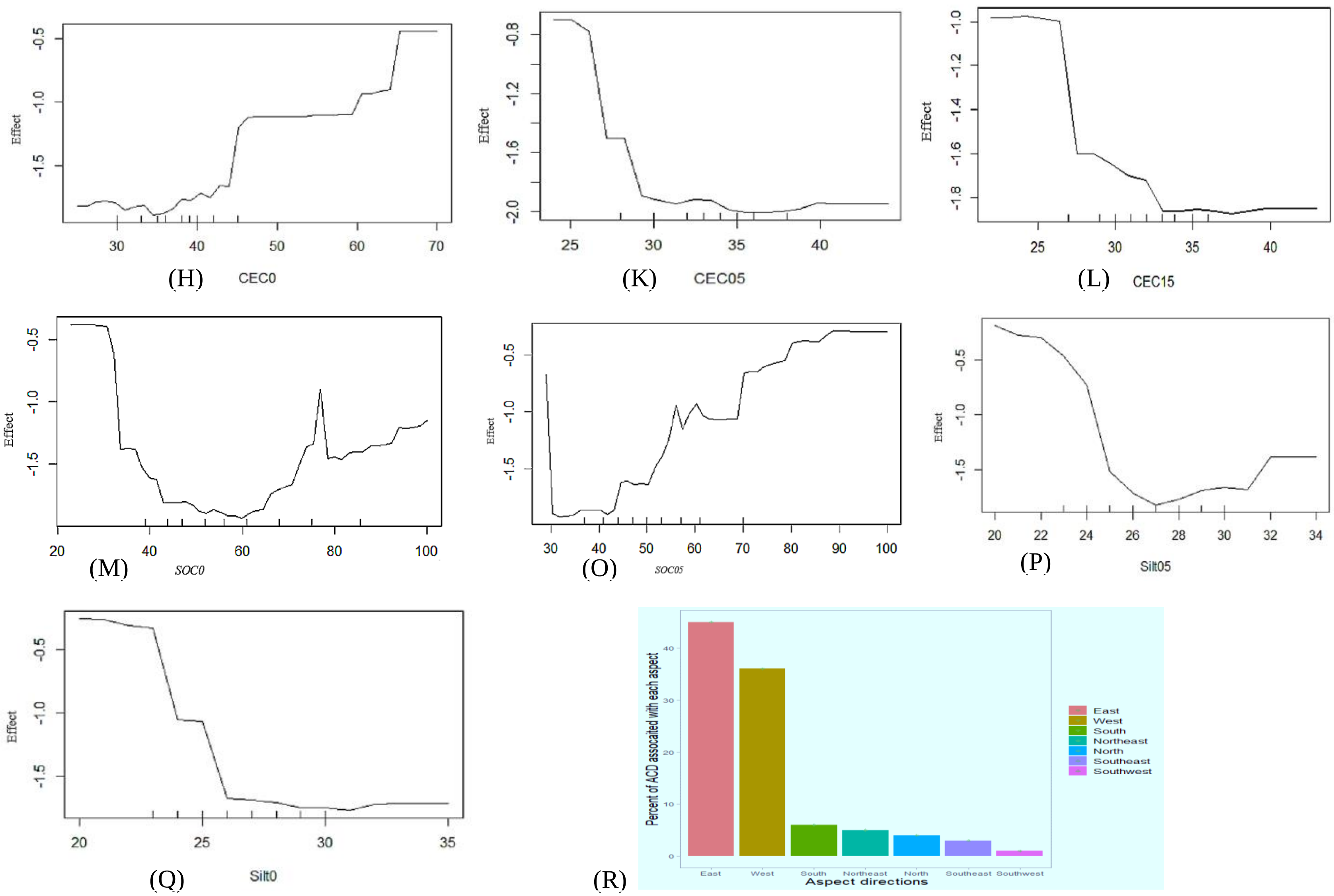

Figure 15: Partial dependency of predicting variables on the spatial distribution of ACD

4.5. Spatial distribution of woody species diversity in the Harana forest

4.5.1. Descriptive statistics of tree abundances and frequencies

The mean abundance of eight woody species was estimated at 2,404 plants per plot of 0.065ha. The Mean abundance of *C. arabica* was 1,395 individuals per plot, accounting for 58% of the total abundance of all woody plant species. The mean abundance of *F. decipenses* was 376 individuals plot^{-1} with a relative abundance of 16%. The mean of *P. falcatus* was 68 individuals plot^{-1} with a relative abundance of 3% while its relative frequency was 39%. *O. capensis* was identified as the smallest woody species in terms of a relative abundance of 1% and a relative frequency of 22% (Table 29).

Table 29: Descriptive statistics of eight woody species in the Harana forest

Species name	Frequency	Relative frequency	Mean Abundance	Relative abundance	Std. Error (+/-)
Coffea arabica	449	40%	1395	58%	99.57
Podocarpus falcatus	434	39%	68	3%	5.8
Croton macrostachyus	570	51%	60	2%	7.24
Celtis Africana	491	44%	236	10%	20.8
Syzygium guineense	384	34%	70	3%	11.01
Olea capensis	245	22%	19	1%	5.42
Diospyros abyssinica	318	28%	178	7%	18.34
Feliucium decipenses	350	31%	376	16%	57.82
Overall mean stem density			2402	100	150

4.5.2. Descriptive statistics of tree stem density within different DBH classes

Small trees with DBH < 10 cm accounted for 16% of the total stem density for each of *P. falcatus and D. abyssinica*, while each of *C. macrostachyus and F. decipenses* accounted for 11% (Table 30). *S. guineense, O. capensis,* and *C. african* were characterized by a small proportion of the stem density for DBH < 10 cm. A large proportion of stem density per ha in each species consisted in the DBH class of 20-60 cm while a proportion of stem density was few in the DBH class that exceeded 60 cm.

Table 30: Stem density of each tree species per ha and its proportion in the Harana Forest

DBH classes	*S. guineense*	*P. falcatus*	*D. abyssinica*	*C. macrostachyus*	*O. capensis*	*F. decipenses*	*C. african*
<10	5%	16%	16%	11%	5%	11%	8%
10-20	13%	20%	17%	19%	6%	25%	13%
20-30	16%	12%	19%	19%	11%	25%	15%
30-40	16%	9%	20%	13%	11%	14%	16%
40-50	12%	9%	9%	11%	12%	10%	18%
50-60	11%	9%	8%	10%	15%	7%	11%
60-70	8%	7%	3%	5%	9%	4%	7%
70-80	6%	5%	3%	4%	11%	2%	5%
80-90	4%	5%	2%	4%	9%	2%	4%
90-100	7%	5%	2%	3%	6%	0%	4%
>100	2%	2%	0%	2%	4%	2%	0%
Proportion	100%	100%	100%	100%	100%	100%	100%
Tree /ha	86	91	58	73	54	90	67

4.5.3. Prediction outputs of the Random Forest

The RF modeling exercise identified that elevation, mean annual temperature, annual precipitation, clay soil content, and available potassium were the major variables to govern the spatial distribution of abundances of many woody species (Fig 16). Specifically, the distribution of the log abundances of *C. arabica* was mainly affected by the annual precipitation, elevation, silt content, mean annual temperature, and clay soil content. The spatial distribution of *P. falcatus* appeared to be influenced by the mean annual temperature, calcium, available potassium, clay content, and carbon-to-nitrogen ratio. The abundance of *F. decipenses* was mainly influenced by elevation, cation exchange capacity (CEC), mean annual temperature, available potassium, and annual precipitation (Fig 16).

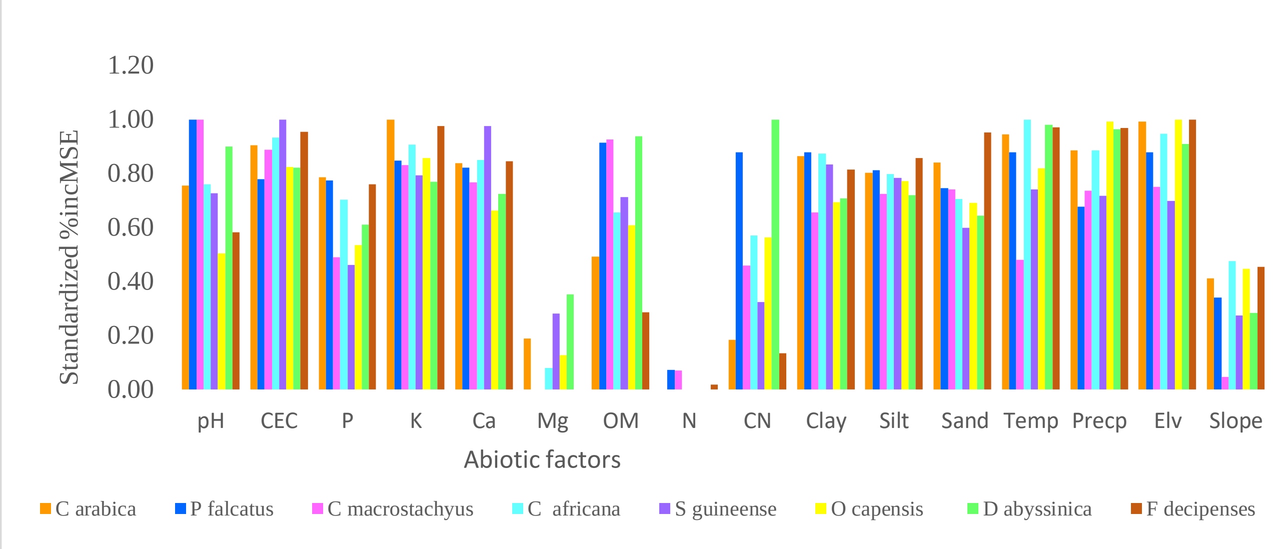

Figure 16: Strength of predicting factors on abundances based on the standardized %incMSE value

4.5.4. Prediction outputs of artificial neural networks

ANNs showed that elevation exerted a negative impact on the log abundances of all species (Table 31). The ANNs showed that SOM was positively related to the log abundances of all species while a strong positive relationship was detected with the log abundances of *D. abyssinica*, and *C. africana*. Total nitrogen exhibited a negative impact on the majority of the log abundances of woody species with a strong negative impact on the log abundances of *C. macrostachyus* and *F. decipenses*. A carbon-to-nitrogen ratio could exhibit a positive effect with all species, except a negative effect was detected on the log abundances of *C. arabica F. decipenses*, and *C. macrostachyus*. Available phosphorus tends to negatively affect the log abundances of all species except a positive impact on the log abundances of *C. arabica* and *F. decipenses*. Available potassium displayed a negative impact on the log abundances of all species apart from the log abundances of C. *arabica*, *C. macrostachyus*, and *S. guineense*. Precipitation exerted strong negative impacts on the log abundances of *D. abyssinica* while temperature appeared to show a positive effect on *F. decipenses* (Table 31).

Table 31: Impacts of variables on abundances of species in terms of Standardized Olden value using ANNs

Variable	*C. arabica*	*P. falcatus*	*C. macrostachyus*	*C. africana*	*S. guineense*	*O. capensis*	*D. abyssinica*	*F. decipenses*
Soil pH	0.2	-0.5	2.7	-0.2	-0.1	-0.1	-0.2	0.3
CEC	0.7	-0.4	0.5	0.0	0.1	-0.3	-0.3	1,0
Phosphorus	0.1	-0.6	-0.8	-0.3	-1.5	-0.4	-0.5	0.5
potassium	0.0	-0.6	0.4	-0.2	0.1	-0.3	-0.3	-0.6
Calcium	0.3	-0.5	0.8	-0.2	-0.4	-0.4	-0.6	0.3
Magnesium	-3.8	3.0	0.0	-2.1	0	-0.5	-0.2	0.1
SOM	0.9	2.1	0.4	3.4	2.2	2.6	3.7	1.1
Nitrogen	-0.2	-0.5	-2.3	0.6	-1.1	-1.1	0.2	-2.6
C/N	-0.2	1.0	-0.2	0.5	2.7	2.7	1.0	-0.1
Clay content	0.7	-0.5	0.4	0.0	-0.3	-0.2	-0.3	0.6
Silt content	0.1	-0.5	0.0	-0.3	-0.2	-0.2	-0.2	0.5
Sand content	0.7	-0.7	0.0	-0.3	-1.0	-0.8	-0.1	-0.6
Temperature	0.3	-0.2	0.0	0.0	0.2	-0.3	-0.3	0.9
Precipitation	0.0	-0.2	-0.1	-0.2	0.0	0.1	-0.4	0.3
Elevation	0.0	-0.2	-1.5	-0.3	-0.4	-0.3	-0.6	-2.2
Slope	0.1	-0.5	-0.2	-0.2	-0.3	-0.2	-0.3	-0.1

4.5.5. Generalized Linear Model (GLM)

The GLM parameter estimates indicated that elevation showed a significant negative relationship with the log abundances of C. *arabica*, *C. macrostachyus*, *C. africana*, and *D. abyssinica*, while a positive effect of elevation showed only with the log abundance of *P. falcatus* $p< 0.05$ (Table 32). SOM appeared to show a positive impact on the log abundances of all species, but a significant effect was detected only with the log abundance of *C. africana* at $p<0.05$. A CN ratio exhibited a positive impact on the log abundances of *P. falcatus*, *C. africana*, *O. capensis*, and *F. decipenses*, whereas a significant negative effect was detected with the log abundance of *C. arabica* $p<0.05$. Available phosphorus and available potassium exhibited significant negative impacts on the log abundances of C. *arabica*, *P. falcatus*, *C. africana*, and *F. decipenses*. Annual precipitation showed a significant negative impact on the log abundances of *C. arabica*, *C. macrostachyus*, and *C. africana*. A mean annual temperature posed a significant negative impact on the log abundances of *C. macrostachyus* but a positive effect on the log abundance of *S. guineense* at $p< 0.05$ (Table 32).

Table 32: Parameter estimates of predictor variables on the abundances of tree species using GLM

Variables	*C. arabica*	*P. falcatus*	*C. macrostachyus*	*C. africana*	*S. guineense*	*O. capensis*	*D. abyssinica*	*F. decipenses*
pH	0.41	0.03	0.5*	-0.11	0.03	0.3	0.05	-0.16
CEC	4.45*	-0.46	1.58	1.52	0.16	-0.61	0.13	0.39
P	-0.93*	-1.35*	-0.4	-1.7*	-0.49	0.78	-0.74	-1.61**
K	-1.09**	-0.9**	0.22	-0.6*	0.12	-0.06	0.26	-1.19**
Ca	1.89*	-0.28	0.83	1.35*	-0.16	-1.17*	0.45	1.14*
Mg	-242**	82.87	-24.9	-105*	-3.37	-38.15	-50.77	-34.67
SOM	76.64	0.82	31.6	147.8*	11.18	93.87	96.92	5.84
N	-12.58	1.9	-7.47	21.7*	-7.07	-6.39	14.73**	-4.61
CN	-17.18*	21.8**	-0.36	14.1*	8.42	32.71**	17.06*	-1.8
Clay	3.2*	-0.4	0.93	0.69	-0.17	-0.41	0.18	-1
Silt	7.78*	-2	-2.73	-3.68	-0.26	-0.59	0.69	3.75
Sand	12.36*	-1.97	0.68	-3.19	-2.29	-4.2	0.74	0.84
Temperature	-0.6	1.2	-1.37*	0.71	1.38*	0.07	-0.43	0.87
Precipitation	-4.78**	1.18*	-1.6*	-3.1*	0.85	2.58**	-3.73**	-1.94**
Elevation	-3.05**	0.99*	-1.5**	-1.9*	-0.25	0.25	-2.34**	-1.93*
Slope	-0.53	-0.19	-0.04	-0.2	0.01	-0.03	0.52*	-0.17

Significant at ** < 0.01; Significant *at < 0.05

4.5.6. Prediction accuracy of ANN, RF, and GLM models

The mean squared error in Table 33 shows that the RF has produced better prediction accuracy as compared with the ANN model. The RF model predicted the spatial distribution of log abundances of *F. decipenses*, *S. guineense*, and *P. falcatus* with small prediction errors (MSE) of 0.28, 0.38, and 0.39, respectively. Consistently, the GLM predicted the log abundances of *F. decipenses* and *S. guineense* with smaller AIC values (Table 4). The RF, GLM, and ANN models predicted the log abundance of *F. decipenses* achieving the R^2 values of 71%, 64%, and 59%, respectively. The ANN model produced larger R^2 values for the log abundances of *P. falcatus*, *C. macrostachyus*, *S. guineense*, and *O. capensis*.

Table 33: Prediction accuracies of the ANN, RF, and GLM models using MSE, AICs and R^2

Species botanical name	ANN MSE	RF MSE	GLM AICs	ANN R^2	RF R^2	GLM R^2
C. arabica	1.19	0.83	3279	41%	58%	47%
P. falcatus	0.49	0.39	2336	42%	32%	23%
C. macrostachyus	0.52	0.52	2471	8%	5%	7%
C. africana	0.65	0.56	2750	48%	48%	40%
S. guineense	0.38	0.38	2094	7%	6%	1%
O. capensis	0.46	0.49	2448	29%	23%	21%
D. abyssinica	0.54	0.6	2543	29%	29%	29%
F. decipenses	0.44	0.28	2067	59%	71%	64%

4.5.7. Spatial distribution

The Random forest model predicted the spatial distribution of the abundances of eight woody species showing more concentration of species abundance in the eastern parts of Harana Forest (Fig 17). The geographical distribution of the log abundance of *C. arabica* was mainly concentrated in the eastern parts of the study area (Fig 17a). The distribution of the log abundances of *P. falcatus* appeared to have a wider ecological range, while its large abundance was detected around a border in the south direction, including a few locations in the central parts of the study area (Fig 17b). The spatial distribution of the log abundances of *F. decipenses* and *C. africana* appeared to be confined to the eastern parts (Figs 17c & d). The log abundance of *D. abyssinica* was found denser in the southeastern parts of the study area (Fig 17e). The distribution of log abundances of *C. macrostachyus,* and *S. guineense* were sparsely distributed (Figs 17f, g & h).

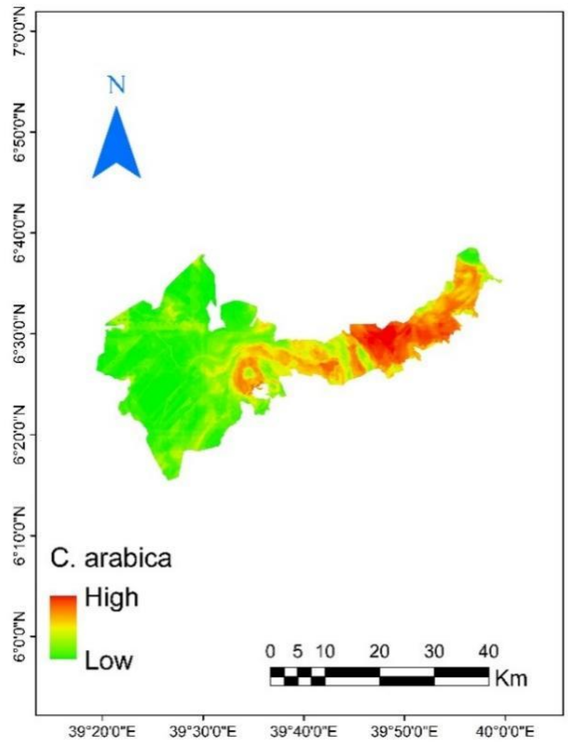

(A). Map of *C. arabica*

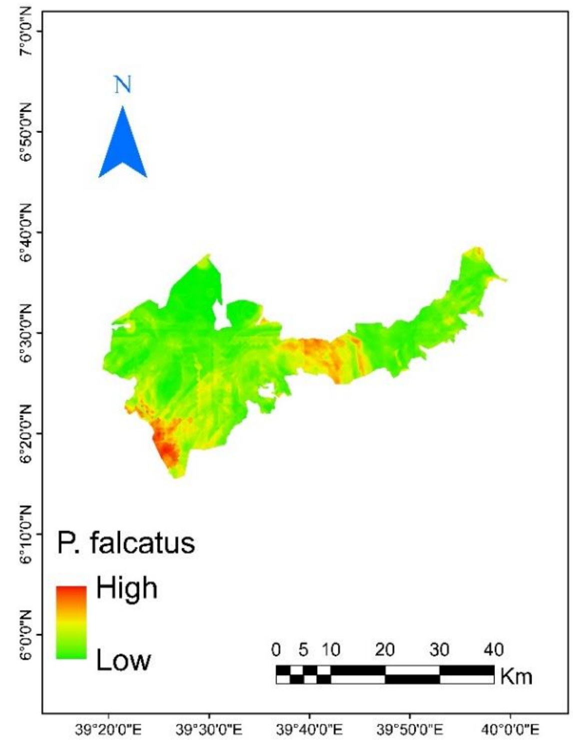

(B). Map of *P. falcatus*

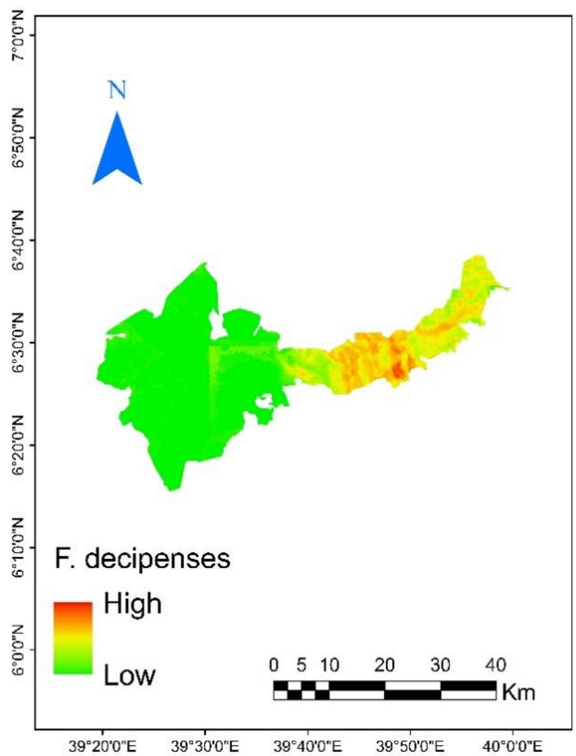

(C). Map of *F. decipenses*

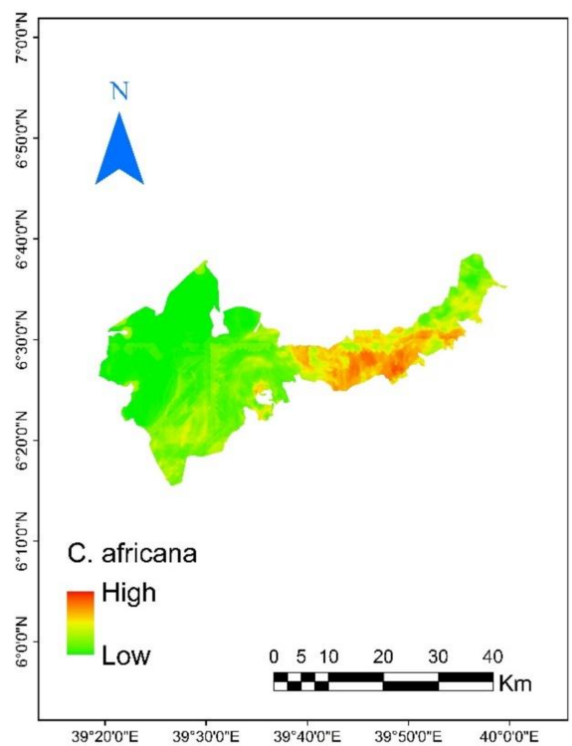

(D). Map of *C. africana*

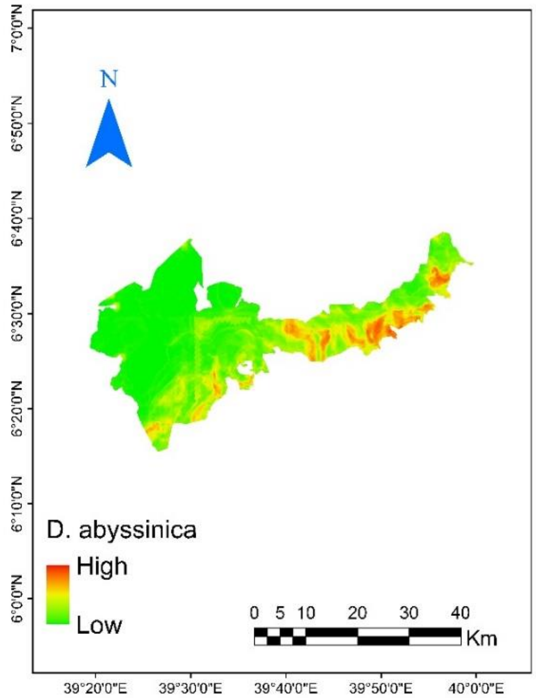

(E). Map of *D. abysinica*

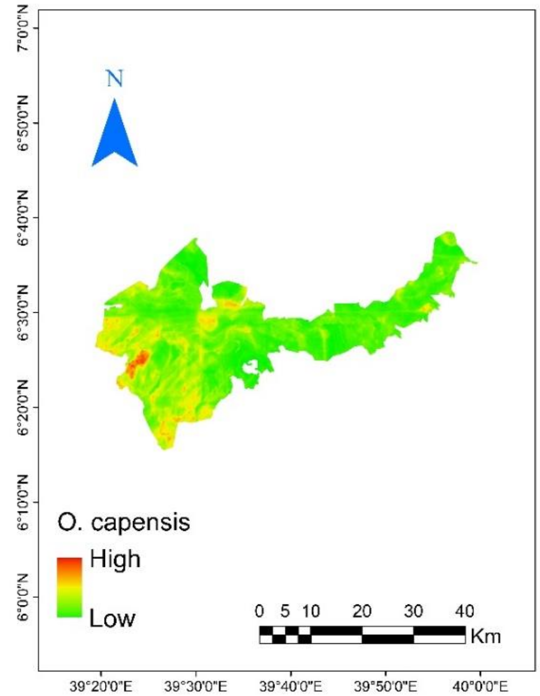

(F). Map of *O. capensis*

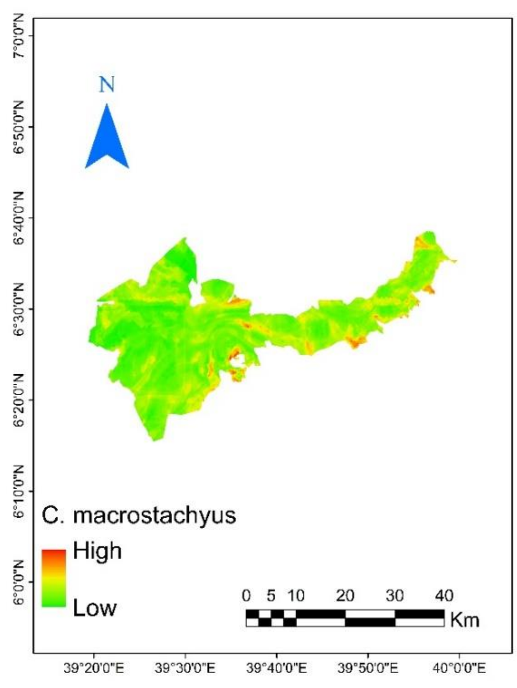

(G). Map of *C.macrostachyus*

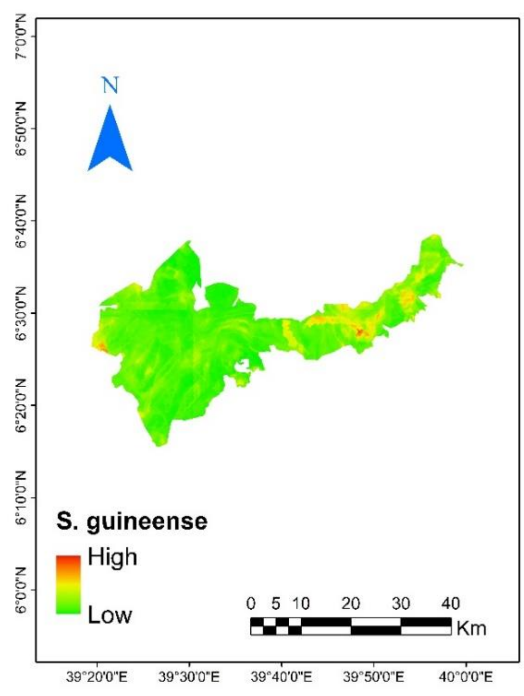

(H). Map of *S.guineense*

Figure 17: Spatial distribution map of the log abundances of species

CHAPTERS 5: DISCUSSION

The discussion chapter comprises five sections where the first section begins with providing the dynamics of ecosystem conditions in terms of the LULC change and monetary value of ecosytem service at the scale of the BMER in different periods. The second section conveys information on the degree of soil loss and spatial distribution of soil losses within different Ecosystems between 2010 and 2022. The third section describes the spatial distributions of the above-ground carbon (ACD) and woody species diversity in forest ecosystems of the BMER. The fourth section presents the impacts of biophysical factors on spatial distributions of ACD in the Harana Forest. The fifth section describes the effects of physical factors on the abundance of the dominant tree species in the Harana forest ecosytem.

5.1. State and dynamics of ecosystem conditions at different periods

5.1.1. Types of ecosystems in the Bale Mountains Ecoregion

Five ecosystem types have been identified from Landsat imageries of 2010, 2015, and 2022 achieving the classification accuracies of > 70%. In this aspect, an overall accuracy above 70% is normally considered an acceptable range of image classification for the LULC classification (Congalton, 1991). Additionally, a Kapp score of > 0.62 has been achieved for the image classifications in 2010, 2015, and 2022, and this Kappa value shows a better accuracy of image classification (Islami *et al.*, 2022). Despite that, the classification of afro-alpine and scrubland has been challenging to distinguish between the two landcover as their features tend to show similar spectral signatures. The reason has been hypothesized that this challenge might be linked to the phenotypical dynamics of Erica vegetation because of the effects of temperature and moisture across elevation gradients (Kidane *et al.*, 2022). This could suggest that a high-resolution image might be required to distinguish between the afro-alpine and scrubland vegetation.

The image classification analysis has shown that the forest ecosystem seems to cover 599,732 ha with a proportion of 16% of the total forest area in the BMER in 2022 (Table 8). This forest area encompasses six National Forest Priority Areas and the Bale Mountains National Park (BMNP (Mezgebu and Workineh, 2017; Kefale *et al.*, 2021). Apart from this potential, the forest ecosystem in the BMER looks to decline because of a conversion of the forest area to woodland and farmland (Fig 4). This forest conversion into other LULC types has resulted in a decline in forest area from 18% to 16% between

2010 and 2022 (Table 8). The finding is consistent with an overall trend of deforestation where 13 million ha of forest area has been globally converted to other LULC types (FAOb *et al*., 2010). Generally, deforesation could lead to carbon emissions which are counted as a cost to society (Zyl, 2015).

The proportion of farmland area conversely seems to show increasing from 14% to 20% between 2010 and 2022 (Table 8). The increase in the farmland ecosystem is manifested at the expense of vegetation. For instance, 103,639 ha of woodland, 59,650 ha of forestland, and 42,558 have been converted to farmland between 2010 and 2022 (Fig 4, Annex 5). This finding complements Hailemariam *et al*., (2015) who have reported the increase of farmland ecosystem in the BMER by 292,294 ha between 1985 and 2015 at the expense of forest land and woodland. The finding is consistent with what has been reported in the literature indicating that increasing of farmland by 35% in the East African countries between 1988 and 2017 at the expense of forest resources (Bullock *et al*.,2021). These findings support to conclusion that farmland expansion is the main driving force for the loss of forest ecosystems (Mandal *et al*., 2011; Mezgebu and Workineh, 2017).

5.1.2. Dynamics of ecosystem services in monetary values

The total ecosystem services value in the BMER has decreased from US$ 103 billion in 2010 to 92.5 billion in 2022 (Table 9). The decrease could be linked to the conversion of vegetation cover to other LULC types. This finding is consistent with the decreasing trend of Ethiopia's ESV from US$ 483 billion to US$ 397 billion between 2000 and 2015 (Sutton *et al*.,2016). Moreover, the impact of LULC has reduced the global ESV from US $145 trillion in 2007 to US $125 trillion in 2011 (Costanza *et al*., 2014). Concerning the specific ecosystem type, the ESV of the forest in the BMER has shown declining from US$ 94.5 billion to 83.2 billion between 2010 and 2022 (Table 9), because of the conversion of forest to farmland (Fig 4). The conversion of forest to farmland has contributed to an increase in the area of farmland from 16% to 20% between 2010 and 2022 (Table 9). This finding complements Fenta *et al*., (2020) who have reported the increase of the ESV of farmland in Sub-Saharan Africa at the expense of forests between 1992 and 2015.

In terms of the bundle of Ecosystem services, the total provisioning services have been estimated at US$ 42.9 billion with 46% of the total ESV of US$ 92.5 billion in 2022 (Table 10); where the provisioning services comprise food, water, and raw material supplies. The ecosystem service value of food has shown an increase of US$ 85 million between 2010 and 2022 (Table 11). This might be directly attributed to the increase in ESV of the farmland from US$4.81 billion to US$ 7.12 billion (Table 9) as the increase in farmland has obviosely contribute to increase crop production (Hailemariam *et al*., 2015; Fenta *et al*., 2020). On the other hand, the ESV of raw materials has shown to decrease from US$ 9.75 billion to US$ 8.36 billion between 2010 and 2022 losing US$1.39 billion (Table 11). This could negatively affect the livelihood of people as many people in rural areas depend on the supply of raw materials from the ecosystem (Narita *et al*.2018). A case study from Ethiopia has shown forest has contributed to 27 % of the annual households' income in Tigray, 39 % in the central Shewa, and 34 % in the BMER (Tesfaye *et al*., 2010). Globally, one-third of the population depends mainly on fuelwood and charcoal supplied from natural ecosystems (FAO, 2022). The ESV of water has shown a decrease from US$ 38.6 billion in 2010 to US$ 35.4 billion in 2022 losing US$ 4.87 billion. This could imply the potential of the water supply has become under compromise where the area consists of 40 springs that flow into Ganale and Wabeshebele river basins (Mezgebu and Workineh,2017).

The total ESV of regulatory ecosystem services has been estimated at US$ 6.54 billion in 2022 (Table 10). These services include regulating water flow, climate regulation, and prevention of soil erosion. The value of regulating water flow has been lost by US$ 439.8 million between 2010 and 2022 (Table 11). This highlights how water regulation services have been threatened which may lead to reducing the flow of water in the Ganale and Wabeshebele river basins while these two water bodies support the livelihood of 30 million people in southeast Ethiopia, Somalia, and Kenya (Kefale *et al*.,2021). ESV of the climate regulation tends to decrease from US$ 775 in 2010 to US$ 699 million in 2022 by losing US$ 7.64 million (Table 11). This loss can be attributed to a change in the area of the forest ecosystem and it has negative implications as forest destruction can cause the release of carbon dioxide which directly contributes to greenhouse gas accumulation (FAOb, 2010). Additionally, the ESV of soil erosion prevention seems to be estimated at US$ 123 million in 2010 but it has shown a loss of US$ 4.66 million between 2010 and 202 2(Table 11). This loss could be linked to the impact of LULC change as different vegetation covers have been converted to farmland (Fig 4). It is evident that LULC change has globally caused annual soil loss of 36 to 75 billion tons (Istanbuly *et al.*, 2021). The loss of soil directly affects human well-being by exacerbating poverty, food insecurity, inequities, and disparities among people mainly in developing countries where people entirely depend on ecosystem services (MEA, 2005; Mandal *et al*. 2011).

5.1.3. Loss of ecosystem services values within different ecosystems

The overall net loss of the ESV in the BMER appears to be US$ 10.8 while a large loss of ESV has been detected in provisioning services between 2010 and 2022 (Table 12). This might induce significant impacts on the livelihood of people where many rural people in Ethiopia depend on the provisioning services such as a supply of raw materials, water, and food (Tesfaye *et al*., 2010; Narita *et al*.2018). A total loss of ESV of US$ 10.8 billion could be associated with the decrease in forest area from 18% to 16% during the same period (Table 9). This finding seems consistent with Hailemariam *et al*., (2015) who reported a decreasing trend in forest ecosytem between 1985 and 2015. The scrubland ecosytem lost the ESV of US$ 84 million between 2010 and 2022 (Table 12) losing an area of 42,558 ha to farmland between 2010 and 2022 (Fig 4). This finding seems to differ from what Hailemariam *et al*., (2015) have reported hypothesizing that scrubland in the BMER could not be susceptible to farmland conversion as scrubland areas are less favorable for crop production due to unfavorable weather conditions.

On the other hand, the grassland ecosytem has lost a total ESV of US$ 835 million between 2010 and 2022 which is directly linked to the conversion of the grassland ecosytem to other LULC types (Fig 4) where its area proportion showing declining from 9% to 3% between 2010 and 2022 (Table 9). It has been reported that the expansion of farmland in the BMER is the main driving force resulting in a decline of the grassland ecosystem (Hailemariam *et al*.,2015). In general, changes in land cover and land use (LCLU) have a profound impact on biodiversity and the delivery of ecosystem services (Maes *et al*., 2015). On the other hand, the tradeoffs among ecosystems show that increasing the ESV of a certain ecosystem may lead to a decrease in the ESV of ecosystems (Xu *et al*., 2021).

5.2. Soil loss intensity and its spatial distribution in the BMER

5.2.1. Driving factors of soil erosion in the BMER

The annual rainfall in the BMER seems to range from 125 to 1216 mm where much rainfall appears to be concentrated in higher elevation areas in the northern parts of the study area while southern parts look to be characterized by a small amount of rainfall (Fig 5a). The lowest rainfall pattern looks to concur with a mean rainfall value of 100 mm that has been reported for the lowland parts of the BMER (Bekele *et al*., 2017). The rainfall erosivity factor in the BMER varies from 62 to 675 MJ mm ha^{-1} h^{-1} yr^{1} (Fig 5b), whereas a higher erosivity tends to be distributed in the western parts with a decreasing trend towards the central parts of the BMER.

A higher erosive factor in the northern parts suggests the possibility of more soil erosion in those areas, whereas, the southern part appears to be characterized by a small R factor closer to 62 MJ mm $ha^{-1}h^{-1}year^{-1}$ (Fig 5b). The rainfall erosivity factor in this study area looks to be lower as compared to 1013.45 to 1157.77 MJ mm ha^{-1} h^{-1} yr^{-1} reported for the Gumara watershed (Belayneh *et al*., 2019), and 496 to 590 MJ mm ha^{-1} h^{-1} yr^{-1} in Stung Sangkae catchment (Nut *et al*., 2021). This could suggest that the BMER appears to be characterized by a small erosivity factor which implies a smaller soil loss as compared with areas that experienced a high erosivity factor.

A maximum value of the C factor which is 0.65 appears to be mainly observed in the northwest and northeast parts of the study area with its elongated pattern into the middle of the study area (Fig 6a). The extent of a pattern of the C factor appears to be expanding from west to east direction in a continuous manner on the map of 2022 (Fig 6b). This observation with higher C values may show the absence of vegetation cover which indicates a higher vulnerability to soil erosion as an increase in the C factor implies a higher rate of erosion (Casermeiroa *et al*., 2004; Luvai *et al*., 2022).

A higher value of the P factor shown in the red color in (Fig 7a) seems to coincide with the distribution pattern of the C factor where a higher value looks to be observed in the northwest and northeast including the elongated distribution pattern from the east to west. The pattern of the P factor in the year 2022 remains similar to that of 2010, though, the area of the P factor seems to be expanded in 2022 (Fig 7b). The areas with a higher P value indicate more soil loss as an increase in the P value shows intensifying soil loss because of the absence of soil conservation measures (Kayet *et al*.,2018; Luvai *et al*., 2022).

On the other hand, the value of soil erodibility factor (K) in the BMER looks to vary between 0.24 and 0.32 where a maximum K value of 0.32 is associated with *Calcaric Regosols* (Rc) and Haplic *Xerosols* (Yh) soil types (Table 13 and Fig 8). The soil erodibility factor in this study area looks to exceed the soil erodibility value of 0.08 to 0.17 which has been reported in Northern Ethiopia (Girmay *et al*., 2020). Contrastingly, it seems to be similar to the erodibility values of 0.16 to 0.48 in the Kelani River basin in Sri Lanka (Fayas *et al*., 2019). A higher range of LS factors in this study area appears to prevail in the northern parts of the area (Fig 9b) which implies that northern parts could be more susceptible to soil erosion as a higher LS value contributes to more soil erosion in connection with a large runoff accumulation and high velocity (Girmay *et al*., 2020; Wagari and Tamiru, 2021).

5.2.2. Status of soil loss under different soil erosion severity classes

A mean annual soil loss in the BMER ranges between 0 and 306 t^{-1} ha^{-1} yr^{-1} in 2010 and slightly increased to 319 t^{-1} ha^{-1} yr^{-1} in 2022 (Figs 10a and b). These values appear to be lower than a mean soil loss of 932.6 t^{-1} ha^{-1} yr^{-1} in the case of the Anger sub-river basin (Moisa *et al*., 2022) and 983.14 $t^{-1}ha^{-1}yr^{-1}$ in the Gilgel Gibe watershed (Tesfaye and Tibebe, 2018). A total soil loss in 2010 was estimated at 4.5 million ha but increased to 7.5 million tons in 2010 while the total area of the BMER is 3,767,400 ha (Table 14). The soil loss in the BMER seems to be lower by far as compared to a total soil loss of 9.7 million t^{-1} yr^{-1} that has occurred in an area of 20,440 ha at Gumara watershed in Ethiopia (Belayneh *et al*., 2019); including the total soil loss of 3.3 million t^{-1} yr^{-1} in 2015 in Stung Sangkae Catchment of Cambodia in an area of 605,170 ha (Nut *et al*., 2021). In comparison with those areas, the soil loss in BMER looks to be small which is possibly attributed to a smaller erosivity factor of 62 to 675 MJ mm ha^{-1} h^{-1} yr^{-1} (Fig 5b) while the rainfall erosivity factor in the Gumara watershed ranges from 1013.45 to 1157.77 MJ mm ha^{-1} h^{-1} $year^{1}$ (Belayneh *et al*., 2019) and 496 to 590 MJ mm ha^{-1} h^{-1} yr^{-1} in Stung Sangkae catchment (Nut *et al*., 2021). These observations indicate that the soil losses might not be necessarily proportional to the size of the study area, rather it depends on the amount of rainfall and rainfall erosivity.

A very slight soil intensity below 5 t^{-1} $ha^{-1}yr^{-1}$ seems to occupy large parts of the BMER having a proportion of 61% of total soil loss in 2010 with 99.7% of the total area, whereas its proportion has increased to 63% of the total soil loss with an area coverage of 99.35% in 2022 (Table 14). This statistical observation is consistent with spatial distribution patterns where a very slight soil loss intensity looks to distribute in the entire parts of the study area in both periods (Fig 10a & b). This finding is in agreement with Nut *et al*., (2021) who have reported about 80% of the total area is occupied by a slight soil intensity in the Stung Sangkae watershed. This may indicate that every part of the land could not be free of soil loss, though, the intensity of rainfall might be small. However, this small intensity should not be overlooked as rainfall can gradually reduce soil fertility by leaching soil nutrients (Nut *et al*., 2021). Loss of soil fertility could have profound implications for human well-being, particularly in developing countries where many people rely heavily on ecosystem services for their livelihoods. Particularly, the loss of soil exacerbates food insecurity, as it directly impacts agricultural productivity and the ability of ecosystems to provide essential resources (MEA, 2005; Mandal *et al*., 2011).

5.2.3. Extent of soil loss under different ecosystems and impacts of slope on soil loss

The extent of soil loss in the farmland ecosystem looks to account for 56% of the total soil loss in 2010 and 69% in 2022 (Table 14). This is consistent with the overall soil erosion trend in Ethiopia where soil erosion is dominant on cropland (Tsegaye, 2019). The vulnerability of farmland to soil loss is mainly linked to improper management of agricultural lands (Alewell *et al*., 2019; Belayneh *et al*., 2023). This soil loss can lead to a reduction in crop productivity and food insecurity (Jemal, 2021). Broadly, soil erosion has been reported to causal factor for about 80% of agricultural land degradation at the global scale (Jemal, 2021). Soil loss in forest land has been shown below 1% in 2010 and 2022 (Table 15) which suggests that the extent of soil vulnerability is minimized by forest as forest canopy intercepts rainfall drops to facilitate water percolation into the ground than producing runoff (Casermeiroa *et al*., 2004; Nut *et al*.,2023; Belayneh *et al*., 2023). A steep slope above 40% looks to account for 58% of the total soil loss in 2010 and 57% in 2022.This observation seems to be logical because higher slope areas could cause water velocities to increase soil erosion (Nyairo, 2024). A flat slope below 5% accounted for 12% of the total soil loss in 2010 and 11% in 2022 (Table 16) and the soil loss on falt slope indicates that any land might not be free of soil erosion though the intensity is lower as compared to slope areas.

5.2.4. Variability of soil losses within different soil types

The total soil loss in *Eutric nitosols* appears to be 2,608,622 t^{-1} ha^{-1} yr^{-1} in 2010 with a proportion of 58% of the total soil loss and increases to 4,540,856$t^{-1}yr^{-1}$ with a proportion of 60% of the total soil loss in 2022 (Table 17). The possible reasons could be explained from different viewpoints. First, *Eutric nitosols* are distributed along higher elevations having a higher erodibility factor (UNDP and FAO,1984; FAO, 2015). Second, the *nitisols* contain heavy loam, and heavy clay with a deep porous, and stable soil structure which shows its good quality for agriculture in terms of having good internal drainage and fair water-holding properties (Yigini *et al*., 2013; FAO, 2015; Paulos, 2021). This suitability of *Nitisols* for agriculture can exacerbate the vulnerability of *Nitisols* to intensive soil loss (Paulos, 2021). Third, *Eutric nitosols* is the largest soil type covering 35% of the study area and this could be a reason for having more total soil loss in proportion to its area coverage.

Soil loss in *Calcaric regosols* (Rc) is estimated to account for 12% of total soil loss in 2010 and is reduced to 11% in 2022 but the absolute value of soil loss has shown increasing. A similar finding has been reported in Ethiopia around the Tigray regional state where *Calcaric regosols* has shown more vulnerable to erosion (Rabia *et al*., 2013) and the increasing soil loss from such soil type leads to a reduction in the soil depth which limits the growth of deep-rooted crops (Kibret, 2014). *Haplic Yermosol* is the fourth soil type in the study area in terms of losing soil which accounts for 11% of the total soil loss in each of 2010 and 2022 (Table 17). *Haplic Yermosols* type is narrowly distributed around a border from south to west and it is widely expanded from west to the central parts of the BMER in lowland areas which is characterized by the flat slope (Fig 8a). This finding is consistent with UNDP and FAO (1984) that have reported *Haplic Yermosols* soil type occurs on a flat slope mainly in the moisture-stressed areas in southern parts of the Bale where the pastoralist community exercises grazing.

5.3. Spatial dynamics of forest structural attributes

5.3.1. Statistical and spatial characteristics of forest attributes

The mean above-ground carbon stock of 97.66 $t^{-1}ha^{-1}$ in the Dry forest and 207.19 $t^{-1}ha^{-1}$ in the moist forest of the BMER (Table 18) appear to show a slight difference as compared with the mean values of 111.39 $t^{-1}ha^{-1}$ in the dry forest and 191.28 $t^{-1}ha^{-1}$in the moist forest that have been reported from the BMER by Asante *et al*., (2013). The possible reason for these differences might be related to the sampling intensity. A total of 236 sample plots with a 15 m radius have been employed in this study while in the previous research, 70 samples have been used with a plot size of 100m by 100 m. Compared with the national mean value, the overall mean ACD of 173.32 t/ha in the Bale forest appears to be higher than the mean value of 106.68 $t^{1}ha^{-1}$ of Ethiopia's forest (Teferi *et al*., 2021). The finding of this study might be more reliable because the forest data collection at the national level might be general and requires downscaling to understand detail variabilities that could occur due to topographic factors, species abundance, and species compositions (Igu *et al*., 2023).

A total of 172 tree species have been recorded in the forest of BMER and this value shows more species richness than 42 tree species recorded in the Dindin forest (Lemi *et al*., 2023). The mean values of the Shann Weiner index and species evenness have been estimated at 1.74$\pm$0.055 and 0.52 $\pm$ 0.033, respectively (Table 18) and these observations look to be consistent with the Shannon Wiener diversity index of 1.74 ± 0.098 and species evenness index of 0.69 ± 0 that have been reported in forest coffee areas of the moist forest of BMER (Kewessa *et al*., 2019). The mean value of species richness, Shannon-Weiner index, and species evenness indices in the Moist Forest appeared to be higher than the mean values recorded in the Dry forest (Table 18). This indicates that a Moist forest could host more species richness than a dry forest. The observed variability could happen as species cannot be evenly distributed in a forest landscape in association with variability in topographic, edaphic, and climatic factors (Amenu, 2016). In terms of tree species diversity, the Shannon-Wiener index appears to range from 0 to 3 in the dry forest and from 0 to 5 in the Moist forest (Table 18). This indicates that the Shannon wiener index $\geq$4 is considered an extraordinarily biodiversity-rich area (Lakićević and Srđević, 2018).

Concerning spatial dependency, semi-variogram analysis of the Shannon Weiner index appears to fit the Gaussian model while species richness, species evenness, and Sqrt-ACD have been fitted to the exponential model (Table 19). This may suggest that the exponential model could better fit to ecological data as compared to the Gaussian model (Table 19). A root-mean-square standardized error (RMSSE) for Shannon Weiner index, species evenness, and Sqrt-ACD, have been computed as 1.014, 1.06, and 1.07, respectively (Table 20). This implies that the RMSSE values closer to one show a better accuracy while RMSSE has a small prediction error (Kalivas *et al*., 2013). Generally, the RMSSE greater than one indicates an underestimated prediction by the kriging technique while values less than one imply overestimation in a prediction (Li and Heap, 2008; Samui, and Sitharam, 2011; Baba *et al*., 2014).

Coming to the spatial variability of forest attributes, the parameters of the Semi-variogram such as range, sill, nugget, and a ratio of sill to nugget have provided descriptions of the spatial dependency of ACD and species diversity (Table 19). Accordingly, spatial dependency of the Sqrt-ACD and species richness appears to occur over shorter distances with a range of 31,440 meters and 34,446 meters, respectively (Table 19). This indicates that similarity in the dataset of ACD and species richness appears to occur over a short distance. In other words, the ACD and species richness can lose spatial continuity or similarity over a short distance. This might be linked to the effects of soil characteristics, moisture, and nutrient availability (Akhavan and Kia-Daliri, 2010). Contrastingly, Shannon Weiner's diversity and species evenness seem to be characterized by having spatial dependency over a long range of 67,712 meters and 62,446 meters, respectively (Table 19). This portrays that the data of the Shannon Weiner index and species evenness exhibit similarity over a long distance because a longer range indicates a strong spatial autocorrelation in a given dataset (Zawadzki *et al.*, 2005; Akhavan and Kia-Daliri, 2010). A sill is another parameter that describes the spatial dependency of forest attributes while a sill represents a maximum point where the spatial dependency of a given attribute can decrease beyond a sill point (Hamilton, 2005; Oindo,2011). A sill value of the ACD in this study has been attained at 33 while a sill of species richness is 30 (Table 19). This implies that moving beyond the sill value, a similarity between a given dataset can decrease. The nugget values for the species richness and ACD appear to be 5 and 10, respectively (Table 19), while the nugget values are assumed to be zero at the origin of the semi-variogram (Park and Lee, 2014). The difference of a value from zero is naturally attributed to a micro-spatial variation occurring at a distance smaller than sampling intervals (Maynou, 1998).

The ACD data have exhibited a strong spatial dependency over a range of 31,440 m with a nugget-to-sill ratio of 23% which indicates a strong spatial dependency as the nugget-to-sill ratio $\leq$ 25% indicates a strong spatial dependency (Table 19). The species richness, Shannon Weiner index, and species evenness have exhibited a moderate spatial dependency with sill-to-nugget ratios of 35%, 45%, and 64%, respectively (Table 19) because a sill-to-nugget ratio between 25% to 75% shows a moderate spatial dependency while the ratio $\geq$75% indicates a weak spatial dependency (Neves *et al*., 2010; Baba *et al*., 2014; Zhang *et al*., 2015). An understanding of spatial dependency is fundamentally required to determine whether mapping is possible or not for a given forest attribute (Lesschen *et al*., 2005; Getis, 2008).

5.3.2. Spatial distribution of forest attributes and impacts of deforestation on tree species

The kriging technique has produced spatial distribution maps of ACD, species richness, Shannon Weiner index, and species evenness. The ACD with a range of 63 to 118 t/ha looks to account for 54% of the total forest area (Table 21). This class of ACD has been mainly distributed in the Adaba-Dodola, Aloshe-Batu, and Kobayo forests including the northern parts of the BMNP (Fig 11a). This may suggest that large parts of the forest might be associated with less stoking of ACD. The highest ACD class (282 to 336 t/ha) appears to occupy only 0.3% of the total forest area showing spatial distribution in the western of the BMNP adjusted to the Harana Kokosa forest (Fig 11a). These findings have shown that the ACD may vary across forest landscapes which might be linked to changes in ecological conditions, biotic interactions, developmental stages of forest resources, and human disturbances (Vayreda *et al*. 2012). This spatial information is useful to understand how ACD varies across a forest landscape which helps to consider an appropriate forest management intervention (Castilho *et al.*, 2006; Labrière *et al*., 2016). The highest species richness class (24.00 to 28.29) has occupied only 0.1% of the total forest area (Table 21), and its spatial distribution pattern looks to occur in the southwestern parts of the Mana Angetu forest (Fig 11b). This indicates that the highest species richness looks to be confined to a small area which might be linked to inaccessible locations. Contrastingly, the lowest tree species richness class of 2.55 to 6.84 seems to occupy 32% of the total forest area with spatial distribution in Adaba Dodola, Aloshie Batu, and Kubyu areas (Fig 11b). This observation might be attributed to natural conditions or anthropogenic factors that reduce species richness in those identified areas (Sintayehu *et al*., 2020; Berhanu *et al*., 2023).

The highest Shannon Weiner class of 2.33 to 3.11 appears to cover 101,557 ha with a proportion of 10% of the total forest area (Table 22). This range of ACD class looks to be distributed in southern parts of the forest of the BMER in Mena Angetu forest whereas the lowest class of (0.57 to 1.02) has occupied 14% of the total forest area and prevails in northern parts of the forest such as in eastern parts of Adaba Dodola forest adjacent to the Aloshie Batu including in northern part of Aloshie Batu forest (Fig 12). These observations might show that more tree species diversity is observed in southern parts of the forest as compared to northern parts which might be attributed to warm temperature in southern parts as warm temperature favors more species richness and species diversity (Rahman *et al*., 2021; Ahmed *et al*., 2022).

An overall mean species evenness appears to be 0.52 (Table 18) and this suggests that tree species in the forest of the BMER seem to be characterized by moderate evenness as a value closer to 0.5 showing a moderate evenness value while getting closer to one could indicate a perfect equitable distribution of species (Hamilton, 2005; Kumar and Mina, 2018). Interestingly, species evenness value in class of (0.44 to 0.57) has been estimated to cover 562,656 ha which is about 53% of the total forest area (Table 22).

This observation reveals that the large parts of the forest areas in the BMER are characterized by a moderate tree species evenness. The observation of having different species evenness classes could imply that every part of the forest landscape cannot exhibit a similar species evenness in association with the effects of various factors such as forest degradation, ecological conditions, and interactions among biotic components (Sintayehu *et al*., 2020; Berhanu *et al*., 2023). Another important point is that the high classes of tree species richness and species diversity appear to share the same area in the southern parts of the study area (Fig 2b and 3a). These observations could happen because the Shannon-Weiner Index is mathematically a derivative of species richness and species evenness (Ozcelik *et al*., 2008; Kent, 2011).

On the other hand, it has been challenging to establish a clear relationship between deforestation and loss of tree species richness and species diversity, though species-area relationships (SARs) have been used to attempt to address the issue (Chisholm *et al*., 2018). In this study, an Arch GIS-based innovative approach has been introduced to provide an indicative relationship between areas of deforestation and a loss of species. For instance, the deforesation of 10356 ha which is 60% of the total deforesation that occurred between 2010 and 2022 has resulted in the loss of species richness class of (6.84 to 11.13). Additionally, the deforestation of 7,745.76 ha has caused the loss of the Shannon-Wiener diversity index (1.36 to 1.67). Moreover, deforestation of 4,978.08 ha of forest area has resulted in the loss of tree species evenness class of (0.44 to 0.57). This technique has contributed to providing insight to answer the question of what is the loss of tree species richness and tree species diversity upon the occurrence of deforestation whereas this question has been a hot topic in tropical forests (Whitmore and Sayer, 1992; Berhanu *et al*., 2023). The technique used in this study seems to provide a better outcome compared to the technique of species-to-area relationships (SARs) that take habitat area as an input and gives species richness as an output. However, the SAR has several limitations. First, SAR ignores the dependence of species loss on the time scale, since habitat destruction occurred. Second, SAR assumes that species persist only in remnant habitat areas but in practice some species may persist in non-habitat area. Third, SAR approach assumes that a total habitat area is the only spatial parameter without considering fragmentated (Chisholm *et al*., 2018).

5.4. Spatial distribution of the ACD in the Harana Forest and influencing factors

5.4.1. The mean above-ground density

The mean ACD in the Harana forest looks to be 131.505 t^{-1} ha^{-1} (Table 25) and it seems greater than the Above-ground carbon (ACD) in the high forest of Ethiopia which has been estimated at 106.68 t/ha (Teferi *et al*.,2021). Conversely, ACD in the Harna seems to be lower than 147.6 t/ha which has been reported from the high forest part of eastern Ethiopia (Sintayehu *et al*., 2020). This variability is obvious as the tropical forest ecosystems sequester large amounts of carbon but remain varied across different landscapes due to various reasons. The variation in the mean ACD might be also affected by a sampling intensity and sampling strategy. For instance, Asante *et al* (2013) used 75 samples with a plot size of one ha which was randomly distributed over a total forest area of 261,053 ha in the moist forest ha of the BMER. Contrastingly, in this study, a total of 1122 sample plots with a sample plot size of 0.07065 ha were systematically distributed across the total forest area of 107,298.673 ha. This shows sampling intensity in this study is 0.7%, which is more than double the sampling intensity of Asante *et al*., (2013). This indicates the difference in a sample plot size and sampling intensity could lead to substantial differences in the estimation of ACD. In the meantime, this observation highlights a grey area where future studies need to focus on examining the efficiency of different sample plot sizes and sample intensity to provide a reliable estimation of ACD.

5.4.2. Effect of plant species richness and species diversity

The species richness and species diversity in this study appear to be the top predictors in shaping the spatial distribution patterns of ACD in the Harana Forest (Table 25). The Pearson correlation reiterates the positive correlation between the ACD and each of the species richness and Shannon Weiner diversity index (Table 28). Other similar findings have been reported by different authors such as Vayreda *et al*., (2012) from the Spain forest; Labrière *et al*., (2016) from the Panama forest; and Day *et al*., (2013) from the Rain Forest of Central Africa. The positive relationships between the ACD and species diversity in this study seem to support the niche complementarity hypothesis which states species diversity provides opportunities for utilizing available resources by plants to store more biomass (Vayreda *et al*., 2012; Labrière *et al*., 2016; Hofhans *et al*., 2020). In this aspect, Sintayehu *et al*., (2020) have indicated that species diversity influences both the magnitude and variability of aboveground biomass of terrestrial ecosystems.

In contrast, 65% of the total ACD in the Harana forest appears to be occupied by 11 dominant tree species (Table 26). This seems to complement the mass ratio hypothesis which explains a biomass accumulation is associated with the presence of dominant tree traits (Labrière *et al.*, 2016; Fotis *et al.*, 2018; Teixeira, *et al*., 2020). A similar finding has been reported indicating that 89.7% of total ACD has been occupied by 10 dominant tree species in the case of the Provincial Nature Reserve forest in China (Hu *et al*., (2015). Evidence from this study supports that the spatial distributions of ACD could be influenced by the presence of dominant tree species as compared with species richness and species diversity. In this aspect, his finding tends to support the mass ratio hypothesis as compared to the niche hypothesis.

5.4.3. Effect of forest structural diversity

A forest structure in this study refers to tree DBH, height, and stem density that has been identified to exert more influence on the spatial distribution of ACD in Harana Forest. The trees with DBH class of 10-50 cm accounted for 68% of the total ACD while those small trees < 10 cm DBH consisted of a large proportion of individual trees but showed a small contribution to the total ACD (Annex 6). Other studies have reported similar findings showing that smaller trees consist of many individual trees but disproportionally contribute to a sum of overall ACD (Vayreda *et al*., 2012; Hu *et al.;* 2015; Padmakumar *et al*., 2018; Getaneh *et al*., 2019). This finding suggests trees with big size store more ACD but it is still important to not overlook the contribution of small trees in the sequestration of carbon dioxide. On the other hand, the stem density has shown a positive correlation with a high clustering of ACD (Table 28). This may differ from the understanding that increasing individual trees could lead to competition for resources which hinders the ability of plants to produce more biomass. The average tree height in this study seems to be positively correlated with the ACD whereas those trees with height classes of 20-40 m tend to account for 94% of the total ACD (Annex 7). This finding complements Fotis *et al.*, (2018) who have reported tall trees consist of a large proportion of ACD. Increasing tree height and DBH could have more influence on the spatial distribution patterns of ACD (Krankina *et al*., 2005; Getaneh *et al*., 2019).

A location with high-high clustering of ACD in this study has shown a strong positive correlation with tree density, DBH, and height, though coffee density appears to indicate a weak relationship with the high-high clustering areas of the ACD. This negative relationship might be linked with farmers' activity of removing a forest regeneration to reduce the effect of tree competition with coffee plants. Previous studies have reported that intensive coffee management practices have affected the condition of forest regeneration in the Harana forest (Senbeta and Manfred, 2006; Kewessa, *et al*., 2019).

5.4.4. Effect of topographic factors

Elevation in this study area seems to show a weak correlation with a high clustering of the ACD (Table 28). This might be associated with increasing humidity and declining temperature at higher elevations which directly influence the distributions of plant species (Wang *et al*., 2007; Getaneh, *et al*., 2019; Wodajo *et al*., 2020). This finding is consistent with similar findings documented in the literature (Wodajo *et al*., 2020; Sun *et al*., 2020). An increase in a slope gradient above 15% appears to show a positive correlation with the ACD with a decreasing trend at a certain point (Fig 15 D), but the Pearson correlation indicates a weak association between the slope and the high clustering area of the ACD (Table 28). The effects of a slope on ACD have considerably varied in literature. For instance, a higher ACD has been reported at lower slopes by Yohannes *et al.,* (2015) while such observation might be related to the removal of soil nutrients from the steep slope and deposited at lower slopes to support vigorous plant growth to store more biomass (Natake, 2012; Wodajo *et al*., 2020). A contrasting finding has been reported to show less ACD at a lower slope in the Awi forest of Ethiopia because of illegal logging activity (Getaneh *et al*., 2019). East and west-faced aspects in this study area appear to occupy a large proportion of the ACD (Fig 15 R). This observation somehow is consistent with Yohannes *et al.*, (2015) who have reported plants associated with northeast and east-faced aspects have a chance of receiving more direct solar energy to facilitate the photosynthetic process (Yohannes, *et al.*, 2015; Kobler, *et al*., 2019). However, the finding of this study seems to be more plausible as the sun rises in the east and sets in the west with a considerable duration of solar radiation.

5.4.5. Impact of edaphic factors

The clay soil content on the top surface including at the depths of 5 cm and 15 cm seems to show a positive association with the ACD along with an increase in the content of clay soil. These appear to be suitable ranges of clay content showing more positive effects on the ACD at a point where the clay content is closer to 40% at different soil depths (Figs 15 G, H & I). The possible reason for such a positive association might be linked to the properties of clay soil which is rich in nutrients and its water-holding capacity to enhance plant growth and productivity (Natake, 2012; Olorunfemi *et al*., 2018; Zhong, 2018;

Kome *et al.*, 2019). Silt soil content beyond 27% in this study looks to be associated with less accumulation of the ACD (Fig15 P & Q). This is possibly linked to the poor water-holding capacity of silt soil which can exert plants under the conditions of moisture stress (Olorunfemi *et al*., 2018**).** The **s**oil organic content (SOC) has shown a positive trend with the ACD(Fig 15 M & O). This may suggest a strong contribution of the SOC in the formation of higher spatial clustering of the ACD. Presumably, soil with high organic content is assumed to be rich in nutrients with good water-holding capacity to support vigorous plant growth (Dölarslan and Erşahin, 2017; Olorunfemi *et al*., 2018). In this study, Figs 15 K & L show that an increase in CEC tends to exert negative impacts on the ACD. This observation is consistent with the Pearson correlation where a negative association is detected between the CEC and ACD (Table 28). The observation seems to contradict the understanding that CEC is a good indicator of soil fertility (Olorunfemi *et al*., 2018). However, similar findings have been reported showing a negative association between CEC and ACD (Poorter *et al*., 2015).

5.4.6. Impacts of climatic factors

Pearson correlation in this study has revealed a positive relationship between temperature and the ACD. Specifically, the partial effect analysis in Fig 15 F has indicated that temperature has shown a positive effect on the ACD at a point when it exceeds 19^0c but tends to show a negative effect as temperature rises. This suggests temperatures below 19^0c might not be suitable ecological ranges for plant growths because a decrease in temperature leads to a decline in the growth of plant height and diameter which reduces the capacity of plants to store biomass (Alvarez-Davila *et al*., 2017). Similarly, extreme temperatures could negatively affect productivity by influencing the metabolic process of plants (Hatfield and Prueger, 2015).

The annual precipitation in this study seems to contribute to the formation of a lower clustering of ACD (Table 28). Effects of precipitation might be considered indirect impact as precipitation may indirectly affect soil textures to influence plant growth and distribution (Natake, 2012). Higher precipitation may create excess water to retain within the capillaries of the clay soil which hinders the availability of water and mobility of nutrients (Olorunfemi *et al*., 2018). Precipitation can further reduce the decomposition of organic matter by limiting the activities of micro-organisms whereas micro-organisms play important roles in decomposing organic matter (Taylor *et al*., 2017). This lower rate of decomposition due to the effect of moisture can reduce the availability of soil organic content which further results in less accumulation of plant biomass.

5.5. Impacts of abiotic factors on the spatial distribution of species abundances

5.5.1. Effects of elevation on the abundances of species

Elevation is one of the abiotic factors that control the spatial distribution of plants at various spatial locations (Nguyen *et al*., 2015; Ahmed *et al*., 2022). The ANN model in this study has indicated elevation could exert a negative impact on the abundance of all species. The GLM revealed a similar observation except a positive impact was shown on the log abundance of *P*. *falcatus* (Table 32). The negative impact of elevation on the log abundance of plant species mainly relates to the drop-in temperature with an increase in elevation that creates unfavorable conditions for plant growth (Rahman *et al*., 2021; Ahmed *et al*., 2022). The positive effect of elevation on abundance of *P*. *falcatus* can suggest this species might be less susceptible to the effect of elevation (Lulekal *et al*., 2008). Eventually, the impact of elevation on plant species could not be a linear relationship as the effects of elevation can be modified by a slope, and edaphic features (Wakjira, 2006; Nguyen *et al*., 2015; Ahmed *et al*., 2022). For instance, at a medium elevation range, a steep slope could develop poor soil fertility which leads to less plant abundance (Nguyen *et al*., 2015).

5.5.2. Effects of soil nutrients on the abundance of different tree species

The ANNs model appears to provide a positive impact of the SOM on the log abundances of all species (Table 31). The observation with the ANNs looks to be consistent with the understanding that soil organic matter is an important nutrient to support the vigorous growth of plant species (Booth *et al*., 2005; Zhou *et al*., 2019; Yaseen *et al*., 2022). Nitrogen is an essential nutrient required in large amounts to construct a plant organ, facilitating metabolism activities, and fruit development (Chapin *et al*., 1987; Xu *et al*., 2020). Contrastingly, the ANN model revealed that total nitrogen could exert a negative impact on the log abundances of all woody species except a positive effect on the log abundances of *C. africana and D. abyssinica* (Table 31). The observed negative impact is probably related to the bondage of nitrogen in the organic materials which could not be easily available for plant use (Matkala *et al*., 2020). This may create that nitrogen might be a limiting factor where the decomposition rate of organic matter is lower (Matkala *et al*., 2020; Rahman *et al*., 2021; Devi, 2022; Gerke, 2022).

The ANN and GLM models appear to display a similar observation in depicting a positive impact of a carbon-to-nitrogen ratio on the log abundances of all woody species, except a negative impact on the abundances of C. *arabica, F. decipenses, and C. macrostachyu*s. This positive observation seems to be reasonable as the carbon-to-nitrogen ratio is an indicator of soil fertility (Zhou *et al*., 2019). The ANN model has indicated a positive effect of magnesium on the log abundance of *P. falcatus* (Table 31). This positive impact could be a reasonable observation as magnesium is an essential element for plant physiological and biochemical processes (Gransee and Führs,2013; Ishfaq *et al*., 2022). Contrastingly, the ANN and GLM models have shown that magnesium exerts a negative impact on the log abundances of C. *arabica*, and *C. africana*. This negative impact might be explained from two different perspectives. First, magnesium tends to form gypsum and magnesium carbonate compounds which create an unavailable form of magnesium for plants (Gransee and Führs, 2013). Second, the availability of magnesium could be reduced by the acidic soil property, particularly for a soil pH < 6 (Gransee and Führs, 2013; Chaudhry *et al*., 2021).

The variable importance analysis using the RF model has indicated that the available phosphorus appears to be a strong variable in influencing the spatial distribution of the log abundances of C. *arabica*, *F. decipenses*, *P. falcatus*, *C. africana,* and *O. capensis*. The ANN and GLM results in Tables 31 and 32, respectively have shown that phosphorus appears to exhibit negative impacts on the majority of the log abundances of woody species. This seems to deviate from the understanding that phosphorous plays an important role in seed germination and plant growth (Rahman *et al*., 2021; Nguyen *et al*., 2015). However, the observed negative impacts of phosphorus might have be occurred as phosphorous exists in unavailable form by creating dihydrogen phosphate and Iron compounds in tropical soil (Vitousek *et al*., 2010; Yaseen *et al*., 2022) where our study area is also located in the tropics. It has been reported that in the absence of phosphorus, species can adapt to low-phosphorus and can grow fast in tropical areas (Yaseen *et al*., 2022).

On the other hand, the ANN model in this study shows a positive effect of phosphorus on the log abundances of *C. arabica*, and *F. decipenses* while the GLM indicates the opposite (Table 31). These observations support Antúnez (2022) who has reported that the use of more than one model is important to check the reliability and consistency of the impacts of abiotic factors on the abundance of woody species under different models.

The RF has shown that the available potassium is identified as one of the top variables to influence the spatial distribution of the log abundances of C. *arabica, F. decipenses, C. africana,* and *P. falcatus* (Fig 16). The ANN model identified that available potassium could exert a positive effect on the log abundances of *C. arabica, C. macrostachyu*s, and *S. guineense.* This positive impact could be directly related to the roles of potassium which helps to enhance the growth of plants (Nguyen *et al*., 2015; Xu *et al*., 2020). Phosphorus is presumed to show a positive effect on plants as it is very essential for plant growth and the transfer of energy in plant cells (Long *et al.*, 2018; Yaseen *et al*., 2022). Differently, The ANN and GLM models have shown available potassium has exerted a negative impact on the log abundances of *P. falcatus, F. decipenses,* and *C. africana.* This observation is consistent with Nguyen *et al*., (2015) who have reported that the impact of potassium might be either positive or negative, depending on the types of plant species.

5.5.3. Effects of climatic factors on the abundances of species

The ANN model in this study looks to show a positive effect of precipitation on the log abundances of *C. arabica*, and *F. decipenses*; but the GLM has displayed a negative impact. The GLM finding looks to be logical as increasing precipitation in the natural forest tends to develop a cooling effect which creates unfavorable conditions for the growth of *C. arabica* while this species prefers to warmer temperatures (Wakjira, 2006). The ANN and GLM models have shown that precipitation could induce a negative impact on the log abundances of many species. This negative impact might be linked to various reasons. First, extreme precipitation may create water saturation in the soil which may affect the nutrient availability to plant roots. Second, high precipitation can cause soil erosion which may result in poor soil fertility that limits the growth of woody species (Wakjira, 2006).

Concerning the impact of temperature on individual plants, the ANN and GLM models look to fail in detecting a similar impact of temperature on the log abundance of many species; except both models have shown a positive impact of the temperature on the log abundance of S. *guineense*; and a negative impact on the log abundance of *C. macrostachyus*. The temperature has been widely reported to show a positive impact on plant growth and distribution (Amissah *et al*., 2014). Despite that, an increase in temperature could negatively affect the physiological processes of plant species (Clark, 2004; Yang *et al*., 2006).

5.5.4. Spatial distribution of the abundance of woody species

The spatial distribution pattern of the log abundance of *C. arabica* looks to be denser in the eastern parts where the elevation range is moderate as compared to a higher elevation in the western parts. This may imply *C. arabica* could be sensitive to the effect of elevation as increasing in elevation directly drops the temperature to the extent where it would be less suitable for the growth of this species. Consistent with this, *C. arabica* in Ethiopia normally grows in elevation ranges of 940 to 2400 m asl (Wakjira, 2006; Lulekal *et al*., 2008; Schmitt *et al*., 2009), and suitable mean annual temperature range from15-20^{0}C (Wakjira, 2006).

The spatial distribution of the log abundance of *P. falcatus* appears to distribute widely in different parts of the study area (Fig 17b) and the GLM has revealed that the log abundance of *P. falcatus* does not show significant interactions with the majority of abiotic factors (Table 32). These findings support to suggestion that the abundance of tree species with wider geographical ranges might not be significantly influenced by environmental factors. The ecological implication of this observation depicts that *P. falcatus* might not be sensitive to the variability of abiotic factors and could grow under different environmental gradients.

Spatial distributions of the log abundances of ***F.*** *decipenses*, *C. africana*, and *D. abyssinica* have shown dense patterns in the eastern parts of the study area (Figs 17c, d, and e) where the area is characterized by a hot temperature as compared to the western parts. This observation implies that the ecological requirement of these three species is limited to a hotter location. Exceptionally, the spatial distribution of the log abundance of *O. capensis* appears to be denser in the southwestern parts of the study area (Fig 17 f). This may suggest *O. capensis* requires a higher elevation which could be characterized by cooler temperatures and higher precipitation.

CHAPTER 6: CONCLUSION AND RECOMMENDATIONS

6.1 Conclusion

Human activities have significantly impacted ecosystem conditions, causing substantial challenges to ecosystem functioning and ecosystem management. Meantime, inadequate understanding and scientific information of these challenges and their effects exacerbate the problems, potentially leading to ineffective planning and interventions to halt the challenges. This PhD research aims to bridge key scientific knowledge gaps by employing diverse geospatial analytical techniques to assess ecosystem conditions in the Bale Mountains Ecoregion (BMER). The findings of this study have shown an overall declining trend in the ESVs of the BMER, implying a critical degradation of the quality of ecosystem services. Contrastingly, the ESV in farmland has shown increasing, though, the soil erosion modeling has revealed that the farmland ecosytem is the most affected by soil erosion. This highlights that the valuation method of a benefit transfer approach fails to consider the quality of the ecosytem as it simply depends on the surface area of a given ecosytem. This implies that the use of more techniques in such research contributes to a better understanding of the conditions of ecosystems. On the other hand, the increasing trend of the farmland's ESV does not necessarily reflect a positive outcome as the increase has been attained at the expense of critical ecosystems, which is detrimental to environmental conservation and sustainability.

The statistical mean value of the ACD in the forest is estimated at 173.31 $t^{-1}ha^{-1}$ which seems better stoking of the ACD in the entire forest of BMER. Contrastingly, the spatial analysis has revealed that 54% of the forest area is occupied by ACD values between 63 and 118 t/ha which is lower than a mean value that implies a large portion of the forest area appears to be under suboptimal condition as compared with a higher ACD of 283 to 336 t/ha that occupied by 0.3% of the total area. This observation highlights that spatial analysis provides a better understanding of the spatial variabilities of the ACD as compared to the statistical mean value. The spatial analysis technique has further indicated that the spatial variabilities of ACD can be more influenced by tree species richness and species diversity compared to the effects of topographic and climatic factors at the local scale. Similarly, 32% of the forest associates with the lowest species richness class of (2.55–6.84 species), whereas better species richness and species diversity are predominantly confined to small locations in the southern parts of the BMER which indicates spatial variation in forest quality in terms of the tree species composition. The association of a large forest area with a small number of tree species richness, species diversity, and ACD implies the deteriorating conditions of large portions of the forest areas. This has adverse implications for forest roles in climate regulation and biodiversity conservation. Moreover, this research study has introduced important spatial analysis techniques to determine the relationship between the area of deforesation and the extent of species loss. The techniques could be very helpful for forest managers and researchers to understand the implications of the area of occurred deforestation in the loss of species richness and diversity.

The modeling of ACD has shown that a substantial proportion of the ACD looks to be concentrated within a few dominant tree species in the Harana forest, and the modeling techniques have revealed that the spatial distributions of the abundance of these dominant tree species are mainly influenced by the combination of topographic, climatic and edaphic factors. Interestingly, the abundance of *Podocarpus falcatus* seems to exhibit neutral interactions with the majority of environmental factors, demonstrating its adaptability to diverse ecological conditions. In conclusion, the findings of this PhD research have provided solid scientific evidence substantiated with quantitative and spatially explicit understandings that could inform decision-making processes to enhance the conservation of the BMER which provides transboundary ecosystem services.

6.2 Recommendations

Based on the empirical research findings, the following recommendations are provided to guide policymakers and resource managers in implementing effective conservation strategies at local, and regional levels.

- The declining trends in ESV of BMER and the deteriorating conditions of forest ecosystems could have far-reaching implications while the area is one of the global biodiversity hotspot areas and water tower in Horn Africa that provide transboundary services. This requires urgent coordination and cooperation among local, regional, and national stakeholders to halt further ESV losses, focusing on preventing the degradation of critical ecosystem services such as forests to mitigate adverse environmental, societal, and economic impacts.
- The BMER exhibits a lower rate of soil erosion, though, northern areas, primarily farmlands, experience higher soil loss due to agricultural activities. Hence, local agriculture offices in the BMER

are required to implement soil and water conservation measures to halt further soil degradation and reduce sedimentation in water bodies while enhancing farmland productivity.

- The kriging techniques have produced the map of ACD that provides insights information of forest attributes and future studies need to incorporate environmental factors to enhance the accuracy of spatial interpolation at the broader scale of the BMER.
- The eastern parts of Harana Forest have been characterized by high ACD and require enhanced conservation measures to avoid the risks of carbon emissions associated with deforestation and forest degradation. Simultaneously, efforts should target the western parts, which exhibit lower ACD, to improve carbon stocking capacity and combat illegal logging.
- Tree species exhibit varying responses to environmental factors, implying the need for site-specific strategies in the processes of ecological restoration. Forest development practitioners should tailor restoration efforts to the ecological requirements of individual species, ensuring high survival rates and improved forest health.
- This study shows the importance of combining ecosystem assessment using valuation, spatial analysis, and modeling to understand ecosystem conditions comprehensively. Future research should expand on this work by integrating advanced techniques and broader environmental factors to refine ecosystem assessment and inform adaptive management.

REFERENCES

Abdulkareem JH, Girei AH, Yamusa AM, and Abdullahi J (20121). AN OVERVIEW OF SOIL Erosion modeling, J of Research in Forestry, Wildlife & Environment Vol. 13(1) March 2021.

Abera E (2014). Assessment of micro-watershed vulnerability for soil erosion in Ribb watershed using GIS and remote sensing, MSc thesis submitted to Mekele University.

Addi A, Demissew S, Soromessa T, Asfaw Z (2019). Carbon Stock of the Moist Afromontane Forest in Gesha and Sayilem Districts in Kaffa Zone: An Implication for Climate Change Mitigation. J Ecosys Ecograph 9: 259. doi: 10.4172/2157-7625.1000259

Adhikari K, and Hartemink AE (2016). Linking soils to ecosystem services, A global review, Geoderma 262 (2016) 101–111, dx.doi.org/10.1016/j.geoderma.2015.08.009.

Ahani H., & Jalilvand, H. (2010). Providing an essay about: a study on the spatial pattern of biodiversity caused by implementing agroforestry methods.li

Ahmadzadeh E, Lee J, and Moon I (2017). Optimized Neural Network Weights and Biases Using Particle Swarm Optimization Algorithm for Prediction Applications J of Korea Multimedia Society, Vol.20, No.8, pp., 1406-1420. doi.org/10.9717/kmms.2017.20.8.1406.

Ahmed S, Lemessa D, and Seyum A (2022). Woody Species Composition, Plant Communities, and Environmental Determinants in Gennemar Dry Afromontane Forest, Southern Ethiopia, Hindawi Scientific Article ID 7970435, P. 10. doi.org/10.1155/2022/797043.

Akhavan R, and Kia-Daliri H (2010). Spatial variability and estimation of tree attributes in a plantation forest in the Caspian region of Iran using geostatistical analysis, Caspian J. Env. Sci., Vol. 8 No.2 pp. 163-172.

Aksu G, Güzeller CO, and Eser MT (2019). The Effect of the Normalization Method Used in Different Sample Sizes on the Success of Artificial Neural Network Model, Int J of Assessment Tools in Education, Vol. 6, No. 2, pp.170–192. doi.org/10.21449/ijate.479404.

Alewell C, Borrelli P, Meusburger K, Panagos P (2019). Using the USLE: Chances, challenges, and limitations of soil erosion modeling; International Soil and Water Conservation Research 7 (2019) 203e225, doi.org/10.1016/j.iswcr.2019.05.004 2095-6.

Al-Mashagbah A, Al-Adamat R, and Salameh E (2012). The use of Kriging Techniques with in GIS Environment to Investigate Groundwater Quality in the Amman-Zarqa Basin/Jordan, Research Journal of Environmental and Earth Sciences 4(2): 177-185.

Alvarez-Davila E, Cayuela L, Gonzolez-Caro S, Aldana AM, Stevenson PR, lips, Jimnez EO (2017). Forest biomass density across large climate gradients in northern South America is related to water availability but not to temperature. PLOS one, 12(3), e0171072.k

Amenu BT (2016). Review on Woody Plant Species of Ethiopian High Forests, Journal of Resources Development and Management www.iiste.org ISSN 2422-8397 An International Peer-reviewed Journal Vol.27, 2016

Amissah L, Mohren GM, Bongers F, Hawthorne WD, and Poorter L (2014). Rainfall and temperature affect tree species distribution in Ghana, Journal of Tropical Ecology, Vol.30, No. 05, pp 435 – 446, DOI: 10.1017/S026646741400025X.

Antúnez P (2022). Main environmental variables influencing the abundance of plant species under risk category, J. For. Res.33:1209-1217. doi.org/10.1007/s11676-021-01425-6

Asante WA, Tadesse WG, & Zerihun G (2013). Final Report Carbon Stocks Inventory of the Bale Mountains Eco Region REDD-plus project (BMERP)in Ethiopia, Final Report of Carbon Stocks Inventory Farm Africa.

Asefa M, Ca M, He Y, Mekonnen E, Song X, and Yang J (2020). Ethiopian vegetation types, climate, and topography, Plant Diversity Vol. 42: pp. 302-311.

Austin M (2007). Species distribution models and ecological theory: A critical assessment and some possible new approaches; ecological modeling 200; 1–19.

Ayele G, Hussein H, Mersha A (2019). Land use land cover change detection and deforestation modeling: in Delomena District of Bale Zone, Ethiopia. J Environ Protection Vol. 10, No.4, pp: 532–561.

Baba *K*, Bahi L, and Ouadif *L,* (2014). Geostatistical Analysis for delineating sterile inclusions in Sidi Chennane's phosphatic series, Morrocco, Eart Sci. Res. J. Vol. 18, No. 2: 143 – 148.

Baer SG and Birgé HE (2018). Soil ecosystem services: an overview, Reaserachagte, Burleigh Dodds series in agricultural science.

Balasubramanian A (2008). Ecosystem and its components, Technical Report, February 2008; www.researchgate.net/publication/314213426.

Balzan MV, Caruana J, Zammit A (2018). Assessing the capacity and flow of ecosystem services in multifunctional landscapes: Evidence of a rural-urban gradient in a Mediterranean small island state,*Land Use Policy 75 (2018) 711–725*.

Barbier EB, Baumgärtner S, Chopra K, Costello C, *et al* (2009). The valuation of ecosystem services, Chapter eight at: https://www.researchgate.net/publication/260534686

Bataineh AL, Oswald BP, Bataineh M, Unger D, Hung I, Kuai & Scognamillo D (2006). Spatial autocorrelation and pseudo replication in fire ecology, J. of Fire Ecology, 2(2),107-118.

Bedane GA, Feyisa GL and Senbeta F (2022). Spatial distribution of above ground carbon density in Harana Forest, Ethiopia, Ecological Processes (2022) 11:4 https://doi.org/10.1186/s13717-021-00345-x

Bekele F, Mosisa N, Terefe D (2017). Analysis of current rainfall variability and trends over Bale-Zone, South Eastern highland of Ethiopia. Climate Change, 2017, 3(12), 889-902.

Belayneh M, Masha M, and Befkadu B (2023). Modelling Soil Loss and Its Association to Site Physical Characteristics in Majang Watershed, Baro Abobo River Basin, Hindawi Applied and Environmental Soil Science Volume 2023, Article ID 6099543, 14 pages https://doi.org/10.1155/2023/6099543.

Belayneh M, Yirgu T, and Tsegaye D (2019). Potential soil erosion estimation and area prioritization for better conservation planning in Gumara watershed using RUSLE and GIS techniques', Environ Syst Res (2019) 8:20 doi.org/10.1186/s40068-019-0149-x.

Benítez FL, Anderson LO, and Formaggio AR (2016). Evaluation of geostatistical techniques to estimate the spatial distribution of aboveground biomass in the Amazon rainforest using high-resolution remote sensing data , ACT Amazonica VOL. 46(2) 2016: 151- 160

Bennett ND, Croke BF, Jakeman AJ, Newham, Lachlan TH, and Norton JP (2010). Performance Evaluation of Environmental Models. Int. Congress on Environmental Modelling and Software. 247, https://scholarsarchive.byu.edu/iemssconference/2010/all/247

Berhanu Y, Dalle G, Sintayehu DW, Kelboro G , Nigussie A(2023). Land use/land cover dynamics driven changes in woody species diversity and ecosystem services value in tropical rainforest frontier: A 20-year history,J Heliyo, 9(2023)e13711,doi.org/10.1016/j.heliyon.2023.e13711.

Binder S, Haight RG, Polasky S, Warziniack T, Mockrin MH, Deal RL, and Arthaud G (2017). Assessment and Valuation of Forest Ecosystem Services: State of the Science Review,General Technical Report NRS-170

Biswa K (2023). Roots of Ecosystem Services from Economics, Asian Journal of Multidisciplinary Research & Review (AJMRR) ISSN 2582 8088 Volume 4, Issue 2,2023, DOI: doi.org/10.55662/AJMRR.2023.4203.

Bonthagorla U, Reddy TSK, Akash S, Srikanth H, and Ahmed M (2022). Effects of soil erosion and control: A review,The Pharma Innovation Journal 2022; SP-11(6): 2925-2933

Booth CA, Fullen MA, Jankauskas B, and Jankauskiene G (2005). The role of soil organic matter content in soil conservation and carbon sequestration studies: case studies from Lithuania and the UK, Sustainable Development and Planning II, Vol. 1, Ecology and the Environment, Vol 84, www.witpress.com, ISSN 1743-3541.

Borrelli P, Alewell C, and Alvarez P *et al*. (2021). Soil erosion modeling: A global review and statistical analysis, Science of the Total Environment 780 (2021) 146494agar

Brander L, Baggethun E, López B, Verma M (2010). Chapter 5 The economics of valuing ecosystem services and biodiversity, The Economics of Ecosystems and Biodiversity: The Ecological and Economic Foundations.

Bullock EL, Healey SP, Yang Z, Oduor P, Gorelick N, Omondi S, Ouko E, Cohen WB (2021). Three Decades of Land Cover Change in East Africa. J Land, vol.10, No. 150, doi.org/10.3390/ land10020150.

Burkhard B, Guerra CA, Davíðsdóttir B (2019). Discussion paper 3: Soil retention (regulating) ecosystem services. Paper submitted to the Expert Meeting on Advancing the Measurement of Ecosystem Services for Ecosystem Accounting, New York, 22-24 January 2019 and subsequently revised. Version of 15 April 2019. Available at: seea.un.org/events/expert-meeting-advancing measurement-ecosystem-services-ecosystem-accounting

Camarero J, Gutilarrez E, Fortin MJ & Ribbens E (2005). Spatial patterns of tree recruitment in a relict population of Pinus uncinata: forest expansion through stratified diffusion, J of Biogeography, 32(11), 1979-1992.

Cao H, Ma S and Li F (2014). Ecosystem Assessment and Fuzzy Systems Management, Advances in Intelligent Systems and Computing 254, DOI: 10.1007/978-3-319-03449-2_1

Casermeiroa MA, Molinab JA, Caravacaa MT, Costaa H,Moreno PS (2004). Influence of scrubs on runoff and sediment loss in soils of Mediterranean climate, Catena 57 (2004), 91 – 107.

Castilho CV, Magnusson WE, Arau´joa RN *et al.* (2006). Variation in aboveground tree live biomass in a central Amazonian Forest: Effects of soil and topography, Forest Ecology and Management 234 (2006) 85–96.

Chapin FS, Bloom AJ, Field CB, and Waring RH (1987). Plant Responses to Multiple Environmental Factors, Physiological ecology provides tools for studying how interacting environmental resources to control plant growth, BioScience, Vol. 37, No. 1, pp. 49-57.

Chapin FS, Matson PA, and Vitousek PM (2011). Principles of Terrestrial Ecosystem Ecology, DOI 10.1007/978-1-4419-9504-9_1, Springer Science+Business Media, LLC 2011.

Chatzinikolaou E (2012). Use and limitations of ecological models, ResearchGate TWB 6 (2012), N.2, www.researchgate.net/publication/256303391

Chaudhry AH, Nayab S, Hussain, SB, Ali M, Pan Z (2021). Current Understandings on Magnesium Deficiency and Future Outlooks for Sustainable Agriculture. Int. J. Mol. Sci. 2021, 22, 1819. doi.org/10.3390/ijms22041819.

Chave J, Andalo C, Brown S, Chambers JQ, and Eamus D (2005). Tree allometry and improved estimation of carbon stocks and balance in tropical forests, J of Oecologia,145: 87–99, DOI 10.1007/s00442-005-0100-x.

Chave J, Coomes D, Jansen S, Lewis SL, Swenson NG, & Zanne AE (2009). Towards a worldwide wood economics spectrum, J of Ecology letters, 12(4), 351-366.

Chen WY, Chan YJ, Lim JW, Liew CS, Mohamad MH, Usman A, Lisak G, Hara H, Tan WN (2022). Artificial Neural Network (ANN) Modelling for Biogas Production in Pre-Commercialized Integrated Anaerobic-Aerobic Bioreactors (IAAB). Water, 14, 1410. doi.org/0.3390/w14091410.

Chisholm RA, Lim F, Yeoh YS, Seah WW, Condit R and Rosindell J (2018). Species–area relationships and biodiversity loss in fragmented landscapes, Ecology Letters (2018) 21: 804–813.

Clark DA (2004). Sources or sinks? The responses of tropical forests to current and future climate and atmospheric composition, Tropical forests and climate change, The Royal Society, DOI 10.1098/rstb.2003.1426.

Collinge S (2010) Spatial Ecology and Conservation. Nature Education Knowledge 3(10):69

Congalton RG (1991). A review of assessing the accuracy of classifications of remotely sensed data. Remote Sensing of Environment, Vol. 37, pp. 35–46.

Cooper DL, Lewis SL, Martin Sullivan MJ, Paulo I. Prado PI (2023, Consistent patterns of common species across tropical tree communities, Nature | Vol 625 | 25 January 2023, https://doi.org/10.1038/s41586-023-06820-z,

Costanza R, de Groot R, Sutton P, Ploeg S, Anderson SJ, Kubiszewski I, Farber SR, and Turner K (2014). Changes in the global value of ecosystem services, Global Environmental Change Vol. 26, No. 152–158.

Crowther T, Glick HB, Covey KR, Bettigole C, Maynard DS, Thomas SM *et al* (2015). Mapping tree density at global scale, ResearchGate, V01.000, Nature, 3, doi:10.1038/nature14967.

Cruz-Cárdenas G, López-Mata L, Villaseñor JL, Ortiz E (2014). Potential species distribution Modeling and the use of principal component analysis as predictor variables, Revista Mexicana de Biodiversidad 85: 189-199.

Cutler DR, Edwards JTC, Beard KH, Cutler A, Hess KT, Gibson J, Lawler JJ (2007). Random forests for classification in ecology. Ecology 88(11):2783–2792

Czúcz B, Keith H, Driver A, Jackson B, Nicholson E, Maes J (2021). A common typology for ecosystem characteristics and ecosystem condition variables. One Ecosystem 6: e58218, doi.org/10.3897/oneeco.6.e58218.

Das S, Bora PK and Das R (2021). Estimation of slope length gradient (LS) factor for the sub-watershed areas of Juri River in Tripura, Modelling Earth Systems and Environment, doi.org/10.1007/s40808-021-01153-0.

Day BB C, Rutishauser E, & Sunderland TC (2013). Relationships between tree species diversity and above-ground biomass in Central African rainforests: implications for REDD. J. of Environmental Conservation, 41(1), 64-72.

De Groot R, Brander L, Solomonides S (2020). Update of global ecosystem service valuation database (ESVD). FSD report No 2020-06 Wageningen, The Netherlands (58 pp).

De Groot R, Brander L, Van der Ploeg S, Costanza R (2012). Global estimates of the value of ecosystems and their services in monetary units, Ecosystem Services, (2012) 50–61.

Deeksha and Shukla AK (2022). Ecosystem Services: A Systematic Literature Review and Future Dimension in Freshwater Ecosystems, J Appl. Sci., 12, 8518, Doi. org/10.3390/app12178518.

Defries R, Pagiola S, Adamowicz WL, Aakaya RK et al (2005).Chapter 2: Analytical approaches for assessing ecosystem condition and human well-being, In: Ecosystems and human well-being. Volume 1: current state and trends, (Millennium Ecosystem Assessment), 37-71.

Devi AS (2022). Influence of trees and associated variables on soil organic carbon: A review, J of Ecology and Environment, 45:5 doi.org/10.1186/s41610-021-00180-3.

Ding D (2006). Analysis on the Economic Valuation of Ecosystem Services: A case study on Lugu Lake basin. MSc thesis, submitted to the Department of Economics, Oslo University.

Dissani BM, Ayenagbo K & N'Souvi K (2021). The Impact of Deforestation on CO2 Emissions: Evidence from WAEMU, Volume: 5, Issue: 5 Year: 2021 Page: 75-87, Int. J of Science and Business.

Dölarslan M, Gγól E, & Ereahin S (2017). Relationship between Soil Properties and Plant Diversity in Semiarid Grassland. J. of Turkish Agriculture-Food Science and Technology, 5(7), 800-806.

Dunn PK, and Smyth GK (2018). Generalized Linear Models with Examples in R, Springer Texts in Statistics, Springer Science Business Media, LLC, part of Springer Nature, doi.org/10.1007/978-1-4419-0118-7-5.

Egendre P (1993). Spatial Autocorrelation: Trouble or New Paradigm?' Jn. Ecological Society of America, 74(6), pp 1659-1673

FAO & ISRIC I (2012). Harmonized world soil database (version 1.1), FAO, Rome, Italy and IIASA, Laxenburg, Austria.

FAO "Food and Agricultural Organization" (2022). The State of the World's Forests 2022. Forest pathways for green recovery and building inclusive, resilient, and sustainable economies. Rome, FAO, doi.org/10.4060/cb9360en.

FAO "Food and Agriculture Organization of the United Nations" (2003). The Digital Soil Map of the World, Version 3.6, Rome.

FAO "Food and Agriculture Organization of the United Nations" (2015). World reference base for soil resources 2014 International soil classification system for naming soils and creating legends for soil maps update 2015, World Roil resources Report, 106, Rome.

FAOa "Food and Agricultural Organization" (2010). Global Forest Resources Assessment, Country Report. Ethiopia, FRA2010/065 Rome, 2010.

FAOb "Food and Agricultural Organization" (2010). Global Forest Resources Assessment Main report Rome.

Faridah-Hanum I, Noor AG, & Nazre M (2010). Assessment of Plant Species Diversity at Pasir Tengkorak Forest Reserve, Langkawi Island, Malaysia, journal of agricultural science, vol., 2, No1.

Fayas CM, Abeysingha NS, Nirmanee KG, Samaratunga D, and Mallawatantri A (2019). Soil loss estimation using RUSLE model to prioritize erosion control in KELANI river basin in Sri Lanka, Int Soil and Water Conservation Research 7 (2019) 130–137.

Fedra K (1993). GIS and environmental modeling, International Institute for Applied Systems Analysis Laxenburg, Austria, Reprinted in 1993 by Novographic, Vienna, Austria. pps. 35- 50. https://www.ddegjust.ac.in

Feng C, Wang H, Lu N, Chen T, He H, Lu Y, and Tu XM (2014). Log-transformation and its implications for data analysis, Shanghai Archives of Psychiatry, Vol. 26, No. 2.

Fentaa AA, Tsunekawaa A, Haregeweyn N (2020). Cropland expansion outweighs the monetary effect of declining natural vegetation on ecosystem services in sub-Saharan Africa, Ecosystem Services 45 (2020) 101154.

Feroz SM, Wum , Sharma S , Li Y , Suwa R , Nakamura K , Hagihara A, Denda T and Yokota M (2009). Floristic composition, woody species diversity, and spatial distribution of trees based on architectural stratification in a subtropical evergreen broadleaf forest on Ishigaki Island in the Ryukyu Archipelago, Japan, TROPICS Vol. 18 (3) Issued November, 2009

Fetene TA (2024). Quantifying Carbon Sequestration of Forest Ecosystem Using GIS and Remote Sensing; the Case of Yeraba State Forest East Gojjam Zone Amhara Regional State,doi: 10.20944/preprints202407.0571.v1

Fibich P, Lepe J, Novotn V, Klimes P, Molem K, Weiblen G D (2016). Spatial patterns of tree species distribution in New Guinea primary and secondary lowland rain forest. J. of Vegetation Science, 27(2), 328-339.

Fischer MM (2006). Spatial Analysis in Geography, Institute for Economic Geography and GIScience. Vienna University of Economics and Business, Nordbergstr. 15/4/AResearchGate,

Fortin MJ and Dale MR (2006). Spatial analysis A Guide for Ecologists,Cambridge University Press The Edinburgh Building, Cambridge cb2 2ru, UK.

Fortin MJ, Dale MRT & Hoef JV (2002). Spatial analysis in ecology, Reserachgate, Volume 4, pp 2051–2058

Fortunel C, Paine CE, Fine PV, Kraft NJ, and Baraloto C (2014). Environmental factors predict community functional composition in Amazonian forests, J., Ecology, 102, 145–155.

Fotis AT, Murphy SJ, Ricart RD, Krishnadas M, Whitacre J, Wenzel JW, Comita LS (2018). Aboveground biomass is driven by massratio effects and stand structural attributes in a temperate deciduous forest. J. of Ecology, 106(2), 561-570.

Fournier A, Barbet-Massin M, Rome Q, Courchamp F (2017). Predicting species distribution combining multi-scale drivers Global Ecology and Conservation 12, 215-226.

Franklin J, Woodcock CE, Phinn SR, and Rogan J (2003). Rationale and conceptual framework for classification approaches to assess forest resources and properties, in Remote Sensing of Forest Environments: Concepts and Case Studies, Wulder M. and Franklin SE, editors, Kluwer Academic Publishers, 279-300

Fu A, Cai Y, Sun T, and Li F (2021). Estimating the Impact of Land Cover Change on Soil Erosion Using Remote Sensing and GIS Data by USLE Model and Scenario Design, Hindawi Scientific Programming Volume 2021, Article ID 6633428, 10 pages, Doi.org/10.1155/2021/6633428.

Fu WJ, Jiang PK, Zhou GM, and Zhao KL (2014). Using Moran's, I and GIS to study the spatial pattern of forest litter carbon density in a subtropical region of southeastern China, Biogeosciences, 11, 2401–2409, 2014.

Ganasri BP, and Ramesh H (2016). Assessment of soil erosion by RUSLE model using remote sensing and GIS - A case study of Nethravathi Basin, Geoscience Frontiers 7 (2016) 953e961.

Gao T, Hedblom M , Emilsson T , Nielsen AB (2014). The role of forest stand structure as biodiversity indicator, Forest Ecology and Management 330 (2014) 82–93,doi.org/10.1016/j.foreco.2014.07.007.

Gashaw T (2015). Threats of Bale Mountains National Park and solutions, Ethiopia, Review paper, J. of Physical Science and Environmental Studies Vol. 1 (2), pp. 10-16, 2015, pearlresearchjournals.org/journals/jpses/index.html

Geary WL, Bode M, Doherty TS, FultonEA, Nimmo DG, Tulloch AT, Tulloch VJ, and Ritchie EG (2020). A guide to ecosystem models and their environmental applications, Nature Ecology & Evolution | VOL 4 | November 2020 | 1459–1471.

Gerke J (2022). The Central Role of Soil Organic Matter in Soil Fertility and Carbon Storage. Soil Syst, 6, 33. https://doi.org/10.3390/ soilsystems6020033.

Getaneh G, Teme S, Tesfaye B, Demel T (2019). Carbon stocks and factors affecting their storage in dry Afromontane forests of Awi Zone, north western Ethiopia. J Ecol Environ 43(1):7

Getaneh ZA, Demissew S, Woldu Z, Aynekulu E (2023). Determinants of plant community along environmental gradients in Geramo forest, the western escarpment of the rift valley of Ethiopia. PLoS ONE 18(11): e0294324, doi.org/10.1371/journal.pone.029432

Getis A (2008). A History of the Concept of Spatial Autocorrelation: A Geographer's Perspective Geographical Analysis 40**;** 297–309 at the Ohio State University.

Getz WM, Marshall CR, Carlson CJ, and Giuggioli L *et al* (2017). Making ecological models adequate, Doi: 10.1111/ele.12893.

Girmay G, Moges A and Muluneh A (2020). Estimation of soil loss rate using the USLE model for Agewmariayam Watershed, northern Ethiopia, Agriculture & Food Security 9:9, doi.org/10.1186/s40066-020-00262-w.

Goldburd M, Khare A, Tevet D, and Guller D (2020). Generalized linear models for insurance rating, CAS monograph series number 5, Second Edition, the Casualty Actuarial Society.

Gómez-Baggethun E, De Groot R, Lomas PL, Montes C (2009). The history of ecosystem services in economic theory and practice: From early notions to markets and payment schemes, Ecological Economics xxx (2009) xxx–xxx, doi: 10.1016/j.ecolecon.2009.11.007.

Gomez-Fern Mendez D, Lopez RS, Zabaleta-Santisteban JA, Medina-Medina AJ, Gonas M, Silva-Lopez JO, Oliva-Cruz M, Rojas-Briceno NB (2024). Landsat images and GIS techniques as key tools for historical analysis of landscape change and fragmentation, *Ecological Informatics 82 (2024) 102738*

Gong W, Liu T, Duan X, Sun Y, Zhang Y, Tong X, Qiu Z (2022). Estimating the Soil Erosion Response to Land-Use Land-Cover Change Using GIS-Based RUSLE and Remote Sensing: A Case Study of Miyun Reservoir, North China. Water 2022, 14, 742. https://doi.org/10.3390/ w14050742.

Gorte RW and Sheikh PA (2010). Deforestation and Climate Change, Congressional Research Service 7-5700 www.crs.gov R41144.

Götzl BM, Tiefenbach M, Tramberend P, and S Condé (2013). Review of recent literature on mapping ecosystem services and analysis of methods used. ETC/BD report for the EEA

Gransee A and Führs H (2013). Magnesium mobility in soils as a challenge for soil and plant analysis, magnesium fertilization and root uptake under adverse growth conditions, Plant Soil (2013) 368:5–21, DOI 10.1007/s11104-012-1567-y.

Guisan A, Edwards, TC and Hastie T (2002). Generalized linear and generalized additive models in studies of species distributions: setting the scene, Ecological Modelling Vol.157, No.89-100.

Haab TC, and McConnell KE (2002). Valuing Environmental and Natural Resources, the Econometrics of Non-Market Valuation, published by Edward Elgar Publishing Limited.

Hadjibiros K (2014). Ecology and Applied Environmental Science ,2014 by Taylor & Francis Group, LLC, CRC Press Taylor & Francis Group 6000 Broken Sound Parkway NW, Suite 300 Boca Raton, FL 33487-2742.

Hadley D, D'Hernoncourt J, Franzén F, Kinell G, Söderqvist T, Soutukorva Å, and Brouwer R (2011). Monetary and non-monetary methods for ecosystem services valuation – Specification sheet and supporting material, Spicosa Project Report, University of East Anglia, Norwich.

Hagos F, van Rooijen D, Haileslassie A, Yehualashet H, Indries H (2018). Investigation of the modalities for an innovative financing mechanism for participatory natural resource management in the Bale Eco-region, Ethiopia. Colombo, Sri Lanka: International Water Management Institute (IWMI). 36p. (IWMI Working Paper 181). Doi: 10.5337/2018.215

Hailemariam SN, Soromessa T, and Teketay D (2015). Land Use and Land Cover Change in the Bale Mountain Eco-Region of Ethiopia during 1985 to 2015; J of Land, Vol.5, No. 41; Doi:10.3390/land5040041.

Haining R (2004). Spatial Data Analysis Theory and Practice, published by the press syndicate of the university of cambridge The Pitt Building, Trumpington Street, Cambridge, United Kingdom.

Hamilton AJ (2005). Species diversity or biodiversity? Journal of Environmental Management 75 (2005) 89–92.

Hanley N, and Czajkowski M (2019). The role of stated preference valuation methods in understanding choices and informing policy. Review of Environmental Economics and Policy, 13(2), pp. 248-266. Doi: 10.1093/reep/rez005

Hao P (2019). Spatial Analysis, The Wiley Blackwell Encyclopedia of Urban and Regional Studies. Edited by Anthony Orum, DOI: 10.1002/9781118568446.eurs0306.

Hatfield JL, & Prueger JH (2015). Temperature extremes: Effect on plant growth and development. J. of Weather and climate extremes, (10), 4-10.

Hatziiordanou L, Fitoka E, Hadjicharalampous E, Votsi N, Palaskas D, Malak D (2019). Indicators for mapping and assessment of ecosystem condition and of the ecosystem service habitat maintenance in support of the EU Biodiversity Strategy to 2020. One Ecosystem 4: e32704. doi.org/10.3897/oneeco.4.e32704

Hegg DA (2006). Valuing Ecological Services and Community Design - Implications for the Private Market and Local Government, MSc thesis submitted to University of Victoria,

Hein L (2014). Biophysical Modelling and Analysis of Ecosystem Services in an Ecosystem Accounting Context, Version 1.

Help CH, Herman PM, & Soetaert K (2001). Indices of diversity and evenness, Netherlands, Institute of Ecology Centre for Estuarine and Coastal Ecology, *institute of oceanography, Oceanis »* vol. 24, No.4. Pp. 61-87

Henderson EB, Ohmann JL, Gregory MJ, Roberts HM, Zald H (2017). Species distribution modelling for plant communities: stacked single species or multivariate modelling approaches? Applied Vegetation Science, 17: 516–527. doi:10.1111/avsc.12085.

Hengl T (2007). A Practical Guide to Geostatistical Mapping of Environmental Variables, European Commission Joint Research Centre Institute for Environment and Sustainability, Italy.

Hill L, Hector A, Hemery G, Smart S, Tanadini M and Brown N (2016). Abundance distributions for tree species in Great Britain: A two-stage approach to modelling abundance using species distribution modelling and random forest, Ecology and Evolution 2017; 7: 1043–1056, DOI: 10.1002/ece3.2661.

Hofhans F, Chacin-Madrigal E, Fuchslueger L, Jenking D, Morera-Beita A, Plutzar C, Dullinger S (2020). Climatic and edaphic controls over tropical forest diversity and vegetation carbon storage. Scientific reports, 10(1), 1-11.

Hofsvang E (2014). State of the rainforest, Rainforest Foundation Norway and GRID Arendal., Norway.

Holling CS *et al*. (I 974). Modelling and simulation for environmental impact analysis, Schloss Laxenburg, A- 2361 Austria.

Hong NT and Izuru I (2019). Forest Ecosystem Services and Local Communities: Towards a Possible Solution to Reduce Forest Dependence in Bach Ma National Park, Vietnam, Human Ecology (2019) 47:465–476, doi.org/10.1007/s10745-019-00083-x.

Hu Y, Su Z, Li W, Li J, & Ke X (2015). Influence of tree species composition and community structure on carbon density in a subtropical forest, PLOS One, 10(8), e0136984.

Humphries HC and Baron J (2001). Ecosystem Structure and Function Modeling 18,A Guidebook for Integrated Ecological Assessments, @ Springer Science+Business Media New York 2001.

Hurni H (1985). Erosion—productivity—conservation systems in Ethiopia. In: Proceedings 4th international conference on soil conservation, Maracay, Venezuela, 3–9 November, 1985, pp 654–674.

Husanoviæ E and Malviæ T (2014). Review of deterministic geostatistical mapping methods in Croatian hydrocarbon reservoirs and advantages of such approach, NAFTA 65 (1) 57-63 (2014)

Huy B (2013). Manuals for Participatory forest/forest carbon measurement (PFM/PCM) (For technical staff).

Ifo SA, Moutsambote JM, Koubouana and Yoka FJ *et al* (2016). Tree Species Diversity, Richness, and Similarity in Intact and Degraded Forest in the Tropical Rainforest of the Congo Basin: Case of the Forest of Likouala in the Republic of Congo, J of Forestry Research Volume 2016, Article ID 7593681, 12 pages, doi.org/10.1155/2016/7593681

Igu NI, Ezenwenyi JU, Ayogu CN, Okolo NV et al (2023). Carbon Storage and Environmental Determinants in a Tropical Rainforest Landscape,Open J. of Ecology, Vol.13 No.4, April 2023

Igwe PU, Onuigbo AA, Chinedu OC, Ezeaku II, Muoneke MM (2017). Soil Erosion: A Review of Models and Applications, [Vol-4, Issue-12, Dec- 2017], International Journal of Advanced Engineering Research and Science *(IJAERS), doi.org/10.22161/ijaers.4.12.22*

Ishfaq M, Wang Y, Yan M, Wang Z, Wu L, Li C and Li X (2022). Physiological Essence of Magnesium in Plants and Its Widespread Deficiency in the Farming System of China. Front. Plant Sci. 13:802274. Doi: 10.3389/fpls.2022.802274.

Islami FA, Tarigan SD, Wahjunie ED and Dasanto BD (2022). Accuracy Assessment of Land Use Change Analysis Using Google Earth in Sadar Watershed Mojokerto, IOP Conf. Series: Earth and Environmental Science,950 (2022) 012091,doi:10.1088/1755-1315/950/1/012091

Istanbuly MN, Dostál T, and Amiri, BJ (2021). Modelling the Soil Erosion Regulation Ecosystem Services of the Landscape in Polish Catchments, Water 2021, 13, 3274. doi.org/10.3390/w13223274.

Jackson LJ, Trebitz AS, and Cottingham KL (2010). An Introduction to the Practice of Ecological ModelingBioScience, August 2000 / Vol. 50 No. 8

Jacquez G (2008). Spatial cluster analysis, chapter 22 In the Handbook of geographic information science, S. Fotheringham and J. Wilson: Blackwell Publishing.

Jafari SM, Zarre S, & Alavipanah SK (2013). Woody species diversity and forest structure from lowland to montane forest in Hyrcanian forest ecoregion. Journal of Mountain Science, 10(4), 609-620.

Jahun BG, Ibrahim R, Dlamini NS, Musa SM (2015). Review of Soil Erosion Assessment using RUSLE Model and GIS; J of Biology, Agriculture and Healthcare www.iiste.org ISSN 2224-3208 (Paper) ISSN 2225-093X (Online) Vol.5, No.9, 2015.

Janitza S, & Hornung R (2018). On the overestimation of random forestβs out-of-bag error. PloS one, 13(8), e0201904.

Jeffers JNR (1988). Practitioner's Handbook on the Modeling of Dynamic Change in Ecosystems. New York: Wiley

Jemal K (2021). Review of Soil Erosion Risk for Soil and Water Conservation Planning Under Ethiopian Condition, Agrotechnology, Vol.10 Iss. 5 No: 217.

Jeyanny V, Husni M, Rasidah KW, Kumar BS, Arifin A & Hisham AM (2014). Carbon stocks in different carbon pools of a tropical lowland forest and a montane forest with varying topography, J of Tropical Forest Science 26(4): 560–571 (2014).

Jiang Z (2012). A Survey on Spatial and Spatiotemporal Prediction Methods, ArXiv:2012.13384v1 [cs. LG] 24 Dec 2020.

Jopp F *et al*., eds. (2011). Modeling Complex Ecological Dynamics, Doi 10.1007/978-3-642-05029-9_3, # Springer-Verlag Berlin Heidelberg 2011

Kalivas DP, Kollias VJ, & Apostolidis EH (2013). Evaluation of three spatial interpolation methods to estimate forest volume in the municipal forest of the Greek island Skyros, Jouranl of Geo-spatail information science. Vol 16, Issue2.

Kankanamge A, and Jayantha I (2021). Economic Valuation of Ecosystem Services Provided by Forest Ecosystems in Sri Lanka: A Study Based on 2010 Forest Cover Classification and the TEEB Database" (2021). MSc thesis submitted to Portland, doi.org/10.15760/mem.72

Kapwata T, and Gebreslasie MT (2016). Random forest variable selection in spatial malaria transmission modelling in Mpumalanga Province, South Africa, Geospatial Health; 11:434, gh_3.qxp_Hrev_master 25/10/16 14:38 Pagina 251.

Kayet M., Pathak K, Chakrabarty A, and Sahoo S (2018). Evaluation of soil loss estimation using the RUSLE model and SCS-CN method in hillslope mining areas, International Soil and Water Conservation Research 6 (2018) 31–42.

Kefale T, Hagos H, Rooijen D, Haileslassie A (2021). Farmers' willingness to pay for alternative resource management practices in the Bale Eco-Region, Ethiopia: An application of choice experiment, Heliyon 7,2021 e08159, doi.org/10.1016/j.heliyon. 2021.e08159.

Kent M (2011). Vegetation description and data analysis: a practical approach: John Wiley & Sons.

Ketema T, Chimdesa C, Eshetu M, Gosa R, Abagaja D, Getachew G (2024). Soil Erosion Mapping and Severity Analysis Based on RUSLE Model on Welmel Catchments of Ganale-Dewa River Basin Bale Lowland South Eastern Ethiopia,East African Scholars J Agri Life Sci,DOI:10.36349/easjals.2024.v07i03.001

Kewessa G, Tiki L, Nigatu D, Datiko D (2019). Effect of forest coffee management practices on woody species diversity and composition in bale eco-region, Southeastern Ethiopia. Open J Forest Vol. 9, No.4, pp: 265–282.

Kflay G, and Kitessa H (2014). Species composition, Plant Community structure and Natural regeneration status of Belete Moist Evergreen Montane Forest, Oromia Regional state, Southwestern Ethiopia, *Momona Ethiopian Journal of Science (MEJS), V6(1):97-101.*

Kibret K (2014). Characterization of agricultural soils in CASCAPE intervention woredas in Eastern Region final Report, Haramaya University.

Kidane Y, Stahlmann R and Beierkuhnlein C(2012).Vegetation dynamics, and land use and land cover change in the Bale Mountains, Ethiopia, Environ Monit Assess. 2012, 184, 7473–7489, DOI 10.1007/s10661-011-2514-8

Kim HS (2006). Soil erosion modelling using RUSLE and GIS on the Imha watershed, South Korea, MSc thesis submitted to Colorado State University.g

Kitikidou K, Milios E, Stampoulidis, A.; Pipinis E, Radoglou K (2024). Using Biodiversity Indices Effectively: Considerations for Forest Management. Ecologies 2024, 5, 42–51, doi.org/10.3390/ecologies5010003

Klobuar D, and Pernar R (2012). Geostatistical approach to spatial analysis of forest damage, Periodicum Biologorum Vol. 114, No 1, 103–110.

Kobler J, Zehetgruber B, Dirnbγάck T, Jandl R, Mirtl M, & Schindlbacher A (2019). Effects of aspect and altitude on carbon cycling processes in a temperate mountain forest catchment. J. of Landscape Ecology, 34(2), 325-340.

Kolli MK, Opp C and Groll M (2021). Estimation of soil erosion and sediment yield concentration across the Kolleru Lake catchment using GIS; Environmental Earth Sciences, 80:161, Doi.org/10.1007/s12665-021-09443-7.

Kome G K, Enang RK, Tabi FO & Yerima BP (2019). Influence of Clay Minerals on Some Soil Fertility Attributes: A Review. Open J. of Soil Science, 9(9), 155-188.

Krankina O, Houghton R, Harmon M, Hogg E, Butman D, Yatskov M, Spycher G (2005). Effects of climate, disturbance, and species on forest biomass across Russia. J. of Canadian Forest Research, 35(9), 2281-2293.

Kukreja H, Bharath N, Siddesh CS, and Kuldeep S (2016). AN Introduction to an artificial neural network, Vol-1 Issue-5 2016 IJARIIE-ISSN (O)-2395-4396.

Kumar J (2021). System Models and System Simulation Lesson No. 01, Paper Code: MCA 504 uploaded document on 14/11/2021.

Kumar P (2005). Market for Ecosystem Services, International Institute for Sustainable Development (IISD), Web site: www.iisd.org/

Kumar P, and Mina U (2021). Fundamentals of Ecology and Environment, third edition, ResearchGate, https://www.researchgate.net/publication/355381814, publisher Pathfinder Publication.

Kumari R , Deepali , Bhatnagar S (2021).Biodiversity Loss: Threats and Conservation Strategies, Int. J. Pharm. Sci. Rev. Res., 68(1), May - June 2021; Article No. 37, Pages: 242-254, DOI: 10.47583/ijpsrr.2021.v68i01.037, doi.org/10.47583/ijpsrr.2021.v68i01.037.

Labrière N, Locatelli B, Vieilledent G, Kharisma S (2016). Spatial congruence between carbon and biodiversity across forest landscapes of northern Borneo,Global Ecology and Conservation 6 (2016) 105–120

Lakićević M, and Srđević B (2018). Measuring biodiversity in forest communities a role of biodiversity indices, Contemporary Agriculture, Vol. 67, No. 1, Pp. 65 - 70, 2018, DOI: 10.2478/contagri-2018-0010.

Latimer Am, Wu S, Gelfand, AE, and Silander, JA (2006). Building Statistical Models to Analyze Species Distributions; *Ecological Applications,* 16(1), pp. 33–50 by the Ecological Society of America.

Legesse F, Degefa S, and Soromessa T (2022). Valuation Methods in Ecosystem Services: A Meta-analysis, World J. of Forest Research, 1(1), 01-12.

Lemi T, Guday S, Fantaye Y, Eshete A, and Hassen N (2023). Woody Species Composition, Structure, and Diversity of Dindin Natural Forest, South East of Ethiopia; Hindawi International J. of Forestry ResearchVolume 2023, Article ID 5338570, 13 pageshttps://doi.org/10.1155/2023/5338570

Lesschen JP, Verburg PH, and Staal SJ (2005). Statistical methods for analyzing the spatial dimension of changes in land use and farming systems, LUCC Report Series No. 7, The International Livestock Research Institute, Nairobi, Kenya & LUCC Focus 3 Office, Wageningen University, the Netherlands.

Li J (2022). Spatial Predictive Modeling with R, CRC Press is an imprint of Taylor & Francis Group, LLC.

Li J, and Heap AD (2008). A Review of Spatial Interpolation Methods for Environmental Scientists, published by Commonwealth of Australia.

Lichtenstern A (2013). Kriging methods in spatial statistics, Bachelor's Thesis, Muunchen University, Germany.

Liedtke TM (2011). A Comparison of Spatial Prediction Techniques Using Both Hard and Soft Data, Theses in Statistics. 7. https://digitalcommons.unl.edu/statisticsdiss/7.

Lindeman RL (1942). The trophic–dynamic aspect of ecology. Ecology 23, 399–418

Liu S, Bai M, Yao M (2021). Integrating Ecosystem Function and Structure to Assess Landscape Ecological Risk in Traditional Village Clustering Areas. Sustainability 2021, 13, 4860, doi.org/10.3390/ su13094860

Liu S, Costanza R, Farber S, and Troy A (2010). Valuing ecosystem services Theory, practice, and the need for a transdisciplinary synthesis, Issue: Ecological Economics Reviews. Ann. N.Y. Acad. Sci. ISSN 0077-8923.

Lof M, Grondard N, Hein L, Barton DN, and Martin FS (2022). Guidance for the Biophysical Modelling and Analysis of Ecosystem Services in an Ecosystem Accounting Context

Long C, Yang X, Long W, Li D, Zhou W, and Zhang H (2018). Soil Nutrients Influence Plant Community Assembly in Two Tropical Coastal Secondary Forests, tropical Conservation Science Vol. 11, pp:1–9; DOI: 10.1177/1940082918817956.

Lopatin J, Dolos K, Hernández HJ, Galleguillos M, & Fassnacht FE (2016). Comparing Generalized Linear Models and random forest to model vascular plant species richness using LiDAR data in a natural forest in Central Chile; Remote Sens Environ Vol.173, pp: 200–210, Doi: 10.1016/j.rse.2015.11.029.

Losonci I (2012). "Valuation of ecosystem services: The case of Orseg National Park, Hungary" (2012). Master's Theses and Capstones. 738, https://scholars.unh.edu/thesis/738.

Lulekal E, Kelbessa E, Bekele T, Yineger H (2008). Plant species composition and structure of the Mana Angetu Moist montane Forest, South-Eastern Ethiopia, J of East African Natural History Vol.97, No.2, pp: 165-185.

Luo W, Taylor MC, and Parker SR (2007). A comparison of spatial interpolation methods to estimate continuous wind speed surfaces using irregularly distributed data from England and Wales, International Journal of Climatology Int. J. Climatol. 28: 947–959.

Luvai A, Obiero J, and Omuto C (2022). Soil Loss Assessment Using the Revised Universal Soil Loss Equation (RUSLE) Model, Hindawi Applied and Environmental Soil Science Volume 2022, Article ID 2122554, 14 pages, Doi.org/10.1155/2022/2122554.

Maes J, Braat L, Jax K, Hutchins M, *et al* (2012).‘A spatial assessment of ecosystem services in Europe: Methods, case studies and policy analysis – phase 1’, PEER Report No 3, Ispra: Partnership for European Environmental Research. Retrieved on 05.07.2012 http://www.peer.eu/fileadmin/user_upload/publications/PEER_report_3_phase_I.pdf

Maes J, Fabrega N, Zulian G, Barbosa A, and Vizcaino P *et al* (2015). Mapping and Assessment of Ecosystems and their Services, Trends in ecosystems and ecosystem services in the European Union between 2000 and 2010, JRC science and policy report.

Mandal FB, Chatterjee C and Ghosh A (2011). Ecosystems and human wellbeing J. Environ. & Sociobiol, Vol. 8, No.1, pp, 25-42.

Mantel S, and Schulp CJ (2014). Modelling of soil degradation and its impact on ecosystem services globally, Part 1: A study on the adequacy of models to quantify soil water erosion for use within the IMAGE modeling framework Report 2014/xx, ISRIC—World Soil Information, Wageningen. 74 pages,28 figures and 12 Tables.

Matkala L, Salemaa M, and Bäck J (2020). Soil total phosphorus and nitrogen explain vegetation community composition in a northern forest ecosystem near a phosphate massif, Biogeo sciences, Vol.17, pp: 1535–1556, doi.org/10.5194/bg-17.

Maynou F (1998). The application of geostatistics in mapping and assessment of demersal resources. *Nephrops norvegicus* (L.) in the northwestern Mediterranean: a case study Journal of Scientia Marina 62 (1): 117-133.

Mcdonald C, Smith R, Scott M, Dick J (2010). Using indices to measure biodiversity change through time, International Workshop on Spatio-temporal mdelling, Santigo de compotela 30 june -2 jul2010.

MEA "Millennium Ecosystem Assessment" (2005). Ecosystems and Human Well-being: Synthesis. Island Press, Washington, DC.

Meier ES (2011). Modelling Spatial Dynamics of Plant Distributions Implementation of Biotic Interactions and Migration Improves Large-scale Projections of Species Distributions during Climate and Land-use Change, Dissertation submitted to University of Zurich.

Merganič JK, Marue TK, RB, & Audolensk V (2012). Plant Diversity of Forests, Forest Ecosystems - More than Just Trees, Dr Juan A. Blanco (Ed.), ISBN: 978-953-51-0202-1, InTech, Available from: http://www.intechopen.com/books/forest-ecosystems-more-than-just-trees/plantdiversity-of-forests

Mezgebu A and Workineh G (2017). Changes and drivers of afro-alpine forest ecosystem: future trajectories and management strategies in Bale eco-region, Ethiopia, Ecological Processes Vol. 6, No. 42, doi 10.1186/s13717-017-0108-2.

Mi C, Huettmann F, Sun R and Guo Y (2017). Combining occurrence and abundance distribution models for the conservation of the Great Bustard, Peer J 5: e4160; DOI 10.7717/peerj.4160

Miller J (2010). Species Distribution Modelling, and Geography Compass 4/6: 490–509, 10.1111/j.1749-8198.2010.00351, published by Blackwell Publishing Ltd.

Mohammed GU, & Belliethathan S (2014). Forest carbon stocks in woody plants of Tara Gedam forest: Implication for climate change mitigation. J. of Science, Technology and Arts Research, 3(1), 101-107.

Moisa MB, Dejeneb IN, Merga BB and Gemeda DO (2022). Soil loss estimation and prioritization using geographic information systems and the RUSLE model: a case study of the Anger River sub-basin, Western Ethiopia, Journal of Water and Climate Change Vol 13 No 3, 1170 doi: 10.2166/wcc.2022.433

Monga P, Radhika, and Sharma M (2017). The Structural and Functional Unit of Environment: Ecosystem, Int J of Advance Research in Science and Engineering, Vol 6, No.03

Morales-Hidalgo, Oswalt SN, Somanathan E (2015). Status and trends in global primary forest, protected areas, and areas designated for conservation of biodiversity from the Global Forest Resources Assessment 2015, Forest Ecology and Management.

Moreno EJC (2007). Ecological and spatial modeling, Mapping ecosystems, landscape changes, and plant species distribution in Llanos del Orinoco, Venezuela , PhD thesis, Enschede, the Netherlands.

Morris EK, Caruso T, Buscot F, Fischer M, Hancock C, Maier TS, Meiners T, Muller C, Obermaier E, Prati D, Socher SA, Sonnemann I, Waaschke N, Tesfaye W, Susanne W, & Rillig MC (2014). Choosing and using diversity indices: insights for ecological applications from the German Biodiversity explanatories, Open access review of Ecology and Evolution 4(18): 3514– 3524.

Moutinho P, and Schwartzman S, (2015). Tropical Deforestation and Climate Change,Amazon Environmental Research Institute (IPAM), Resaerachgate .

Mulatu DW (1976). Linking the Economy to the Ecosystems: land use change and ecosystem services valuation at basin level, ITC dissertation submitted to the university of Twente, The Netherlands.

Mwakisunga B. and Majule AE (2012).The influence of altitude and management on carbon stock quantities in Rungwe forest, southern highland of Tanzania, Vol.2, No.4, 214-221 (2012) Open J of Ecology, doi.org/10.4236/oje.2012.24025.

Naidu MT, and Kumar OA (2016). Tree diversity, stand structure, and community composition of tropical forests in Eastern Ghats of Andhra Pradesh, India, Journal of Asia-Pacific Biodiversity.

Narita DN, Lemenih M, Shimoda Y, Ayana AN (2018). Economic Accounting of Ethiopian Forests: A Natural Capital Approach, Forest Policy, and Economics, ISSN 1389-9341, Elsevier, Amsterdam, Vol. 97, pp. 189-200, doi.org/10.1016/j.forpol.2018.10.002.

Natake T (2012). Patterns of soil texture and root biomass along a humid tropical forest hillslope catena. University of California.

Nchimbi G (2021). Tree species diversity, composition, population structure and associated herbivore abundance in human-impacted and nonimpacted areas of Marang' forest, Northern Tanzania, MSc thesis submitted to Life Sciences of the Nelson Mandela African Institution of Science and Technology Arusha, Tanzania.

Neba SG (2013). Assessment and prediction of above-ground biomass in selectively logged forest concessions using field measurements and remote sensing data: case study in southeast Cameroon, Thesis submitted to the University of Helsinki.

Negese A, Fekadu E and Getnet H (2021). Potential Soil Loss Estimation and Erosion-Prone Area Prioritization Using RUSLE, GIS, and Remote Sensing in Chereti Watershed, Northeastern Ethiopia, Air, Soil and Water Research Volume 14: 1–17.

Nelson A (2012) General Management Planning for the Bale Mountains National Park, Walia-Special Edition on the Bale Mountains

Neves, DA, Lemos F, Gonzaʿlez, AP, Vieira SR, & Siqueira GM. (2010). Using geoestatistics for assessing biodiversity of forest reserve areas, Bragantia, 69, 131-140.

Newbold T (2010). The value of species distribution models as a tool for conservation and ecology in Egypt and Britain. PhD thesis, University of Nottingham Submitted to the University of Nottingham.

Nguyen TV (2012). Ecosystem-based fishery management: A review of concepts and ecological economic models. Journal of Ecosystems and Management 13(2)1–14. Published by FORREX Forum for Research and Extension in Natural Resources. http://jem.forrex.org/index.php/jem/article/viewFile/142/460

Nguyen TV, Mitlöhner R, Bich NV and Do, TV (2015). Environmental Factors Affecting the Abundance and Presence of Tree Species in a Tropical Lowland Limestone and Non-limestone Forest in Ben

En National Park, Vietnam, J of Forest and Environmental Science Vol. 31, No. 3, pp: 177-191, dx.doi.org/10.7747/JFES.2015.31.3.177.

Nurhssen S (2016). The Role of Tourism on Local Economic Development of Gondar City, Amhara Regional State, Ethiopia. J Glob Econ 4: 207, doi: 10.4172/2375-4389.1000207.

Nut N, Mihara M, Jeong J, Ngo B, Sigua G, Prasad PV, Reyes MR (2023). Land Use and Land Cover Changes and its Impact on Soil Erosion in Stung Sangkae Catchment of Cambodia. Sustainability 2021, 13, 9276. https://doi.org/10.3390/ su13169276.

Nyairo R (2024). Effect of slope on water run-off and soil vulnerability in an unglaciated sub-watershed: A case study of Conservation Practices, *Environmental Systems Research* (2024) 13:50.

OFWE "Oromia Forest and Wildlife Enterprise", Farm Africa and SOS Sahel Ethiopia (2014). Bale Mountains Eco-Region Reduction of Emission from Deforestation and Forest Degradation (REDD+) Project Ethiopia.

Oindo BO (2011). Spatial Patterns of Species Diversity in Kenya, phD thesis, Wageningen University.

Olden JD, and Jackson DA (2002). Illuminating the ‘‘black box’’: a randomization approach for understanding variable contributions in artificial neural networks, Ecological Modelling vol.154, pp: 135–150.

Olea, R.A., 2009. A practical primer on Geostatistics: U.S. Geological Survey, Open-File Report 2009-1103, 346.

Olorunfemi IE, Fasinmirin JT, & Akinola FF (2018). Soil physico-chemical properties and fertility status of long-term land use and cover changes: A case study in forest vegetative zone of Nigeria. J. of Eurasian of Soil Science, 7(2), 133-150.

Osaragi T (2008). Classification methods for spatial data representation, center for advanced spatial analysis Working Paper Series, 40, Reserachgate.

Osborne JW (2016). Notes on the use of data transformations. Practical Assessment, Research & Evaluation, 8(6). Available online: http://ericae.net/pare/getvn.asp?v=8&n=6.1.

Ozcelik R, Gul, AU, Merganic J, & Merganicova K (2008). Tree species diversity and its relationship to stand parameters and geomorphology features in the eastern Black sea region forests of turkey. J. of Environmental Biology, 29(3), 291-298.

Padmakumar B, Sreekanth NP, Shanthiprabha V, Paul J, Sreedharan K, Augustine T, Ramasamy, EV (2018). Tree biomass and carbon density estimation in the tropical dry forest of Southern Western Ghats, India. J. of Forest-Biogeosciences and Forestry, 11(4), 534.

Pallaris K (1998). Modelling the Distribution of Cecropia Species Using GIS based Techniques Implications for Tropical Forest Conservation, MSs submitted *King's College*, *Londonun*

Panagos P, Borrelli P, Poesen J, Ballabio C, Lugato E, *et al* (2015). The new assessment of soil loss by water erosion in Europe, /Environmental Science & Policy 54 (2015), doi.org/10.1016/j.envsci.2015.08.012.

Paramasivam and Venkatramanan S (2019). An Introduction to Various Spatial Analysis Techniques Chapter 3, GIS and Geostatistical Techniques for Groundwater Science, doi.org/10.1016/B978-0-12-815413-7.00003-1.

Park JS, and Lee EJ (2014) Geostatistical analyses and spatial distribution patterns of tundra vegetation in Council, Alaska, J. Ecol. Environ. 37(2): 53-60.

Patarkalashvili T (2017). Forest biodiversity of Georgia and endangered plant species, journal of Annals of Agrarian Science 15, 349-351.

Pauli N (2010). The Tropical Forest Governance 21st Century, briefing document by the James Martin 21st Century School, University of Oxford.

Paulos D (2021). Soil and Water Resources and Degradation Factors Affecting their Productivity in the Ethiopian Highland Agro-ecosystems. International Conference on African Development Archives. 1. https://scholarworks.wmich.edu/africancenter_icad_archive/.

Payna TW, Hill RB, HoÈcka BK, Skinner MF, Thorn AJ, and Rijkse WC (1999). Potential for the use of GIS and spatial analysis techniques as tools for monitoring changes in forest productivity and nutrition, a New Zealand example, journal Forest Ecology and Management 122, 187-196.

Pearson RG (2007). Species' Distribution Modelling for Conservation Educators and Practitioners. Synthesis. American Museum of Natural History. Available at http://ncep.amnh.org.

Pelissar AL, Filho AF , Ebling AA , CARLOS R. *et al* (2018). Spatial variability of tree species diversity in a mixed tropical forest in Southern Brazil,Anais da Academia Brasileira de Ciências (2018) 90(2 Suppl. 1): 2491-2500.

Peng G, Shao Y, and Leslie LM (2002). Environmental modeling and prediction, Reserachgate, Springer-Verlag Berlin Heidelberg, https://www.researchgate.net/publication/259618525.

Perng BH, Lam TY, Cheng ST, Su SH *et al* (2024). Mapping distribution of woody plant species richness from field rapid assessment and machine learning, Taiwania 69(1): 1–15, 2024 DOI: 10.6165/tai.2024.69.1

Pham TG, Degener J, Kappas M (2018). Integrated universal soil loss equation (USLE) and Geographical Information System (GIS) for soil erosion estimation in A Sap basin: Central Vietnam, International Soil and Water Conservation Research 6 (2018) 99–110; doi.org/10.1016/j.iswcr.2018.01.001.

Phinzi K and Ngetar NS (2019). The assessment of water-borne erosion at catchment level using GIS-based RUSLE and remote sensing: A review, International Soil and Water Conservation Research 7 (2019) 27–46, doi.org/10.1016/j.iswcr.2018.12.002.

Pierzynski G, Caon L and Vargas R (2017). Threats to soils: global trends and perspectives, a Contribution from the Intergovernmental Technical Panel on Soils, Global Soil Partnership Food and Agriculture Organization of the United Nations, Global land outlook working paper.

Pittroff W, and Pedersen EK (2005). Ecological Modelling, Encyclopedia of life Sciences & 2005, John Wiley & Sons, Ltd. www.els.net

Poorter L, van der Sande MT, Thompson J, Arets EJ, Boit A (2015). Diversity enhances carbon storage in tropical forests. J. of Global Ecology and Biogeography, 24(11), 1314-1328.

Prasad B and Tiwa HL (2016).GIS-based soil erosion modeling, Int. J. of Civil Engineering and Technology (IJCIET) Volume 7, Issue 6, November-December 2016, pp. 166–171, Article ID: IJCIET_07_06_018.

Prasad S (2022). Structure and functions of ecosystem course**,** Environmental geography, academic year of 2022/2023**,** Mukherjee, University, Ranchi.

Puheim M, and Madarász L (2014). Normalization of Inputs and Outputs of Neural Network Based Robotic Arm Controller in Role of Inverse Kinematic Model, a conference paper.

Rabia HA, Afifi RR, Gelaw AM, Bianch S *et al* (2013). Soil mapping and classification: a case study in the Tigray Region, Ethiopia, J. of Agriculture and Environment for International Development - JAEID 2013, 107 (1): 73 – 99.

Rahman A, Khan SM, Ahmad Z, Alamri S, *et al* (2021). Impact of multiple environmental factors on species abundance in various forest layers using an integrative modelling approach, Global Ecology and Conservation29, e01712.

Rebelo H, and Jones G (2009). Ground validation of presence-only modelling with rare species: a case study on barbastelles Barbastella barbastellus (Chiroptera: Vespertilionidae), J of Applied Ecology.

Redowan M (2015). Spatial pattern of tree diversity and evenness across forest types in Majella National Park, Italy. Forest Ecosystems, 2(1), 1-10.

Relethford JH (2008). Geostatistics and Spatial Analysis in Biological Anthropology, American Journal of Physical Anthropology 136:1–10.

Renard KG, Foster GR, Weesies GA, McCool DK, & Youder DC (1997). Predicting soil erosion by water: A guide to conservation planning with the revised universal soil loss equation (RUSLE), USDA (Agriculture Handbook Number 703).

Rendon P, Erhard M, Maes J & Jahunhard B (2019) Analysis of trends in mapping and assessment of ecosystem condition in Europe, Ecosystems and People, 15:1, 156-172, DOI: 10.1080/26395916.2019.1609581.

Reyers B, Bidoglio G, Dhar U, Gundimeda H *et al* (2010). Chapter 3 Measuring biophysical quantities and the use of indicators, the Economics of Ecosystems and Biodiversity: The Ecological and Economic Foundations.

Ridwan MA, Radzi NA, Ahmad WS, Mustafa IS, Din NM, Jalil YE, Isa AM, Othman NS, Zaki W (2018) Applications of Landsat-8 Data: a Survey, Int. J of Engineering & Technology, 7 (4.35) (2018) 436-441

Riisgard HU (2017). General ecology outline of contemporary ecology for university students, 1st edition, http://bookboon.com/

Rion V (2010). Modeling the plant species richness: a comparison between two approaches, Master thesis of Science in Behavior, Evolution, and Conservation Lausanne University.

Rodrigues AR, Botequim B, Tavares C, Pécurto P and Borges J (2020). Addressing soil protection concerns in forest ecosystem management under climate change, Forest Ecosystems (2020) 7:34, doi.org/10.1186/s40663-020-00247-y.

Rossi RE, Mulla DJ, Journe AJ, Fran EH (1992). Geostatistical Tools for Modeling and Interpreting Ecological Spatial Dependence`, journal of *Ecological.Ecological Molonographs* 62(2), pp. 277-314.

Sahragard HP, Ajorlo M, & Karami P (2018). Modelling habitat suitability of range plant species using random forest method in arid mountainous rangelands. J. of Mountain Science, 15(10), 2159-2171.

Sakate DM and Kashid DN (2016). A new robust model selection method in GLM with application to ecological data, Environ Syst Res (2016) 5:9 DOI 10.1186/s40068-016-0060-7.

Sales MH, Souza JR, CM, Kyriakidis PC, Roberts DA, & Vidal E (2007). Improving spatial distribution estimation of forest biomass with geostatistics: A case study for Rondnia, Brazil. J. of Ecological Modelling, 205(1-2), 221-230.

Samui P, and Sitharam, TG (2011). Application of Geostatistical Models for Estimating Spatial Variability of Rock Depth, J of scientific research, Engineering, 3, 886-894.ich

Sanders L (2007). Introduction to Models in Spatial Analysis. Lena Sanders. Models in Spatial Analysis, ISTE, London, PP.xv-xxvii, 2007, Geographical Information Systems series. ffhalshs-00226417.

Santos CGA, Watanabe M and Suzuki MK (1998). A conceptual soil erosion model, Annual J of Hydraulic Engineering, JSCE, VOL.42, 1998,

Scarnati L, Attorre F, Farcomeni A, Francesconi F, and Sanctis MD (2009). Modelling the spatial distribution of tree species with fragmented populations from abundance data, J. of Community Ecology, 10(2),215-224, DOI: 10. 1556.comEc.10.2009.2.12.

Scheller RM, & Mladenoff DJ (2007). An ecological classification of forest landscape simulation models: tools and strategies for understanding broad-scale forested ecosystems. Landscape Ecology, 22(4), 491-505.

Schmitt CB, Denich M, & Boehmer H J (2009). Plant diversity and conservation of Afromontane forest with Coffea arabica in the Bonga region (SW Ethiopia). In: X. van der Burgt, J. van der Maesen & J.M. Onana (eds), Systematics and Conservation of African Plants, pp. 679–690. Royal Botanic Gardens, Kew.

Schröter M (2015). Conceptual basis and spatial modeling to account for and conserve multiple ecosystem services in Telemark County, Norway, MSc Thesis submitted to Wageningen University

Schroter M, Zanden EH, Alexander PE van Oudenhove *et al* (2014). Ecosystem Services as a Contested Concept: A Synthesis of Critique and Counter-Arguments, Conservation Letters, 2014, 7(6), 514–523.

Sciarrettam Am and Trematerra P (2014). Geostatistical Tools for the Study of Insect Spatial Distribution: Practical Implications in the Integrated Management of Orchard and Vineyard Pestsm , Plant Protect. Sci. Vol. 50, No. 2: 97–110.

Selivanov E, Hlaváčková P (2021). Methods for monetary valuation of ecosystem services: A scoping review. J. For. Sci., 67: 499–511.

Senbeta F, & Denich M (2006). Effects of wild coffee management on species diversity in the Afromontane rainforests of Ethiopia. J. of Forest Ecology and Management, 232(1-3), 68-74.

Sharma R, Rima B, Baral H, Nehren U *et al* (2019). Impact of Land Cover Change on Ecosystem Services in Tropical Forested Landscape, Vol.8, pp. 18, doi:10.3390/resources8010018.

Sharma S, Hussain S, and Singh AN (2021). Integrated Approaches of Ecology and Economy for Sustainable Development with Special Emphasis on Ecosystem Services: A Review, Journal of Scientific Research, Volume 65, Issue 3, 2021; DOI: 10.37398/JSR.2021.650312

Sheate WR, Eales RP, Daly E , Baker J, Murdoch A, Hill C , Ojike U and Karpouzoglou (2012). Spatial representation and specification of ecosystem services: a methodology using land use/land cover data and stakeholder engagement, Journal of Environmental Assessment Policy and Management Vol. 14, No. 1 (March 2012) 1250001 (36 pages).

Shuang S, Costanza R, Farber S, and Austin TA (2010). Valuing ecosystem services Theory, practice, and the need for a transdisciplinary synthesis, Ann. N.Y. Acad. Sci. 1185 (2010) 54–78 c 2010, New York Academy of Sciences

Silvis HJ, and Heide CM (2013). Economic viewpoints on ecosystem services. Wageningen, Statutory Research Tasks Unit for Nature and the Environment (WOT Natuur & Milieu). Wot-rapport 123. 68 p. 7 Fig.; 9 Tab.; 91 Ref.

Simeon M and Wana D (2024). Impacts of Land use Land cover dynamics on Ecosystem services in maze national park and its environs, southwestern Ethiopia, Heliyon 10 (2024) e30704, doi.org/10.1016/j.heliyon.2024.e30704

Sing L, Ray D and Watts K (2015). Ecosystem services and forest management, ResearchGate, forestry Commission, UK.

Sintayehu DW, Belayneh A, and Dechassa N (2020). Aboveground carbon stock is related to land cover and woody species diversity in tropical ecosystems of Eastern Ethiopia, Ecological Processes (2020) 9:37

Skidmore AK, Franklin J, Dawson TP and Pilesjö P (2011). Geospatial tools address emerging issues in spatial ecology: a review and commentary on the Special Issue, International J of Geographical Information Science, 25:3, 337-365, DOI: 10.1080/13658816.2011.554296.

Soberón J, and Peterson AT (2005). Interpretation of models of fundamental ecological niches and species' distributional areas, *Biodiversity Informatics*, 2, pp. 1-10.

Sola J, and Sevilla J (1997). Importance of input data normalization for the application of neural networks to complex industrial problems.

Solomon N, Segnon AC, and Birhane E (2019). Ecosystem Service Values Changes in Response to Land-Use/Land-Cover Dynamics in Dry Afromontane Forest in Northern Ethiopia, Int. J. Environ. Res. Public Health 2019, 16, 4653; doi:10.3390/ijerph16234653.

Spash C (2008). Ecosystems Services Valuation, Socio-Economics and the Environment in Discussion CSIRO Working Paper Series 2008-03 CSIRO Sustainable Ecosystems, Canberra.

Steimer C (2017). Review of various methods for interpolation of rainfall and their applications in hydrology Bachelor Thesis, Hogenbergstr, München.

Stockwell DR, and Peterson T (2002). Effects of sample size on accuracy of species distribution models. Ecological Modelling 148, 1-13.

Sun L, Wang M, & Fan X (2020). Spatial pattern and driving factors of biomass carbon density for natural and planted coniferous forests in mountainous terrain, eastern Loess Plateau of China. J. of Forest Ecosystems, 7(1), 9.

Sutton P, Anderson S, Costanza R, Kubiszewski I (2016). The ecological economics of land degradation: impacts on ecosystem service values. Ecology. Econ. Vol.129, No. 182–192.

Szmyt J, and Stoyan D (2014). Spatial autocorrelation of tree attributes in naturally regenerated managed beech (Fagus sylvatica) forests in the Beskid Niski Mountains, southern Poland, Journal of Dendrology, vol 71, 129–136.

Tadesse L, Suryabhagavan KV, Sridhar G, and Legesse G (2017). Land use and land cover changes and Soil erosion in Yezat Watershed, North Western Ethiopia, International Soil and Water Conservation Research 5 (2017) 85–94.

Tamire C, Elias E, and Argaw M (2023). A systematic review of ecosystem services assessments, trends, and challenges in Ethiopia, Watershed Ecology and the Environment. 5, pp. 38–45.

Tan L, Zhang P, Zhao X, Fan C, Zhang C, Yan Y, von Gadow K (2020). Analysing species abundance distribution patterns across sampling scales in three natural forests in Northeastern China. iForest 13: 482-489, doi: 10.3832/ifor3211-013.

Tanács E, Bede-Fazekas Á, Csecserits A, Kisné Fodor L, Pásztor L, Somodi I, Standovár T, Zlinszky A, Zsembery Z, Vári Á (2022) Assessing ecosystem condition at the national level in Hungary, indicators, approaches, challenges. One Ecosystem 7: e81543.//doi.org/10.3897/oneeco.7.e81543.

Taylor PG, Cleveland CC, Wieder WR, Sullivan BW, Doughty CE, Dobrowski SZ, & Townsend, AR (2017). Temperature and rainfall interact to control carbon cycling in tropical forests. J. of Ecology letters, 20(6), 779-788.

TEEB "the Economics of Ecosystems and Biodiversity" (2010). Mainstreaming the Economics of Nature: A Synthesis of the Approach, Conclusions and Recommendations of TEEB: 40.

Teferi E, Bantider A, Zeleke G, Bewket W and Kassawmar T (2021). 'Mapping Aboveground Carbon Stocks and Emissions Induced by Land Use and Land Cover Change in Ethiopia: A Remote Sensing Approach'. Working Paper No. 3. Water and Land Resource Centre, Addis Ababa University: Addis Ababa.

Teixeira, LH, Oliveira BF, Krah FS, Kollmann J & Ganade G (2020). Linking plant traits to multiple soil functions in semi-arid ecosystems, J of Arid Environments, 172, 104040.

Tenedório JA and Rocha J (2018). Introductory Chapter: Spatial Analysis, Modeling, and Planning, ResearchGate,at: https://www.researchgate.net/publication/329280860

Tesfaye G and Tibebe D (2018). Soil Erosion Modelling Using GIS Based RUSEL Model in Gilgel Gibe-1 Catchment, South West Ethiopia, Int J Environ Sci Nat Res 15(5): IJESNR.MS.ID.555923.

Tesfaye Y, Roos A, Campbell BM, Bohlin F (2010). Forest Incomes and Poverty Alleviation Under Participatory Forest Management in the Bale Highlands, Southern Ethiopia, International Forestry Review, Vol. 12, No.1, pp. 66-77.

Thokchom A and Yadava PS (2017). Biomass and carbon stock along an altitudinal gradient in the forest of Manipur, Northeast India, Tropical Ecology 58(2): 389–396, 2017 ISSN 0564-3295.

Thomas J, Joseph S, and Thrivikramji KP (2018). Assessment of soil erosion in a tropical mountain river basin of the southern Western Ghats, India using RUSLE and GIS, Geoscience Frontiers 9 (2018) 893-906.

Thorson JT, Ianelli JN, Larsen EA, Ries L, Scheuerell MD, Szuwalski C, and Zipkin EF (2016). Joint dynamic species distribution models: a tool for community ordination and spatio-temporal monitoring. Global Ecology and Biogeography, J. Global Ecol. Biogeogr.

Tinch DR, Beamont N, Sunderland T, Ozdemiroglu E *et al*. (2019). Economic valuation of ecosystem goods and services: a review for decision makers, Journal of Environmental Economics and Policy on available, tandfonline.com/10.1080/21606544.2019.1623083.

Tsegaye B (2019). Effect of Land Use and Land Cover Changes on Soil Erosion in Ethiopia. Int J Agric Sc Food Technol 5(1): 026-034: Doi.org/10.17352/2455-815X.000038.

Tsegaye L and Bharti R (2021). Soil erosion and sediment yield assessment using RUSLE and GIS-based approach in Anjeb watershed, Northwest Ethiopia, SN Applied Sciences, 3:582, /doi.org/10.1007/s42452-021-04564-x.

UNDP and FAO (1984). Assistance to land use planning Ethiopia geomorphology and soils, Report prepared for the Government of Ethiopia the Food and Agriculture of the United Nations acting as existing agency for the United Nations development Programme.

UNFCCC (2015). Measurements for estimation of carbon stocks in afforestation and reforestation project activities under the clean development mechanism, a field manual. Retrieved 01 July 2021.

Unnasch RS, Braun DP, Comer PJ, Eckert GE (2008). The Ecological Integrity Assessment Framework: A Framework for Assessing the Ecological Integrity of Biological and Ecological Resources of the National Park System**.** Report to the National Park Service.

Vargas-guzma´ JA, Warrick, AW, Myers DE, Musil, SA, and Artiola JF (2004). Statistics and Geostatistics in Environmental Monitoring book chapter in Environmental Monitoring and Characterization Publisher: Elsevier Science & Technology Books.

Vayreda J, Gracia M, Canadell JG, and Retana J (2012). Spatial Patterns and Predictors of Forest Carbon Stocks in Western Mediterranean, Ecosystems,15, 1258–1270 DOI: 10.1007/s10021-012-9582-7.

Verdonschot PFM, van der Lee GH, and Verdonschot RCM (2020). Integrating measures of ecosystem structure and function to improve assessments of stream integrity, Freshwater Science. 2020. 39(4):601–604, doi.org/10.1086/711708

Vincenzia S, Zucchetta M, Franzoi P, Pellizzato M, Pranovi F, Deleo GA, Torricelli P (2011). Application of a Random Forest algorithm to predict the spatial distribution of the potential yield of Ruditapes philippinarum in the Venice lagoon, Italy. Ecol Model Vol. 222, No.8, pp.1471–1478.

Vitousek PM, Porder S, Houlton BZ, Chadwick OA (2010). Terrestrial phosphorus limitation: Mechanisms, implications, and nitrogen–phosphorus interactions. Ecol. Appl. 2010, 20, 5–15.

Vogiatzakis IN (2003). GIS-based Modelling and Ecology: A Review of Tools and Methods, Geographical Paper No. 170, Department of Geography, The University of Reading, Whiteknights.

Wagari M, Tamiru H (2021). RUSLE Model Based Annual Soil Loss Quantification for Soil Erosion Protection: A Case of Fincha Catchment, Ethiopia, Air, Soil and Water Research Volume 14: 1–12.

Wahab MA (2017). Interpolation and Extrapolation; “Topics in System Engineering” – Winter Term 2016/17, ResearchGate, www.researchgate.net/publication/313359516.

Wakjira FS (2006). Biodiversity and ecology of Afromontane rainforests with wild Coffea arabica L. populations in Ethiopia, Ecology and Development Series No. 38.

Wang B, Zheng F, Guan Y (2016). Improved USLE-K factor prediction: A case study on water erosion areas in China, International Soil and Water Conservation Research 4 (2016) 168–176, doi.org/10.1016/j.iswcr.2016.08.003.

Wang C, Shan L, Liu X, Yang Q et *al* (2020). Impacts of horizontal resolution and downscaling on the USLE LS factor for different terrains, International al Soil and Water Conservation Research 8 (2020) 363e372, doi.org/10.101

Wang CT, Long RJ, Wang QJ, Ding LM, & Wang MP (2007). Effects of altitude on plant-species diversity and productivity in an alpine meadow, QinghaiTibetan plateau. J. of Australian Botany, 55(2), 110-117.

Wang L (2013). Species Distribution Modeling: Implications of Modeling Approaches, Biotic Effects, Sample Size, and Detection Limit, PhD Dissertation, submitted to Department of Ecology and Evolutionary Biology University of Toronto.

Wang T (2021). Climatic & Ecological Modelling for Adaptive Forest Applications, onlinebook, University of British Columbia.

Watson C (2007). Direct consumptive use valuation of ecosystem goods and services in the Bale Mountains Eco-region, Ethiopia, MSc thesis submitted to Imperial College London Faculty of Natural Sciences.

Webster R, Oliver MA (2007). Geostatistics for Environmental Scientists Second Edition, published by John Wiley & Sons Ltd, The Atrium, Southern Gate, Chichester.

Wen D, Ma S, Zhang A, Ke X (2021). Spatial Pattern Analysis of the Ecosystem Services in the Guangdong-Hong Kong-Macao Greater Bay Area Using Sentinel-1 and Sentinel-2 Imagery Based on Deep Learning Method. Sustainability 2021, 13, 7044. https://doi.org/ 10.3390/su13137044.

Whitmore TC, and Sayer JA (1992) Tropical Deforestation and Species Extinction. Chapman & Hall, London, xvii + 147 pp.

Williams AK (2003). The Influence of Probability of Detection When Modeling Species Occurrence Using GIS and Survey Data, PhD dissertation submitted to the Faculty of the Virginia Polytechnic Institute and State University

Williams SD, Vivero JL, Spawls S, Shimelis, & Kelbessa A (2005). Ethiopian Highlands. In: Mittermeier, R. (ed) Hotspots revisited. Conservation International and Cemex.

Wischmeier WH and Smith DD (1965). Predicting rainfall erosion from cropland east of the Rocky Mountain: Guide for selection of practices for soil and water conservation. U.S. Department of Agriculture Handbook, No. 282

Wischmeier WH, & Smith DD (1978). Predicting rainfall erosion losses, a guide to conservation planning. U.S. Department of Agriculture (Agriculture Handbook No. 537).

Wisz MS, Hijmans, RJ, Li J, Peterson AT, Graham CH, Guisan A, and Nceas (2008). Effects of sample size on the performance of species distribution models, Diversity Distribution, 14, 763–773.

Wodajo A, Tesfaye MA, Mohammed M (2020). Floristic composition and carbon pools along altitudinal gradient: the case of Gara Muktar forest, west Hararghe Zone, Eastern Ethiopia. J. of Int Forest Res Eng 2020;4(1):42-50. DOI: 10.15406/freij.2020.04.00098.

Wulder MA, Hermosilla T, JWhite JC, Bater, CW, Hobart G, and Bronson SC (2024). Development and implementation of a stand-level satellite-based forest inventory for Canada, Forestry: An International Journal of Forest Research, 2024, 1–18, doi.org/10.1093/forestry/cpad065

Xu X, Du X, Wang F, Sha J, Chen Q, Tian G, Zhu Z, Ge S and Jiang Y (2020). Effects of Potassium Levels on Plant Growth, Accumulation and Distribution of Carbon, and Nitrate Metabolism in Apple Dwarf Rootstock Seedlings. Front. Plant Sci. 11:904. Doi: 10.3389/fpls.2020.00904.

Yang Y, Watanabe MF, Lii F, Zhang J, Zhang W, and Zhai J (2006). Factors affecting forest growth and possible effects of climate change in the Taihang Mountains, northern China, Forestry, Vol. 79, No. 1, doi:10.1093/forestry/cpi062.

Yaseen M, Fan G, Zhou X, Long W, Feng G (2022). Plant Diversity and Soil Nutrients in a Tropical Coastal Secondary Forest: Association Ordination and Sampling Year Differences. Forests, 13, 376. doi.org/10.3390/f13030376.

Ye J (2008). Geostatistical Methods for Spatio-Temporal Analysis of Magnetic Resonance Imaging data, PhD dissertation, Athens, Georgia.

Yigini Y, Panagos P, and Montanarella L eds (2013). Soil Resources of Mediterranean and Caucasus Countries", Office for Official Publications of the European Communities, Luxembourg.

Yineger H, Kelbessa E, Bekele T and Lulekal E (2008). Floristic composition and structure of the Dry Afromontane forest at Bale mountains national park, Ethiopia, SINET: Ethiop. J. Sci., 31(2):103–120, 2008

Yohanis K and D'Huart JP (2014). Assessment of the Present Distribution of the Forest Hog (Hylochoerusmeinertzhageni) in Ethiopia. J. of Mountain Ecology, Vol.3, pp. 46-48.

Yohannes H, Soromessa T, & Argaw M (2015). Carbon stock analysis along slope and slope aspect gradient in Gedo Forest: implications for climate change mitigation. J. of Earth Science and Climate Change, 6(9).

Young NE (2010). Regional data refine local abundance models: Modelling plant species abundance distributions on the central plains, Msc thesis submitted Colorado State University, Fort Collins, Colorado.

Yu CX, Kai A, Yang Y, Gaodi X and Chunxia L (2014). Forest Carbon Storage Trends Along Altitudinal Gradients in Beijing, Journal of Resources and Ecology Vol.5 No.2, DOI: 10.5814/j.issn.1674-764x.2014.02.007.

Yudaputra A, Robiansyah I, and Sumeru RD (2019). The Implementation of Artificial Neural Network and Random Forest in Ecological Research: Species Distribution Modelling with Presence and Absence Dataset, Research Center for Plant Conservation and Botanic Gardens, Indonesian Institute of Sciences Jl. Ir. H. Juanda No.13, Bogor-Indonesia.

Zare C, MA (2010). Predicting the distribution of plant species using logistic regression (Case study: Garizat rangelands of Yazd province), Journal of Desert 15,151-158.

Zawadzki J, Cieszewski CJ, Zasada M & Lowe RC (2005). Applying geostatistics for investigations of forest ecosystems using remote sensing imagery. Silva Fennica 39(4): 599–617.

Zhang C, Wang K, Yue, Y, Qi X, Zhang M (2023). Assessing Regional Ecosystem Conditions Using Geospatial Techniques, A Review. Sensors 2023, 23, 4101. https://doi.org/10.3390/s23084101.

Zhang H, Zhuang S, Qian H, Wang F, Ji H (2015) Spatial Variability of the Topsoil Organic Carbon in the Moso Bamboo Forests of Southern China in Association with Soil Properties. PLos one 10(3): e0119175, Doi: 10.1371/journal.pone.0119175.

Zhang L, Huettmann F, Zhang X, Liu S, Sun P, Yu Z, Mi C (2019). The use of classification and regression algorithms using the random forests method with presence-only data to model species distribution, Methods Vol. X No.6:pp.2281–2292.

Zhang L, Xu M, Qiu S, Li R, Zhao H, Shang H, Lai C & Zhang W (2016). Improving the estimate of forest biomass carbon storage by combining two forest inventory systems, Scandinavian Journal of Forest Research, DOI: 10.1080/02827581.2016.1226946.

Zhanga H, Weia J, Yangb Q, Baartmanc JE, *et al* (2017). An improved method for calculating slope length (λ) and the LS parameters of the Revised Universal Soil Loss Equation for large watersheds, Geoderma 308, 36–46.

Zhong Z, Chen Z, Xu Y, Ren C, Yang G, Han X, Ren G, and Feng Y (2018). Relationship between Soil Organic Carbon Stocks and Clay Content under Different Climatic Conditions in Central China, J. of Forests, 9, 598; doi:10.3390/f9100598.

Zhou W, Han G, Liu M, Li X (2019). Effects of soil pH and texture on soil carbon and nitrogen in soil profiles under different land uses in Mun River Basin, Northeast Thailand. Peer J 7:e7880. dOI 10.7717/peerj.7880.

Zhu, AX, Lu G, Liu J, Qin CZ and Zhou C (2018). Spatial prediction based on Third Law of Geography, Annals of GIS, 24:4, 225-240, DOI: 10.1080/19475683.2018.1534890 To link to this article: https://doi.org/10.1080/19475683.2018.1534890.

Zimmermann NE, Edwards, TC, Graham CH, Pearman, PB, and Svenning JC (2010). New trends in species distribution modelling.

Zulian G, Stange E, Woods H, Carvalho L, Dick J *et al* (2018). Practical application of spatial ecosystem service models to aid decision support, Ecosystem Services 29 (2018) 465–480,

Zyl H (2015). The Economic Value and Potential of the Wildlife Protected Areas of Ethiopia Case Study on 14 Federal Protected Areas, the Sustainable Development of the Protected Areas System of Ethiopia (SDPASE) project, and the Ethiopian Wildlife Conservation Authority.

APPENDICES

Annex 1: Ecosytem services values adopted from De Groot *et a*l., (2020)

Ecosystem services	(Int$/hectare/year) adjusted to the price of 2022				
	Tropical forest	Woodland and shrubland	Grassland	Cultivated land	Afroalpine
Provision					
Food	692	8	0	586	4
Water	55063	1.15	360	694	180.575
Raw materials	13502	0	732	6.9	366
Genetic resources	18	0	0	0	0
Medicinal resources	3.45	1.15	0	0	0.575
Ornamental resources	0	0	0	0	0
Regulation					
Air quality regulation	355	8	10	11.5	9
Climate regulation	756	102	83	11.5	92.5
Moderation of extreme events	124	0	0	1142	0
Regulation of water flows	442	81	49	19	65
Waste management	13	100	13	46	56.5
Erosion prevention	694	33	694	199	363.5
Maintenance of soil fertility	48	21	48	39	34.5
Pollination	1008	28	1008	1723	518
Biological control	16	0	16	714	8
Maintenance of life cycles of migratory species	21	0	21	0	10.5
Supportive					
Maintenance of life genetic diversity	8	0	0	0	0
Disease control	0	0	0	0	0
Photosynthesis	0	0	0	0	0
Nutrient cycle	0	0	0	0	0
Soil formation	0	0	0	0	0
Water cycling	0	0	0	0	0
maintenance of genetic diversity	0	0	0	0	0
Nursery	0	0	0	0	0
Cultural					
Aesthetic information	0	44	0	454	22
Opportunities for recreation and tourism	60826	142	105	3567	123.5
Inspiration for culture, art, and design	6	142	326	18.4	234
Spiritual experiences	0	0	0	0	0
Information for cognitive development	0	246	169	0	207.5
Existence and bequest values	3404	2.3	0	0	1.15

Annex 2: Ecosystem services values of five LULC types of the study area in 2010

Ecosystem services	2010					
	Forest	Woodland	Grassland	Farmland	scrubland	sum
Provision	4.78E+10	1.73E+07	3.66E+08	6.71E+08	2.90E+08	4.91E+10
Food	4.77E+08	1.34E+07	0.00E+00	3.06E+08	2.11E+06	7.98E+08
Water	3.80E+10	1.93E+06	1.21E+08	3.62E+08	9.52E+07	3.86E+10
Raw materials	9.31E+09	0.00E+00	2.46E+08	3.60E+06	1.93E+08	9.75E+09
Genetic resources	1.24E+07	0.00E+00	0.00E+00	0.00E+00	0.00E+00	1.24E+07
Medicinal resources	2.38E+06	1.93E+06	0.00E+00	0.00E+00	3.03E+05	4.62E+06
Ornamental resources	0.00E+00	0.00E+00	0.00E+00	0.00E+00	0.00E+00	0.00E+00
Regulation	2.40E+09	6.27E+08	6.52E+08	2.04E+09	6.10E+08	6.32E+09
Air quality regulation	2.45E+08	1.34E+07	3.36E+06	6.00E+06	4.74E+06	2.72E+08
Climate regulation	5.21E+08	1.71E+08	2.79E+07	6.00E+06	4.87E+07	7.75E+08
Moderation of extreme events	8.55E+07	0.00E+00	0.00E+00	5.95E+08	0.00E+00	6.81E+08
Regulation of water flows	3.05E+08	1.36E+08	1.64E+07	9.91E+06	3.43E+07	5.02E+08
Waste management	8.97E+06	1.68E+08	4.36E+06	2.40E+07	2.98E+07	2.35E+08
Erosion prevention	4.79E+08	5.55E+07	2.33E+08	1.04E+08	1.92E+08	1.06E+09
Maintenance of soil fertility	3.31E+07	3.53E+07	1.61E+07	2.03E+07	1.82E+07	1.23E+08
Pollination	6.95E+08	4.71E+07	3.38E+08	8.98E+08	2.73E+08	2.25E+09
Biological control	1.10E+07	0.00E+00	5.37E+06	3.72E+08	4.22E+06	3.93E+08
Maintenance of life cycles of migratory species	1.45E+07	0.00E+00	7.05E+06	0.00E+00	5.53E+06	2.71E+07
Supportive	5.52E+06	0.00E+00	0.00E+00	0.00E+00	0.00E+00	5.52E+06
Maintenance of life genetic diversity	5.52E+06	0.00E+00	0.00E+00	0.00E+00	0.00E+00	5.52E+06
Disease control	0.00E+00	0.00E+00	0.00E+00	0.00E+00	0.00E+00	0.00E+00
Photosynthesis	0.00E+00	0.00E+00	0.00E+00	0.00E+00	0.00E+00	0.00E+00
Nutrient cycle	0.00E+00	0.00E+00	0.00E+00	0.00E+00	0.00E+00	0.00E+00
Soil formation	0.00E+00	0.00E+00	0.00E+00	0.00E+00	0.00E+00	0.00E+00
Water cycling	0.00E+00	0.00E+00	0.00E+00	0.00E+00	0.00E+00	0.00E+00
maintenance of genetic diversity	0.00E+00	0.00E+00	0.00E+00	0.00E+00	0.00E+00	0.00E+00
Nursery	0.00E+00	0.00E+00	0.00E+00	0.00E+00	0.00E+00	0.00E+00
Cultural	4.43E+10	9.69E+08	2.01E+08	2.11E+09	3.10E+08	4.79E+10
Aesthetic information	0.00E+00	7.40E+07	0.00E+00	2.37E+08	1.16E+07	3.22E+08
Opportunities for recreation and tourism	4.20E+10	2.39E+08	3.52E+07	1.86E+09	6.51E+07	4.41E+10
Inspiration for culture, art and design	4.14E+06	2.39E+08	1.09E+08	9.59E+06	1.23E+08	4.85E+08
Spiritual experiences	0.00E+00	0.00E+00	0.00E+00	0.00E+00	0.00E+00	0.00E+00
Information for cognitive development	0.00E+00	4.13E+08	5.67E+07	0.00E+00	1.09E+08	5.80E+08
Existence and bequest values	2.35E+09	3.87E+06	0.00E+00	0.00E+00	6.06E+05	2.35E+09
Total	1.41E+11	3.21E+09	2.07E+09	8.95E+09	2.13E+09	1.58E+11

Annex 3: Ecosystem services values of five LULC types of the study area in 2015

Ecosystem services	2015					
	Forest	Woodland	Grassland	Farmland	scrubland	sum
Provision	4.38E+10	1.85E+07	3.31E+08	7.64E+08	2.19E+08	4.51E+10
Food	4.37E+08	1.44E+07	0.00E+00	3.48E+08	1.59E+06	8.01E+08
Water	3.48E+10	2.07E+06	1.09E+08	4.12E+08	7.17E+07	3.54E+10
Raw materials	8.53E+09	0.00E+00	2.22E+08	4.10E+06	1.45E+08	8.91E+09
Genetic resources	1.14E+07	0.00E+00	0.00E+00	0.00E+00	0.00E+00	1.14E+07
Medicinal resources	2.18E+06	2.07E+06	0.00E+00	0.00E+00	2.28E+05	4.48E+06
Ornamental resources	0.00E+00	0.00E+00	0.00E+00	0.00E+00	0.00E+00	0.00E+00
Regulation	2.20E+09	6.72E+08	5.88E+08	2.32E+09	4.60E+08	6.23E+09
Air quality regulation	2.24E+08	1.44E+07	3.03E+06	6.83E+06	3.57E+06	2.52E+08
Climate regulation	4.78E+08	1.84E+08	2.51E+07	6.83E+06	3.67E+07	7.30E+08
Moderation of extreme events	7.84E+07	0.00E+00	0.00E+00	6.78E+08	0.00E+00	7.56E+08
Regulation of water flows	2.79E+08	1.46E+08	1.48E+07	1.13E+07	2.58E+07	4.77E+08
Waste management	8.22E+06	1.80E+08	3.94E+06	2.73E+07	2.24E+07	2.42E+08
Erosion prevention	4.39E+08	5.94E+07	2.10E+08	1.18E+08	1.44E+08	9.71E+08
Maintenance of soil fertility	3.03E+07	3.78E+07	1.45E+07	2.31E+07	1.37E+07	1.20E+08
Pollination	6.37E+08	5.04E+07	3.05E+08	1.02E+09	2.06E+08	2.22E+09
Biological control	1.01E+07	0.00E+00	4.85E+06	4.24E+08	3.18E+06	4.42E+08
Maintenance of life cycles of migratory species	1.33E+07	0.00E+00	6.36E+06	0.00E+00	4.17E+06	2.38E+07
Supportive	5.06E+06	0.00E+00	0.00E+00	0.00E+00	0.00E+00	5.06E+06
Maintenance of life genetic diversity	5.06E+06	0.00E+00	0.00E+00	0.00E+00	0.00E+00	5.06E+06
Disease control	0.00E+00	0.00E+00	0.00E+00	0.00E+00	0.00E+00	0.00E+00
Photosynthesis	0.00E+00	0.00E+00	0.00E+00	0.00E+00	0.00E+00	0.00E+00
Nutrient cycle	0.00E+00	0.00E+00	0.00E+00	0.00E+00	0.00E+00	0.00E+00
Soil formation	0.00E+00	0.00E+00	0.00E+00	0.00E+00	0.00E+00	0.00E+00
Water cycling	0.00E+00	0.00E+00	0.00E+00	0.00E+00	0.00E+00	0.00E+00
maintenance of genetic diversity	0.00E+00	0.00E+00	0.00E+00	0.00E+00	0.00E+00	0.00E+00
Nursery	0.00E+00	0.00E+00	0.00E+00	0.00E+00	0.00E+00	0.00E+00
Cultural	4.06E+10	1.04E+09	1.82E+08	2.40E+09	2.34E+08	4.45E+10
Aesthetic information	0.00E+00	7.92E+07	0.00E+00	2.69E+08	8.74E+06	3.57E+08
Opportunities for recreation and tourism	3.84E+10	2.56E+08	3.18E+07	2.12E+09	4.90E+07	4.09E+10

Inspiration for culture, art and design	3.79E+06	2.56E+08	9.88E+07	1.09E+07	9.29E+07	4.62E+08
Spiritual experiences	0.00E+00	0.00E+00	0.00E+00	0.00E+00	0.00E+00	0.00E+00
Information for cognitive development	0.00E+00	4.43E+08	5.12E+07	0.00E+00	8.24E+07	5.76E+08
Existence and bequest values	2.15E+09	4.14E+06	0.00E+00	0.00E+00	4.57E+05	2.16E+09
Total	1.29E+11	3.44E+09	1.87E+09	1.02E+10	1.61E+09	1.47E+11

Annex 4: Ecosystem services values of different ecosystems in the BMER in USD in 2022

Ecosystem services	2022					
	Forest	Woodland	Grassland	Farmland	scrubland	Sum
Provision	4.15E+10	1.84E+07	1.16E+08	9.93E+08	2.70E+08	4.29E+10
Food	4.15E+08	1.43E+07	0.00E+00	4.52E+08	1.96E+06	8.83E+08
Water	3.30E+10	2.06E+06	3.81E+07	5.35E+08	8.86E+07	3.37E+10
Raw materials	8.10E+09	0.00E+00	7.75E+07	5.32E+06	1.79E+08	8.36E+09
Genetic resources	1.08E+07	0.00E+00	0.00E+00	0.00E+00	0.00E+00	1.08E+07
Medicinal resources	2.07E+06	2.06E+06	0.00E+00	0.00E+00	2.82E+05	4.41E+06
Ornamental resources	0.00E+00	0.00E+00	0.00E+00	0.00E+00	0.00E+00	0.00E+00
Regulation	2.09E+09	6.68E+08	2.06E+08	3.01E+09	5.68E+08	6.54E+09
Air quality regulation	2.13E+08	1.43E+07	1.06E+06	8.87E+06	4.41E+06	2.42E+08
Climate regulation	4.53E+08	1.83E+08	8.79E+06	8.87E+06	4.54E+07	6.99E+08
Moderation of extreme events	7.44E+07	0.00E+00	0.00E+00	8.81E+08	0.00E+00	9.55E+08
Regulation of water flows	2.65E+08	1.45E+08	5.19E+06	1.47E+07	3.19E+07	4.62E+08
Waste management	7.80E+06	1.79E+08	1.38E+06	3.55E+07	2.77E+07	2.51E+08
Erosion prevention	4.16E+08	5.91E+07	7.35E+07	1.54E+08	1.78E+08	8.81E+08
Maintenance of soil fertility	2.88E+07	3.76E+07	5.08E+06	3.01E+07	1.69E+07	1.18E+08
Pollination	6.05E+08	5.01E+07	1.07E+08	1.33E+09	2.54E+08	2.34E+09
Biological control	9.60E+06	0.00E+00	1.69E+06	5.51E+08	3.92E+06	5.66E+08
Maintenance of life cycles of migratory species	1.26E+07	0.00E+00	2.22E+06	0.00E+00	5.15E+06	2.00E+07
Supportive	4.80E+06	0.00E+00	0.00E+00	0.00E+00	0.00E+00	4.80E+06
Maintenance of life genetic diversity	4.80E+06	0.00E+00	0.00E+00	0.00E+00	0.00E+00	4.80E+06
Disease control	0.00E+00	0.00E+00	0.00E+00	0.00E+00	0.00E+00	0.00E+00
Photosynthesis	0.00E+00	0.00E+00	0.00E+00	0.00E+00	0.00E+00	0.00E+00
Nutrient cycle	0.00E+00	0.00E+00	0.00E+00	0.00E+00	0.00E+00	0.00E+00
Soil formation	0.00E+00	0.00E+00	0.00E+00	0.00E+00	0.00E+00	0.00E+00
Water cycling	0.00E+00	0.00E+00	0.00E+00	0.00E+00	0.00E+00	0.00E+00
maintenance of genetic diversity	0.00E+00	0.00E+00	0.00E+00	0.00E+00	0.00E+00	0.00E+00
Nursery	0.00E+00	0.00E+00	0.00E+00	0.00E+00	0.00E+00	0.00E+00
Cultural	3.85E+10	1.03E+09	6.35E+07	3.12E+09	2.88E+08	4.30E+10
Aesthetic information	0.00E+00	7.88E+07	0.00E+00	3.50E+08	1.08E+07	4.40E+08

Opportunities for recreation and tourism	3.65E+10	2.54E+08	1.11E+07	2.75E+09	6.06E+07	3.96E+10
Inspiration for culture, art and design	3.60E+06	2.54E+08	3.45E+07	1.42E+07	1.15E+08	4.21E+08
Spiritual experiences	0.00E+00	0.00E+00	0.00E+00	0.00E+00	0.00E+00	0.00E+00
Information for cognitive development	0.00E+00	4.40E+08	1.79E+07	0.00E+00	1.02E+08	5.60E+08
Existence and bequest values	2.04E+09	4.12E+06	0.00E+00	0.00E+00	5.64E+05	2.05E+09
Total	1.23E+11	3.42E+09	6.54E+08	1.32E+10	1.98E+09	1.42E+11

Annex 5: The net contributions of LULC categories to other categories between 2010 & 2022

		LULC in 2022						
	LULC types	Forest	Farmland	Grassland	Woodland	Scrubland	Unclassified	A net gain or loss
LULC in 2010	Forest		-59650	-62000	-37802	-18737	-7662	-185851
	Farmland	59650		17100	103639	42558	-2270	220677
	Grassland	62000	-17100		16390	-1481	-1865	57944
	woodland	37802	-103639	-16390		-26671	-6444	-115342
	Scrubland	-18737	-42558	1481	26671		-1469	-34612
	Unclassified	7662	2270	1865	6444	1469		19710

Annex 6: Sum of ACD in each diameter class of sample plots in the Harana Forest

Diameter class in cm	The sum of ACD in a ton	Percentage of the total
0- 10	5	1%
10-20	741	0%
20-30	2105	10%
30-40	2110	29%
40-50	1098	29%
50-60	808	15%
60-70	287	11%
> 70	150	4%
Total ACD	7227	100%

Annex 7: Sum of ACD in each height class of sample plots in the Harana Forest

Class	Height class in meter	The sum of ACD in a ton	Percentage of the total ACD
1	0-10	0	0%
2	10-20	145	2%
3	20- 30	4023	56%
4	30- 40	2764	38%
5	> 40	295	4%
	Sum	7227	100%

Annex 8 Bedane et al , 2022 ACD in Harana

Annex 9 Bedane et al 2023 Abudances of w

Annex 10 Manuscript ecosystem service val

Annex 11 Manuscript Soil loss in BMER.pdf

Annex 12 Manuscript ACD and species dive